Phase inversion temperature emulsification: from batch to continuous process

Marino, Helene

Award date:
2010

Awarding institution:
University of Bath

Phase Inversion Temperature Emulsification: From Batch to Continuous Process

Helene Marino

A thesis submitted in candidature for the degree of Doctor of Philosophy

University of Bath
Department of Chemical Engineering

April 2010

Abstract

Emulsion systems are encountered in many everyday products such as milk, agrochemicals or shampoo. This thesis presents an attempt to create an experimental set-up working in continuous flow to produce monodispersed food-grade oil nanoemulsions (< 0.1 μm in diameter) with a low-energy emulsification method. Preparation of O / W nano-emulsions with formulation Soya bean oil / Brij 97 / Water was performed using the phase inversion temperature (PIT) emulsification method with 2 different techniques.

The first technique was the emulsification in batch where the pre-emulsion was heated to its hydrophilic-lipophilic balance (HLB) temperature and then quickly cooled down to room temperature. The appearance of the resultant emulsions varied from unstable white to stable transparent. Cooling rate seemed to be a critical parameter to obtain transparent nanoemulsions. Reproducible results were difficult to obtain since a good temperature control was not achieved with the batch set-up.

Requirements for the conception of the second technique, e.g. the continuous emulsification rig, were deduced from the results of the batch experiments. The designed set-up continuously pumped the emulsion premix through a pipe immersed into a heating bath at the HLB temperature and then through a cooling micro-heat exchanger. In order to obtain small average size, narrow size distribution and transparency special attention needed to be paid to the heating treatment.

The nanoemulsions prepared with the PIT method showed a good stability over time. For instance, a fresh nanoemulsion made with 10 % (w / w) of soya bean oil in the continuous set-up displayed an average droplet size of 21 nm. A month and a half later, this average size had increased only 5 nm. The average size and polydispersity index of the emulsions obtained using both techniques were similar. The continuous device allowed the preparation of emulsions more rapidly and in a more reproducible way than the batch set-up.

Acknowledgements

I would like to thank my supervisors Dr Tom Arnot and Dr Pawel Plucinski for their advice and guidance throughout the course of this project.

I am also very grateful towards Unilever Corporate Research for providing the financial support for this research in the form of an Industrial PhD Studentship. I would like to acknowledge especially Dr Steve Moore and Dr Shiping Zhu for the valuable meetings that we had.

I want to thank all the technical and administrative staff in the Department of Chemical Engineering for their precious help.

Finally, I owe special thanks to my family and friends who provided me with a positive environment for this work.

Table of Contents

LIST OF SYMBOLS

surface (m^2)	A
Absorbance (a.u.)	Abs.
constant for the linear relationship relating $d_{droplet}$ to d_{pore} (-)	c
Critical Micellar Concentration (mol L^{-1})	CMC
specific heat of a material at constant pressure (J g^{-1} K^{-1})	C_p
average droplet diameter (m)	$d_{droplet}$
average pore diameter (m)	d_{pore}
mass flow rate (g s^{-1})	G
correlation function (-)	$G(\tau)$
Hydrophilic-Lipophilic Balance (-)	HLB
intensity of the scattered light at time t (-)	I(t)
Internal Diameter of the copper coil (m)	ID
length of the copper coil (m)	L
net energy consumption per unit volume (J m^{-3})	p
transmembrane pressure (Pa)	ΔP_{tm}
pressure of the disperse phase outside the membrane (Pa)	P_d
pressure at the inlet of the membrane module (Pa)	$P_{c,1}$
pressure at the outlet of the membrane module (Pa)	$P_{c,2}$
Phase Inversion Temperature (ºC)	PIT
Laplace pressure (Pa)	p_L
Polydispersity Index (-)	PdI
heat transfer by unit time (J s^{-1})	Q
principal radii of curvature of a curved interface (m)	R_1 and R_2
time (s)	t
measured temperature (°C)	T
difference of temperature between 2 fluids (ºC)	ΔT
overall heat transfer coefficient of a material (W m^{-2} K^{-1})	U
volume flow rate (m^{-3} s^{-1})	$\dot{V}$
interfacial tension (N m^{-1})	γ
power or energy density (W m^{-3})	ε
difference of temperature on side 1 and side 2 of the heat exchanger (ºC)	θ_1 nd θ_2
logarithmic mean temperature difference (ºC)	θ_m
density (kg m^{-3})	ρ
light wavelength (nm)	λ
delay time (s)	τ

Introduction and thesis structure

A colloid is a two-phase system, in which one phase is dispersed into a continuous phase. These colloidal systems are encountered in many everyday products such as chocolate, milk, agrochemicals, shampoo, toothpaste **[1]**.

This project focuses on the preparation of nanoemulsions. Nanoemulsions are colloidal systems for which the internal phase and the external phase are both liquid and whose dispersed phase displays a very small size (< 0.1 μm in diameter). When in suspension in water, they have the potential to be transparent and very stable which makes them particularly attractive for the customer. Nanosized materials have also been of particular interest during the past few decades since they are a potential delivery system for bioactive compounds with applications in personal and health care, cosmetics and food products **[2, 3]**. However, techniques enabling formation of colloids in this size range are usually very energy-consuming.

The aim of this project is to develop an experimental set-up that could produce monodispersed nanoemulsions continuously using a low-energy method and low-toxicity components since it would be desirable to use these new systems in the preparation of food or health care products. The following thesis reports the attempt to create such a device based on the Phase Inversion Temperature (PIT) emulsification method which relies on the use of temperature-sensitive constituents. It is divided in 6 distinct parts: literature review, materials and methods, batch emulsification experiments, rig design, continuous emulsification experiments and an overall conclusion.

Chapter 1 is the literature review. It is composed of 4 sections. The first section deals with the properties of emulsions and nanoemulsions. It provides the reader the necessary background to understand what emulsions are, their different types and main characteristics. The following sections concern the different ways to produce nanoemulsions. Section 1.2 presents the most commonly used techniques to prepare small droplets, i.e. the high-energy emulsification methods, whereas Section 1.3 is about membrane emulsification, an alternative technique with moderate energy consumption that allows the preparation of systems with narrow size distributions. Finally, Section 1.4 deals with the low-energy emulsification methods which enable the preparation of very small droplets without the need of mechanical energy. One of these methods, the Phase Inversion Temperature (PIT) emulsification, is the technique that will be studied in more details in the next chapters.

Chapter 2 presents the materials and methods used for the experiments on Phase Inversion Temperature emulsification. It focuses especially on the determination of the PIT for an emulsion system and on the different modes of nanoemulsion production with the PIT emulsification methods. The various analyses performed on the prepared emulsions are detailed and the technique that determines the size and size distribution of the emulsions is also explained.

Chapter 3 gathers the different batch emulsification results. Indeed, batch emulsification is studied first in order to identify the requirement for the building of the rig. The chosen system for the emulsification process is a mixture of soya bean oil, Brij 97 and water. It allows the production of transparent nanoemulsions under certain conditions. Under optimal conditions with the batch emulsification set-up, it is possible to prepare soya oil droplets as small as 10 nm with a narrow droplet size distribution. It is observed that a fast cooling rate is a critical operational parameter to achieve the formation of small droplets at high soya bean oil concentration.

Chapter 4 explains the conception of the continuous emulsification rig. Indeed, after all the important parameters for successful nanoemulsion production have been identified from the batch experiments in Chapter 3, it is possible to design an experimental set-up that will allow to produce rapidly and in a continuous way Soya bean oil / Brij 97 / Water nanoemulsions. The different items of equipment

selected for the construction of the rig are presented. This chapter also describes the preliminary experiments performed on the emulsification rig and its subsequent improvements.

Chapter 5 concentrates on the operational parameters of the continuous set-up such as the emulsion flow rate, the cooling treatment or the heating treatment and deals with their effects on the characteristics of the resulting Soya bean oil / Brij 97 / Water emulsions. It focuses on the droplet size and droplet size distribution of these emulsions as well as on their stability over time. The last section of this chapter is a short comparison between the experiment results obtained with the batch and the continuous processes.

Finally, the conclusion summarises the main points that have been made throughout the study and draws the eventual future works that could be undertaken.

Chapter 1 – Literature review

1.1- Properties of emulsions and nanoemulsions

1.1.1- Generalities about emulsions

1.1.1.1- Emulsion type

An emulsion is a colloidal system in which the dispersed and continuous phases are liquids, usually immiscible with each other (e.g. oil and water). The structure of emulsions consists of droplets of the dispersed (or internal) phase in the continuous (or external) phase. Two types of emulsion can be distinguished, water-in-oil (w / o) and oil-in-water (o / w) in which water or oil are the dispersed phase respectively **[4]**.

1.1.1.2- Emulsion and size

Generally, emulsion droplet size (Figure 1.1) lies in the micrometer range, a size range in which droplets are attracted by gravity forces **[5]**. Microemulsions whose characteristic droplet size lies in the range 1-100 nm must be distinguished from emulsions (also called macroemulsions to accentuate this difference). Indeed, they are thermodynamically stable: they form spontaneously and present no discernible change in the number, size distribution and spatial arrangement of drops within the experimental timescale. Contrary to microemulsions, macroemulsions require energy input for formation and can only be stable in a kinetic sense **[6]**.

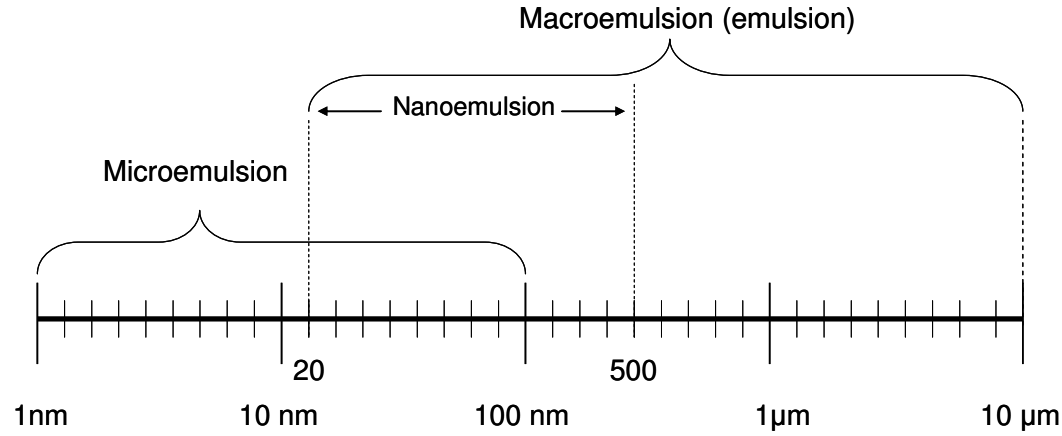

Figure 1.1 : Droplet sizes in macroemulsions (emulsions) and microemulsions

1.1.1.3- Emulsion stability

1.1.1.3.1- definition of hydrophilic and hydrophobic interactions

Water molecules are polar: the hydrogen atoms are positively charged while the oxygen atom is negatively charged. These charges confer them a strong tendency to form hydrogen bonds with other water molecules (Figure 1.2) and other materials **[7]**.

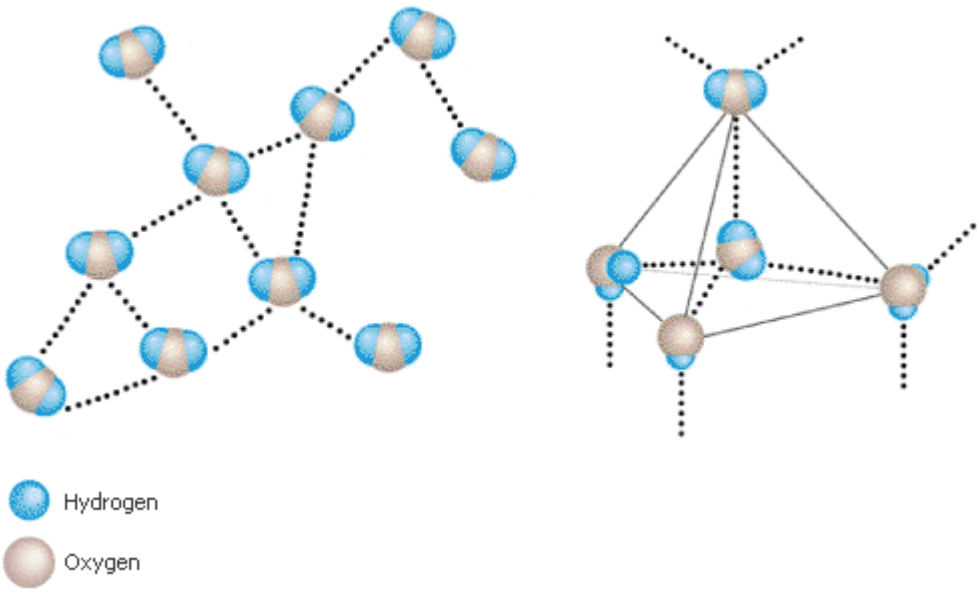

Figure 1.2: Hydrogen bonding in water[8]

When the other material is an ion, a polar compound or a charged surface, the neighbouring water molecules arrange themselves with their charges opposite sign towards the other material. This energetically-favourable process is called hydration. Materials for which there is extensive hydration are described as hydrophilic. Some atoms form hydrogen bonds when in certain compounds such as oxygen in alcohol or polyethylene oxide chains **[7]**.

On the contrary, when the molecule is non-polar such as a hydrocarbon chain, the water molecules arrange themselves into a cage-like structure around it (Figure 1.3) in order to minimize the number of unused potential hydrogen bonds. The water

molecules are more ordered than in the bulk liquid, which results in a low solubility of the solute. Such non-polar substances are called hydrophobic. When two hydrophobic molecules encounter one another in an aqueous solution, the exposed hydrophobic area decreases which is energetically favourable **[7]**.

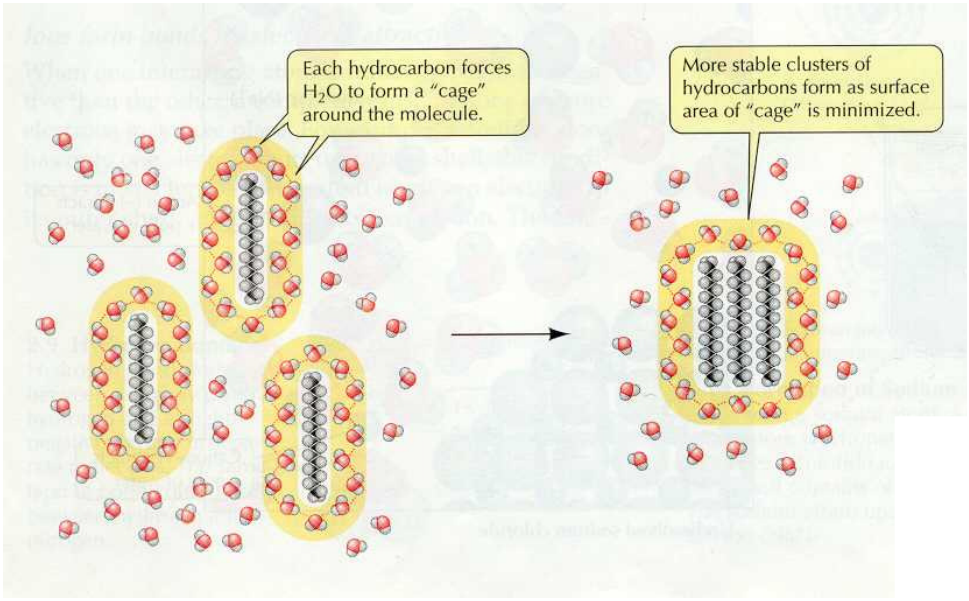

Figure 1.3: Interactions of Water and Non-Polar Substances
Non-polar substances dispersed in water will slowly cluster together, forming larger and larger droplets **[9]**

1.1.1.3.2- break-up processes

The hydrophilic-hydrophobic interactions previously described are one of the main reasons why emulsions are not thermodynamically stable. Indeed, these interactions result in net attractive forces between dispersed droplets. As a consequence, they tend to flocculate: the emulsion drops aggregate, without rupture of the stabilizing layer at the interface. The flocculation (Figure 1.4) can be weak (reversible) or strong (irreversible) **[6]**. This latter phenomenon is also called coagulation. Flocculation could lead to coalescence (Figure 1.5) if the droplets merge. Aggregation will be reduced if the volume fraction of the dispersed phase is small as the chances of collision get smaller.

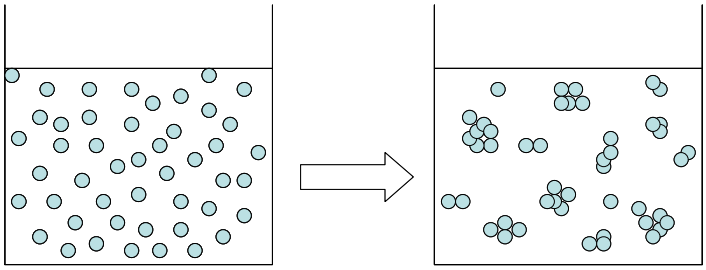

Figure 1.4: Flocculation / Aggregation

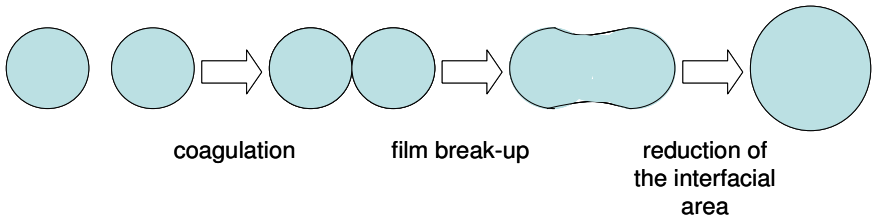

Figure 1.5: Coalescence of 2 droplets

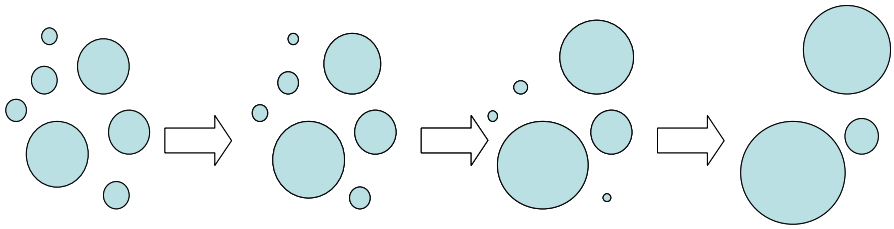

Figure 1.6: Ostwald ripening

Emulsions can also break up on account of other processes: Ostwald ripening, creaming and sedimentation. Ostwald ripening (Figure 1.6) involves large droplets growing at the expense of small ones **[10]**. If the dispersed phase is significantly soluble in the continuous phase, it can be transported through the continuous phase from smaller droplets to larger ones. As larger droplets have a lower surface to volume ratio than the smaller ones, Ostwald ripening occurs with a net reduction in interfacial energy and therefore is energetically favourable **[11]**. To avoid this degradative process, the emulsion droplets must be as monodispersed as possible that is to say that their size distribution needs to be very narrow. Creaming (Figure 1.7) or sedimentation (Figure 1.8) is a build up of a droplet concentration gradient.

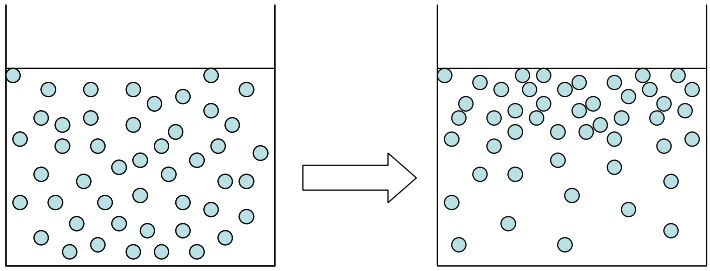

Figure 1.7: Creaming phenomenon

The dispersed phase density is lower than the continuous phase density, hence the droplets tends to concentrate towards the surface.

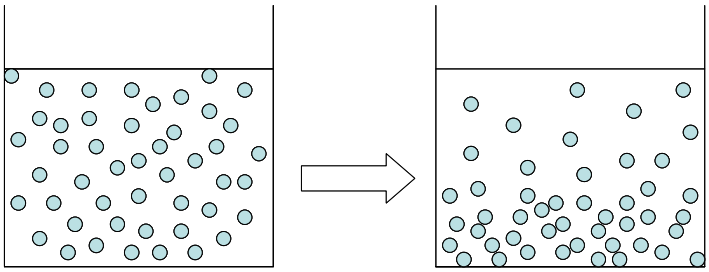

Figure 1.8: Sedimentation phenomenon

The dispersed phase density is higher than the continuous phase density, hence the droplets tends to concentrate towards the bottom of the beaker.

It occurs because of the density difference between the two phases. Hence, it is possible to decrease the intensity of these processes by reducing the density difference. This can be done by making multiple emulsions (W / O / W or O / W / O, Figure 1.9) **[4]**. As for Ostwald ripening, the monodispersity of the emulsion is important: a polydispersed emulsion (i.e an emulsion with a large size distribution) will tend to break-up by sedimentation or creaming faster than a monodispersed one. Generally, flocculation will also lead to enhanced creaming or sedimentation since aggregates move faster than individual drops due to their large effective radius **[6]**. As a consequence, it is very important to limit as much as possible droplet aggregation resulting from the hydrophilic-hydrophobic interactions.

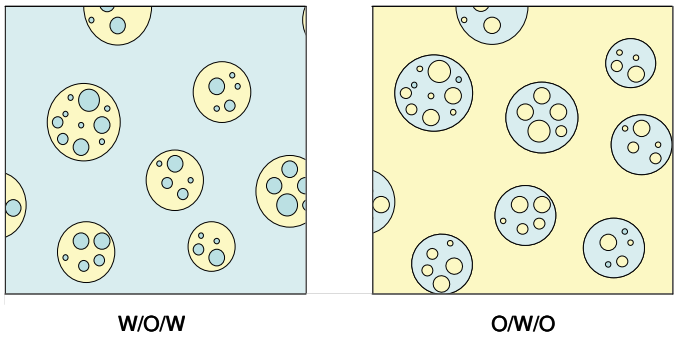

Figure 1.9: Multiple emulsions

1.1.2- Stabilizing emulsions

Emulsions are almost always stabilized using emulsifiers or emulsifying agents. They can be either surface-active agents, proteins or finely divided solids. It must be noted that the features described below can also be used for the stabilization of solid suspensions.

1.1.2.1- Surface-active agents or surfactants

1.1.2.1.1- definition and characteristics

Surfactant molecules consist of two blocks, one with affinity to water and the other to oil: they are amphiphiles (Figure 1.10). When added to a mixture of oil and water, they adsorb at the oil-water interface, so that the hydrophilic block stays in water and the hydrophobic one remains in oil. The presence of the surfactants at the interface induces a decrease of the interfacial tension.

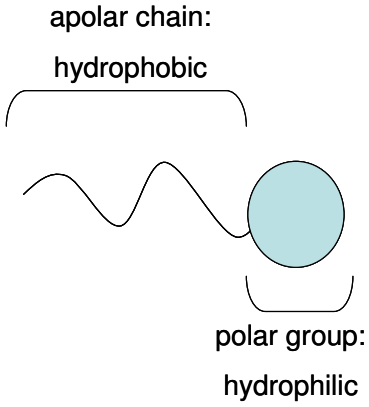

Figure 1.10: Amphiphilic molecule

As the surfactant concentration increases, the monolayer at the oil-water interface becomes more densely populated and the interfacial tension decreases. At a certain concentration, the interface is saturated with surfactant molecules and they begin self-assembling in the bulk of one of the phases, forming supramolecular aggregates, called micelles (Figure 1.11). This specific concentration is known as the Critical Micellar Concentration (CMC). At concentrations above the CMC, the surfactant chemical potential stays constant, because all surfactants added are associating in micelles **[12]**. The surface tension reached its minimum value at the CMC and remains constant above it.

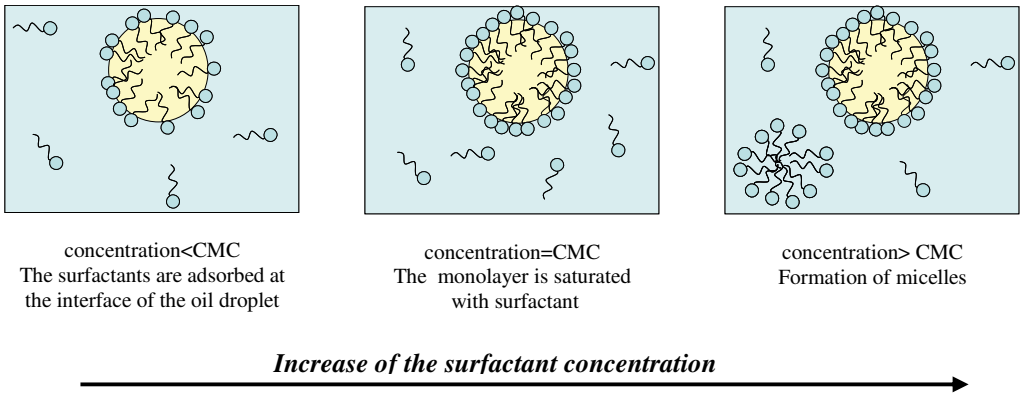

Figure 1.11: Surfactant adsorption in an O / W emulsion and micelle formation

1.1.2.1.2- stabilization by formation of a membrane

Surfactants lower the interfacial tension hence favour the formation of interfaces. Once the droplets are formed, the surfactant molecules stabilize them mechanically by formation of a membrane at the interface. This membrane can prevent coalescence because of *two static effects*:

1- the reduction of interfacial tension caused by the surfactant and the consequent decrease in the thermodynamic drive towards coalescence

2- the physical barrier that the adsorbed layers impose: strong and elastic enough to support the emulsion and prevent the coalescence of dispersed droplets **[7]**.

The Gibbs-Marangoni effect described below (Figure 1.12) is a self-stabilizing *dynamic effect*. This mechanism only works if the surfactant is in the continuous phase **[13]**.

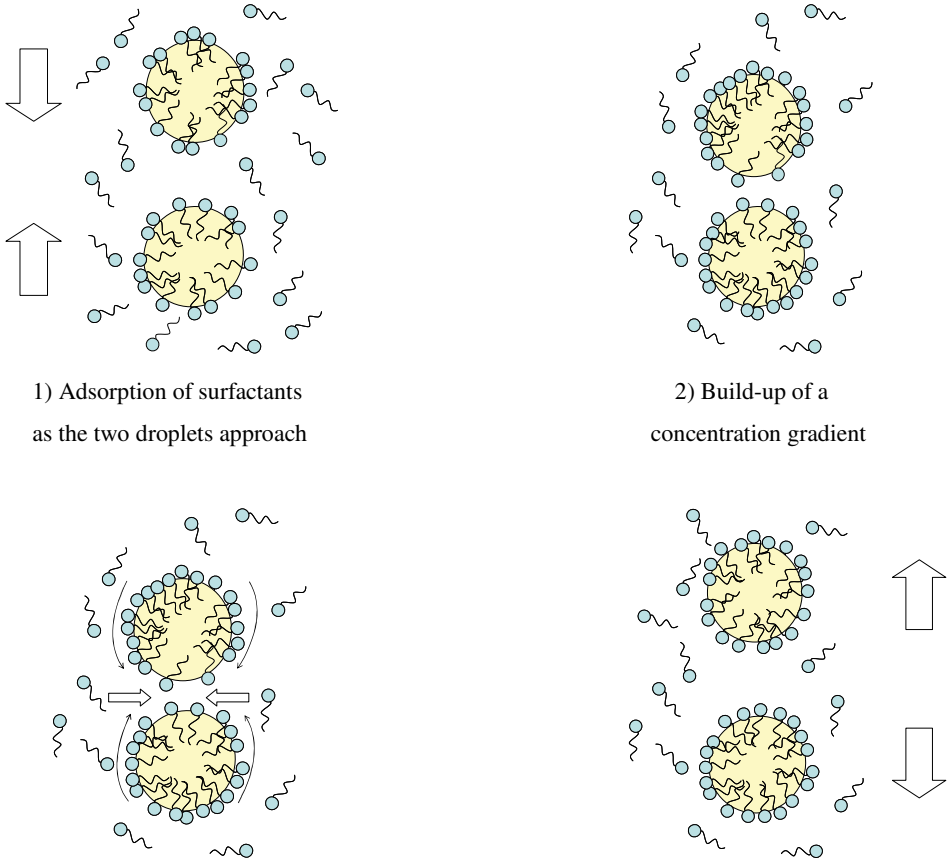

Figure 1.12: Gibbs-Marangoni effect

1.1.2.1.3- electric stabilization

Many surfactants used to stabilize emulsions are ionised. This results in an electric charge carried at the surfaces of the emulsion droplets. In O / W emulsions, the presence of such surface charges lead to the formation of an electrical double layer around the droplets (Figure 1.13): it is composed of the Stern layer (a single layer of oppositely charged ions (e.g counterions) of finite size adjacent to the surface) and the diffuse layer (which extends out from the Stern layer) where the

imbalance between oppositely charged and like-charged ions decreases with distance from the interface until a balance is reached **[7]**.

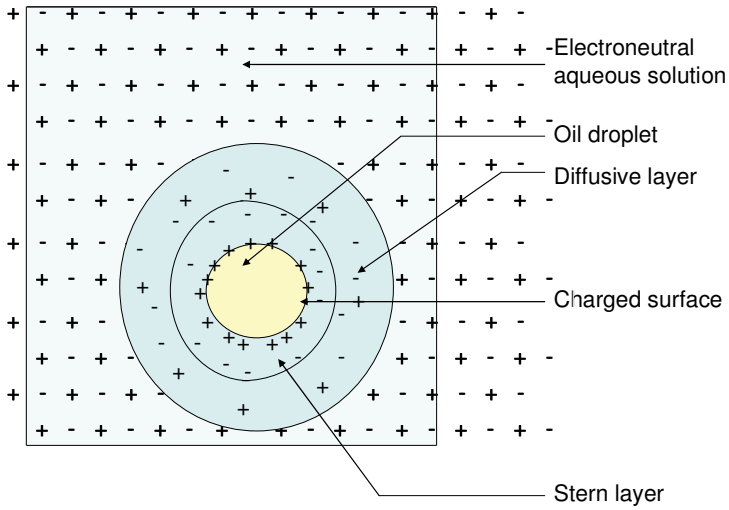

Figure 1.13: Electrical double layer

The zeta potential gives the value of the potential at the boundary between the Stern layer and the diffuse layer. It is measured by electrophoresis. A high absolute zeta potential reveals a strong Coloumbic repulsion between the particles. Therefore, it counteracts the impact of the Van der Waals force which results from the attraction between electric dipoles **[14]**.

If the concentration of ions in the aqueous phase is increased, the effective thickness of the diffusive layer decreases because compensation for the surface charge occurs more readily. O / W emulsions are more stable when the concentration of ions in the aqueous phase is low. Conversely, aggregation can occur by adding salts **[7]**.

1.1.2.1.4- steric stabilization

Another mechanism of stabilization is found when the surfactant is polymeric. The polymer forms loops and tails into the two phases (Figure 1.14). This promotes the formation of a stabilizing layer. Steric stabilization may be effective in non-aqueous dispersion media where charge stabilization cannot be used **[7]**.

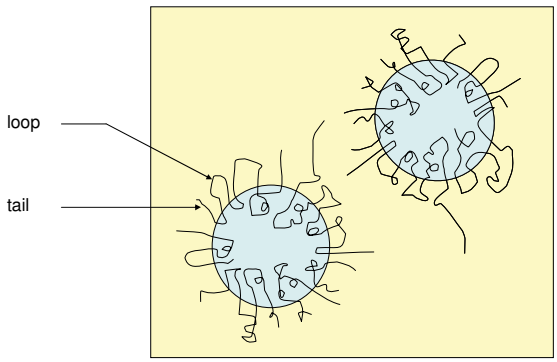

Figure 1.14: Schematic diagram of polymer molecules at a surface of a liquid particle

1.1.2.1.5- HLB

The activity of surfactant emulsifiers is often quantified through the hydrophilic-lipophilic balance (HLB) scale. This concept was introduced by Griffin as a means of predicting emulsion type from surfactant molecular composition. The HLB values can be evaluated experimentally with a number of emulsion stability tests or calculated using empirical equations based on the molecular formula of some surfactants. The more hydrophilic the amphiphile, the higher its HLB **[12]**.

In order to make and stabilize a W / O emulsion, the HLB value should be between 3.5 and 6, while for an O / W emulsion a value between 8 and 18 is desirable. Most of the common surfactants lie outside these ranges, hence have little use as emulsifiers **[12]**. Typical examples of "natural" emulsifiers are lecithin and monoglycerides. Common synthetic emulsifiers include sorbitan fatty acid esters known as Spans (low HLB and oil-soluble) and polyoxyethylene sorbitan esters called Tweens (high HLB and water-soluble) **[4]**.

1.1.2.2- Use of stabilizer

An emulsifier is a substance that promotes emulsion formation by interfacial action and stabilizes it. In the food industry, the term emulsifier is often improperly used to describe materials that promote the shelf-life of food. Rigorously, they

should be called stabilizers. They must be distinguished from emulsifiers, since they only stabilize an emulsion that has already been formed. For example, polysaccharides such as carrageenan or xanthan are common additives to foods. Their thickening properties impart stability to the colloids **[4]**. Another example of stabilizer is finely divided solid particles. They have to be amphiphilic so that they sit at the oil-water interface. Their presence does not make emulsification easier, they only migrate to the interface after the emulsion has formed **[4]**.

1.1.3- Nanoemulsions

Owing to their small droplet size (Figure 1.1), nanoemulsions (also called miniemulsions, fine-dispersed emulsions, submicron emulsions, unstable microemulsions, or translucent emulsions...) resemble microemulsions. Indeed, they may both appear bluish or optically clear **[15, 16]**. As a consequence, they are often difficult to distinguish from each other. But whereas microemulsions are thermodynamically stable, nanoemulsions are only kinetically stable **[3, 16]**. No matter how the components are added, the microemulsion will form spontaneously as long as the final composition is adequate. Contrary to microemulsions, the formation of nanoemulsions requires special operating conditions, reflecting that these colloidal dispersions are not thermodynamically stable **[17]**.

Why make nanoemulsions which are unstable when it is already technologically possible to make microemulsions which are indefinitely stable and have a similar range of size? In fact, nanoemulsions present a number of advantages over microemulsions. Indeed, unlike microemulsions which require a high concentration of surfactants for their preparation (usually 10-30 wt %), nanoemulsions can be made at moderate surfactant concentrations (4-8 wt %) **[18]**. In addition, many microemulsion systems are not dilutable, i.e. they break down at increased water concentration **[2]**. Nanoemulsions can be diluted with water without changing the droplet size distribution **[19]**. Finally, nanoemulsions are metastable (unstable but relatively long-lived). Because of their small droplet size, Brownian motion prevents sedimentation or creaming, hence offering increased stability **[19]**.

Nanoemulsion formation requires energy input, generally from mechanical devices or from the chemical potential of the components **[20]**. The methods using mechanical energy are called dispersion or high-energy emulsification methods. The high-energy input is generally achieved by means of high-shear stirring, high-pressure homogenizers or ultrasound generators (Figure 1.15). In the dispersing zones of these machines high shear stresses are applied to deform and disrupt large droplets **[21]**. A procedure to make emulsion with intermediate energy consumption (Figure 1.15) is membrane emulsification, a promising way to produce such systems with narrow size droplet distributions **[22]**. Finally, the methods that make use of the chemical energy stored in the components are referred to as condensation or low-energy emulsification methods. These techniques take advantage of the phase transition occuring during the emulsification process **[15]**.

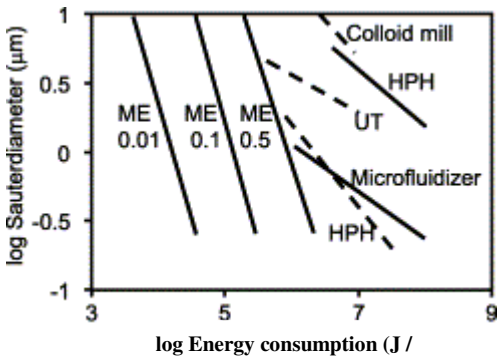

Figure 1.15: Droplet diameter as a function of the energy consumption p supplied by different types of equipment [22]

ME: cross-flow membrane emulsification, numbers denote the dispersed phase fraction; HPH: high-pressure homogenizer; UT: Ultra Turrax. Solid lines reprinted from **[23]**, dashed lines reprinted from **[24]**.

The major source of instability of nanoemulsions is Ostwald ripening **[3]**. The larger droplets grow at the expense of the smaller ones. As a consequence, the more monodispersed the droplets are, the less the nanoemulsions will be affected by Ostwald ripening **[3].** Thus, it is important to find a way to produce nanoemulsions with a narrow size distribution as it could prevent Ostwald ripening. Besides, droplet size and droplet size distribution are the main factors influencing the properties of the product such as rheology, appearance, chemical reactivity, stability and physical properties **[25]**.

1.2- High-energy emulsification techniques

For large-scale production, conventional emulsification devices such as colloid mills, high-pressure homogenizers and ultrasonic transducers are generally used. They often involve inhomogeneous extensional and shear forces and high energy input per unit volume so as to rupture droplets. These methods usually generate emulsions with small mean droplet sizes but wide droplet size distributions.

1.2.1- Why is an important amount of energy needed?

Breaking up droplets requires a significant amount of energy because the deformation of the droplet is opposed by the Laplace pressure. The Laplace pressure p_L is the difference in pressure between the two sides of a curved interface and is given by:

$$p_L = \gamma\left(\frac{1}{R_1}+\frac{1}{R_2}\right) \qquad \textbf{Equation 1.1}$$

where γ is the interfacial tension and R_1 and R_2 are the principal radii of a curvature. In order to break up a spherical droplet of radius 0.2 μm with interfacial tension of 0.01 N m^{-1}, a stress must overcome a Laplace pressure of 10^5 Pa **[13]**. The net energy consumption per unit volume of emulsion is given by:

$$p = \int \varepsilon(t)dt \qquad \textbf{Equation 1.2}$$

where t is the time during which emulsification occurs and ε is the power or energy density in W m^{-3} (average amount of energy per unit time and unit volume of the emulsion). Break-up of drops will only occur when ε is high, which means that energy dissipated at low ε levels is wasted **[26]**. The residence time in the dispersing zone also influences the resulting size of emulsion droplets **[27]**.

Batch processes will generally be less efficient than continuous ones, since it is difficult to produce a high value of ε throughout the whole apparatus. For example, in a large vessel, a stirrer will dissipate most of the energy applied at low energy intensity level. Hence, the energy will not be used to deform the droplets. Moreover, the larger the vessel relative to the stirrer, the longer the process must last before all

the emulsion droplets have finally been broken up into small ones. **[26]**. Finally, a poor reproducibility of the emulsions is observed from batch-to-batch even when similar experimental conditions are deployed **[28]** which must be a consequence of the inhomogeneity of the flow.

High-energy emulsification devices have a main drawback: a significant waste of energy. Indeed, most of the energy is used as heat rather than in effectively producing the droplets **[29]** since the energy density does not overcome the Laplace pressure at all times and everywhere in the tank. Walstra illustrated this with the following example **[13]**: the preparation of an emulsion of oil droplets with a radius of 1 μm and a volume fraction of 0.1. The interfacial tension was 0.01 N m^{-1}. The calculated net surface energy needed to create the emulsion was 3 kJ m^{-3}. But in practice, it needed about 3 MJ m^{-3}. Another disadvantage of the high energy inputs is the impossibility to use shear-sensitive ingredients as they may lose their functional properties **[21]**.

1.2.2- Colloid mill or rotor-stator device

Colloid mills are used to reduce the particle size of one phase suspended in a liquid. The phase can be of any state e.g. gaseous, liquid or solid **[30]**. They are widely used in the food industry for example in the preparation of mayonnaise, ketchup, mustard or salad dressing and in the pharmaceuticals and cosmetics field where they are useful for making lipsticks or creams for instance.

In the following paragraph, the mixing of 2 liquid phases, that is to say the process of emulsification, will be looked at in more details. In a colloid mill, the droplets of a coarse emulsion prepared by stirring are broken up by shear stresses in the small space between the rotor and the stator (Figure 1.16).

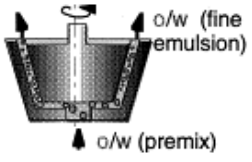

Figure 1.16: Colloid mill [27]

Colloid mills are particularly suitable for producing emulsions with a continuous phase of medium to high viscosity. A narrow droplet size distribution is obtained if the energy density in the space between rotor and stator is well controlled. In a colloid mill, the highest shear stress attainable is about 10^4 Pa **[26]** with energy consumption up to 10^7 J m^{-3} (Figure 1.15). The minimum droplet sizes are around 1 μm **[22]**.

1.2.3- High-pressure homogenizer

High-pressure homogenization is used for the production of beauty creams, lotions, nail varnishes, shampoos, toothpastes, and emulsions containing different oils. In a high-pressure homogenizer, a coarse emulsion is pushed with high pressure (100-2000 bar) through a narrow gap in the range of a few microns (Figure 1.17). The droplets are broken up in the nozzle by turbulence and cavitation and their size can be reduced down to 0.1 μm **[22]**. High pressure homogenizers are the most widely used devices to make nanoemulsions **[15]**.

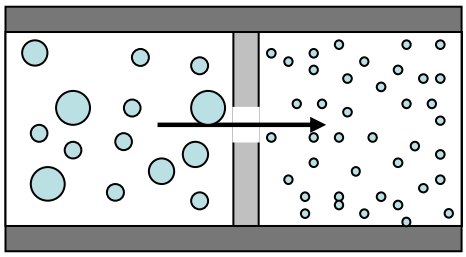

Figure 1.17: High-pressure homogenizer schematic

Cavitation is the phenomenon of formation, followed by a rapid collapse, of cavities. Whenever the instantaneous pressure at a point in a liquid becomes negative, the liquid ruptures at that point, giving a void filled either with the vapour of the liquid or with the gases that are dissolved in the liquid. The collapse of such voids results in a strong shock wave on a microscale **[31]**. This phenomenon leads to the formation of very fine but polydispersed droplets. In the process of homogenization the particle size is reduced to such an extent that Brownian motion is

sufficient to prevent the creaming action. In a high-pressure homogenizer, the energy density ε may be as high as 10^{12} W m^{-3} and the energy consumption p can go up to 10^{8} J m^{-3} **[26]**.

1.2.4- Ultrasonic devices

The ultrasonic range of frequencies lies above the limit of audibility (20 kHz) right up to several gigahertzes. Emulsification is feasible only below about 5 MHz s^{-1}.

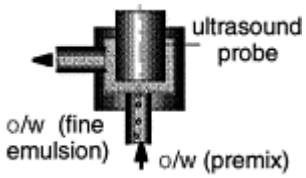

Figure 1.18: Ultrasound emulsification [27]

Several devices can be used to convert electrical energy into mechanical vibrations (Figure 1.18): piezoelectric transducers, magnetostriction transducers, electromagnetic generators, liquid jet generators. The latter is very popular in industrial emulsification **[31]**. In a liquid jet generator, a vibrating blade breaks the liquid into small droplets due to vigorous cavitation **[27]**.

Ultrasound is a very efficient way for reducing the droplet size but can only be used for small quantities. As a consequence, it is more frequently used at lab scale. A liquid jet generator uses less pressure than a homogenizer. As a consequence, it consumes less energy than ordinary homogenizers for the preparation of emulsion droplets with the same size. A typical energy consumption is around 10^{7} J m^{-3} **[26]**. Ultrasonic devices allow the preparation of very small droplets (around 0.1 μm) but the relative width of the size distribution is large. Ultrasonic methods have one particular feature: the possibility to obtain concentrated (30 % (v / v)) highly dispersed emulsions without the use of any surfactant **[31]**.

1.2.5- Improvement by formulation engineering

A better understanding of the chemical system and optimum composition could be a way to decrease the size of the droplets, enhance their stability and reduce the consumption of energy **[32]**. A procedure called concentrate demulsification enables the production of a highly concentrated O / W emulsion (internal phase = 70 % (v / v)) by means of a low speed mechanical mixing. It is then possible to dilute the emulsion to the required concentration **[33]**.

1.3- Intermediate-energy consumption technique: Use of membranes

1.3.1- Direct membrane emulsification

The membrane emulsification technique was first proposed by Nakashima *et al.* **[34]** in 1991. Since then, this technique has seen an increasing interest as it presents a number of advantages. Indeed, this method requires little quantity of surfactants **[35]** and in spite of a low energy consumption, it could have the potential to produce monodispersed emulsions of very fine droplets **[22]**. Moreover, membrane emulsification could be achieved with shear-sensitive systems **[36]**.

1.3.1.1- Principles of droplet formation

To prepare emulsions by membrane emulsification, the phase to be dispersed is pressed into a continuous phase through a porous membrane using a low transmembrane pressure ΔP_{tm} (Figure 1.19) **[34]**. The transmembrane pressure is defined as the difference between the pressure of the dispersed phase P_d and the mean pressure of the continuous phase P_c:

$$\Delta P_{tm} = P_d - \frac{(P_{c,1} + P_{c,2})}{2} \qquad \textbf{Equation 1.3}$$

where P_d is the pressure of the dispersed phase outside the membrane, $P_{c,1}$ and $P_{c,2}$ are respectively the pressures at the inlet and outlet of the membrane module.

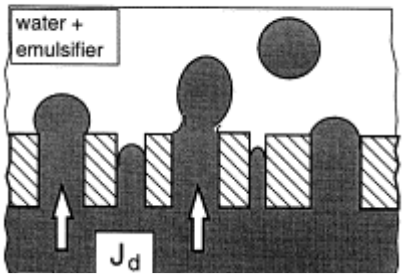

Figure 1.19: Membrane emulsification schematic [37]

Using this technique, several types of emulsions can be obtained ranging from the simple oil-in-water (O / W) or water-in-oil (W / O) to multiple emulsions like W / O / W **[38]** depending on the type of continuous and dispersed phases utilized.

Droplets are produced at the pore openings. They grow at the membrane surface until they reach a certain size at which point they are detached **[39]**. A great number of interactions occur during the droplet formation and many parameters have to be taken into account to understand the droplet formation. The particular influence of the membrane material will be discussed in more details in the next paragraph.

1.3.1.2- Membrane material

Many papers reported that the characteristics of the membrane material have an important impact on the resulting emulsions. Indeed, the droplet size is directly influenced by the pore size of the membrane. For example, it has been shown that with Shirasu Porous glass, the average droplet could be related to the average by a linear relationship:

$$d_{droplet} = c\, d_{pore} \qquad \textbf{Equation 1.4}$$

where $d_{droplet}$ is the average droplet diameter, d_{pore} the average pore diameter of the SPG membrane and c a constant for particular conditions. The values of c are

typically ranging from 2 to 10. Therefore, the smaller the pore size, the smaller the droplets **[34, 40]**.

The polydispersity of the membrane pores was also shown to have an effect on the size of the droplets since the coarse pores tend to produce droplets preferentially **[40]**. As a consequence, a monodispersed emulsion can be obtained only if the membrane pore size distribution is sufficiently narrow **[41]**. In order to work with any desired pore size and to avoid the problem of pore polydispersity, microengineered membranes **[42, 43]** and microchannels **[44, 45]** have been fabricated. Microchannel emulsification allows the formation of very monodispersed emulsions because the pore size is well controlled, but usually results in larger droplets than membrane emulsification.

Finally, it must be noted that membrane characteristics are not sufficient to determine the final droplet size and size distribution (Table 1.1). Indeed, there are many other process parameters involved in the formation of droplets such as the nature of the dispersed and continuous phases, the choice and concentration of the surfactant **[46]**, the transmembrane pressure **[47]**, the possible use of a cross flow **[42, 48]**.

Table 1.1: Direct ME results found in the literature ranked in the base of droplet size

Ref.	Membrane Material	Dispersed Phase	Continuous Phase	d_{pore} in µm	$d_{droplet}$ in µm
[29]	Ceramic	Mineral oil	Water	0.2	0.56
[35]	α-Alumina	Vegetable oil	Skimmed milk	0.5 & 0.2	> 1
[38]	Al_2O_3-SiO_2	Soya bean oil	Water	0.36	1.07
[49]	SPG	Rapeseed oil	Water	0.4	1.4
[46]	Aluminium Oxide	Vegetable oil	Water	0.2	~2
[50]	SPG	Corn oil	Water	0.57	2.66
[51]	Sol-Gel Silica	Aqueous colloidal silica	Toluene	0.6	3
[44]	α-Al_2O_3	Rapeseed oil	Water	1.4	3.5
[36]	SPG	Sunflower oil	Water + skimmed	0.2	5

			milk powder		
[52]	SPG	Corn oil	Water	1.1	5.48
[53]	SPG	Rapeseed oil	Water	5	15

1.3.2- Modification of emulsion features by means of a membrane

A number of papers have reported the utilization of membranes to change the properties of pre-existing emulsions. To achieve this, two different methods have been used: membrane filtration **[54, 55]** and premix membrane emulsification **[56]**. The first technique simply uses the membrane as a sieve through which only the smaller droplets will go **[57]**. As a result, one will obtain a permeate containing a smaller mean droplet size and a narrower distribution. In premix membrane emulsification, the whole emulsion is pushed through the membrane. Thus, the preformed droplets will be forced to deform and eventually break into smaller ones in order to reach the other side of the membrane. These two processes have a common drawback: a high tendency for rapid fouling of the membranes **[33, 58]**.

1.4- Low-energy emulsification methods

Submicron emulsions can be obtained by exploiting the physicochemical properties of the system. These methods are generally referred to as low-energy emulsifications. The Ouzo effect relies on the homogeneous nucleation of the oil droplets **[59]**. Phase inversion methods make use of the spontaneous curvature change of the surfactant **[15]**.

1.4.1- The Ouzo effect

When water is added to Ouzo, an alcoholic Greek drink, the anise oil dissolved in the Ouzo spontaneously nucleates into many small droplets **[59]**. Indeed, when water is added to a dilute binary solution of a solute, whose solubility in water is very small (e.g. anise oil), in a water-miscible solvent (e.g. ethanol), most of the solute will rapidly come out of solution as it becomes greatly supersaturated, which results in the nucleation of droplets **[60]** (Figure 1.20). This phenomenon has been termed "the Ouzo effect" **[59]** and has proved to lead to the formation of droplets with diameters as small as 200 nm (**[61]** as cited by **[60]**).

The Ouzo effect can be used to create metastable liquid-liquid dispersions without the addition of surfactants, stabilizers, or any form of mechanical agitation **[59]**. Of course, surfactants can be mixed with the aqueous phase prior to emulsification as it enhances the stabilization of the emulsions **[60]**.

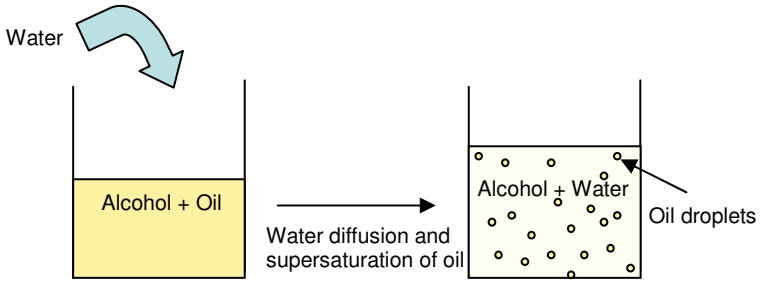

Figure 1.20: The Ouzo Effect

However, this technique for producing nanoemulsions presents some drawbacks. First, only a very low oil content can be dispersed. Indeed, it has been shown that the droplet diameter is a function of the ratio of excess oil to ethanol, which means that to obtain small droplets, the initial amount of oil must be very low. Secondly, the Ouzo effect has to be applied to specific systems where the solvent must be soluble in water in all proportion **[60]**. Finally, the removal of solvent might be a limitation **[15]**.

1.4.2- Phase inversion emulsification

Phase inversion in emulsions can be of two types: catastrophic phase inversion (CPI) and transitional phase inversion (TPI) **[3]**. Emulsions are called normal when the emulsifier is more soluble in the continuous phase. They are called abnormal if the emulsifier is more soluble in the dispersed phase. Abnormal emulsions are highly unstable. They can only be maintained in this state under vigorous mixing and for a short period of time **[62]**. A catastrophic phase inversion occurs between a normal emulsion and an abnormal one whilst a transitional inversion is a process happening between two normal emulsions **[63]**.

The CPI technique is often used when a very viscous oil needs to be dispersed. In most cases, it consists in adding water little by little to the oil phase in which a hydrophilic surfactant was initially dissolved or dispersed. At first, an abnormal W / O emulsion is prepared **[64]**. The rate of water droplet coalescence increases greatly as the water fraction in the emulsion gets higher. After a certain amount of water is added, the balance between the rate of droplet coalescence and the rate of droplet break-up (i.e. droplet formation) cannot be maintained anymore and the abnormal emulsion switches irreversibly to a normal O / W emulsion **[62]**.

Contrary to catastrophic phase inversion, transitional phase inversion is a gradual process. The shift in the continuous phase occurs due to a continuous change in the affinity of the surfactant toward the dispersed phase. This process is reversible i.e. the initial state of the emulsion can be restored if the change in the variable is reversed **[64]**. TPI enables the preparation of nanoemulsions **[65]** and can be induced by factors such as temperature, salt concentration or pH **[66]**. Within a limited range of HLB, it can also occur by changing the oil-water ratio at a constant temperature. This latter technique is known as the Emulsion Inversion Point (EIP) method **[67]**.

In order to prepare nanoemulsions, the Emulsion Inversion Point (EIP) and Phase Inversion Temperature (PIT) methods are the most commonly used **[68]**. They are described in more details in the following paragraphs.

1.4.2.1- The EIP Method

In this method, change in the spontaneous radius of curvature is obtained by changing the composition at constant temperature. By adding water into oil / surfactant mixtures, water droplets are first formed in a continuous oil phase. With the increase in the water volume the spontaneous curvature of the surfactant changes from stabilizing a W / O emulsion to an O / W emulsion via the Emulsion Inversion Point (Figure 1.21) **[65]**.

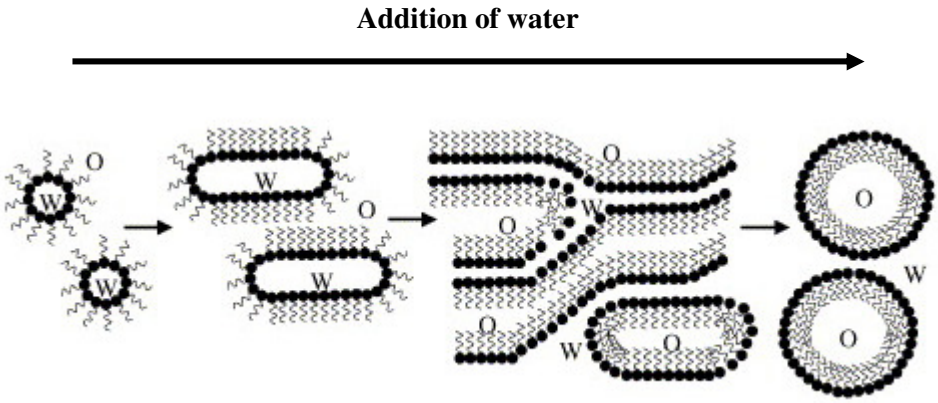

Figure 1.21: Scheme of the EIP emulsification procedure [65]

At the EIP, the affinity of the surfactant toward both phases is balanced and a microemulsion phase or lamellar liquid crystal with possible excess water and oil forms (Figure 1.22). The interfacial tension reaches a minimum and the system crosses a point of zero spontaneous curvature **[15]**. When the system is further diluted with water, this structure break up into a O / W nanoemulsion.

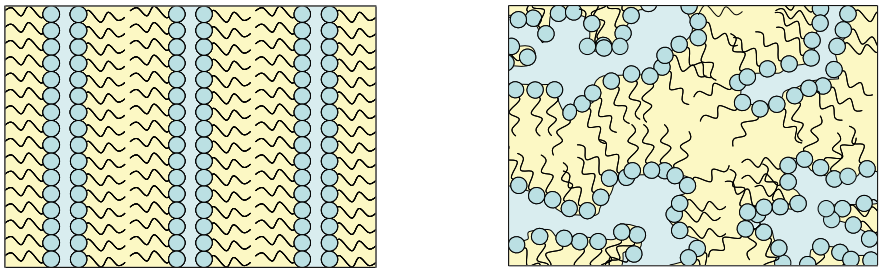

Figure 1.22: Lamellar (left) and bicontinuous (right) surfactant structures

Nanoemulsions using the EIP method are obtained depending on the order of addition of components and if the water to oil ratio is over a certain value, which can be determined with a phase diagram. Above this value, excess of water may be added without any affect on the droplet size. A critical surfactant concentration is necessary for the preparation of submicrometer-sized droplets as the oil has to be solubilized completely at the EIP **[65]**. Besides, the resulting size distribution mainly depends on the surfactant to oil ratio, suggesting that the size of the droplets is governed by the structure at the inversion point **[65]**.

The group of Forgiarini *et al.* has reported the preparation of O / W nanoemulsions with average droplet size of 50 nm in the system water / $C_{12}E_4$ / decane. **[5]**. Sadurní *et al.* managed to prepare water / non-ionic surfactant (Cremophor EL) / oil (Mygliol 812) nanoemulsions with droplet sizes from 14 to 39 nm **[17]**. Following the same method, Usón *et al.* made W / O nanoemulsions with droplet sizes ranged between 60 and 160 nm, by adding oil to mixtures of water and surfactant **[20]**. Stability studies showed that the breakdown of the nanoemulsions was due to Ostwald ripening and coalescence mechanism, depending on the final compositions **[69]**.

1.4.2.2- The PIT method

The Phase Inversion Temperature (PIT) method was introduced by Shinoda *et al.* **[70]**. They used non-ionic ethoxylated surfactants whose properties at the droplet interface are highly dependent on temperature. These surfactants are subjected to the dehydration of the polyethyleneoxide chain with increasing temperature **[71]**. As a consequence, the surfactants get more lipophilic. Mixtures of oil, water and surfactant are prepared at their Phase Inversion Temperature (PIT), also referred to as hydrophilic-lipophilic balance (HLB) temperature, which is the temperature for which the affinities of the surfactant for water and oil are balanced

[72]. Then, the solutions are quickly heated or cooled in order to obtain water-in-oil (W / O) or oil-in-water (O / W) emulsions respectively **[19]**.

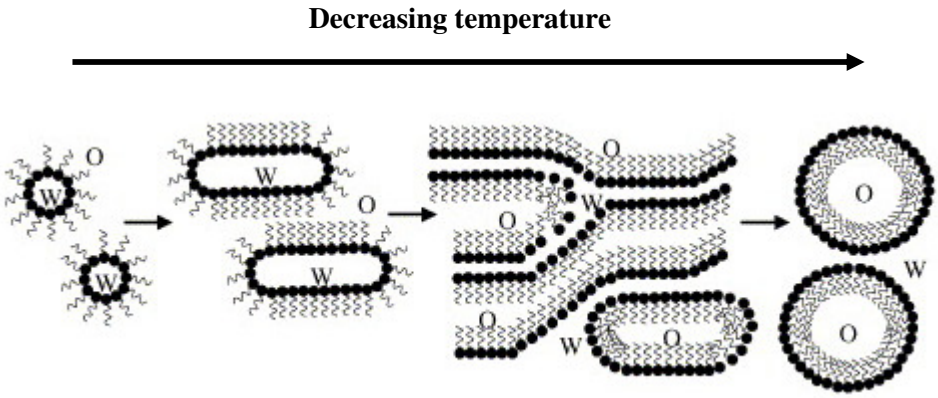

Figure 1.23: Scheme of the PIT emulsification procedure [65]

Indeed, at low temperature, O / W macroemulsions can be formed and are quite stable as the surfactant has more affinity with the aqueous phase. On increasing the temperature, the O / W emulsion stability decreases and the macroemulsion finally resolves at the HLB temperature (both O / W and W / O emulsions are unstable). In this temperature zone, the interfacial tension reaches a minimum and the system crosses a point of zero spontaneous curvature. At higher temperature, W / O emulsions become stable. By preparing the emulsion in the region of the PIT and proceeding with rapid cooling (or heating), the system is subjected to a transitional inversion and nanoemulsions may be produced (Figure 1.23).

HLB temperatures can be measured with conductimetry, by gradually increasing the temperature until a conductivity jump is produced **[73]**. They can also be determined by visual observation of phase separation **[19]**. The PIT value depends on the phase volume ratio, the nature of the oil, and the type of surfactant **[72]**. If the surfactant is monodistributed, then the PIT is independent of its concentration. Commercial surfactants usually display a certain polydispersity in the number of ethylene oxide groups. Since the most ethoxylated surfactants impose their behaviour

at the interface **[74]**, the HLB temperature increases with decrease in concentration of these commercial surfactants **[64]**. This effect becomes less important at high surfactant concentration.

Generalized by the surfactant affinity difference (SAD) concept **[65]**, the PIT method can be applied using other parameters rather than the temperature. Salt concentration or pH value may be considered as well **[66]**. These latter techniques have some advantages over their thermal counterpart since they do not require a temperature-sensitive surfactant and would not result in eventual thermal degradation. However, these changes can often be applied in one direction only. For example, increasing salinity can easily be obtained by adding a small amount of concentrated brine whilst decreasing it would considerably change the overall emulsion composition **[64]**.

As for the EIP emulsification, the size of the nanoemulsion droplets is governed by the surfactant structure (bicontinuous or lamellar (Figure 1.22)) present at the phase inversion point **[75]**. One of the main requirements for the formation of O / W nanoemulsions with the smallest droplet size is to achieve a complete solubilization of the oil phase at the HLB temperature **[19]**; if there is water in excess, it acts as a dilution medium for the dispersed oil droplets **[15, 65]** and vice-versa if the preparation of small droplets of water in oil is desired. Temperature cycling around the PIT might also improve the size of the nanoemulsion droplets because it increases the concentration of amphiphiles that get trapped in the interfacial region **[76]**.

Another parameter to take into account for the successful preparation of fine nanodroplets is the rate of cooling or heating. If the cooling or heating process is not fast enough, coalescence predominates and polydispersed coarse emulsions are formed **[77]**. It was also shown that relatively stable O / W type emulsions are obtained when the PIT of respective systems are about 20 to 65 °C higher than the storage temperature **[70]**. Finally, the stability of the nanoemulsions decreases with the increase in oil solubility in the continuous phase, as it results in an increase in the oil diffusion rate and therefore enhances Ostwald ripening.**[18]**.

Nanoemulsions with a droplet size in the range 50-130 nm have been obtained in the system water / polyoxyethylene lauryl ether (abbreviated as $C_{12}E_4$ for the 12 C in the carbon chain and an average of 4 mol of ethylene oxide per surfactant molecule) / hexadecane at 20 wt % oil concentration and at concentration of surfactant higher than 3.5 wt % by the group of Izquierdo *et al.* **[18]**. Morales' team managed to prepare O / W nanoemulsions with droplet sizes as low as 40 nm in the system water / hexaethylene glycol monohexadecyl ether ($C_{16}E_6$) / mineral oil **[19]**.

1.5- Conclusion and objectives

Nanoemulsions when in suspension in water have the potential to be transparent and very stable which make them particularly attractive for the customer. To obtain this transparency and good stability, the droplets must not only be in the nanosize range but also have a size distribution as narrow as possible, since Ostwald ripening is the main source of instability for nanoemulsions. Rotor-stator devices, high-pressure homogenizers and ultrasound generators are the most commonly used techniques enabling formation of colloids in the nanosize range. They require a high-energy input and do not achieve the preparation of very monodispersed particles. Membrane emulsification, an alternative technique with moderate energy consumption, allows the preparation of systems with narrow size distributions. The droplet formation at the membrane surface is influenced by many interactions and an important number of parameters have to be controlled in order to achieve successful production of nanoemulsions. Finally, the low-energy emulsification methods enable the preparation of very small droplets without energy input since they rely on the chemical energy stored in the components. However, these techniques can only be applied to a few emulsion formulations. For example, in order to produce nanoemulsions using the phase inversion temperature process, non-ionic ethoxylated surfactants need to be used.

Nanoemulsions can be used as a potential delivery system for bioactive compounds for application in personal and health care, cosmetics and food products **[2, 3]**. Indeed, it is possible to add lipophilic drugs or vitamins in the oil droplets

[78]; their small sizes can enhance the penetration of actives in specific site of action such as the skin or the digestive system **[79, 80]**. Nanoemulsification techniques can also enable the preparation of nanoparticles. They either involve the polymerization of monomer nanoemulsions or are based on the nanoemulsification of preformed polymers **[81-83]**. The aim of the project is to produce monodispersed nanoemulsions (20-40 nm) using low-energy methods and, as much as possible, with low-toxicity components since it would be desirable to use these new systems in the preparation of food or health care products. In order to improve time efficiency and reduce the cost of production, developing a method of preparation of nano-emulsions based on continuous emulsification is also considered.

Phase Inversion Temperature emulsification is a low-energy technique already widely used in industry **[84]**. It is an advantageous method since the only basic equipment required to prepare nanoemulsions is a heat source. As a consequence, it should be relatively rapid to gather data about the chosen system. PIT emulsification is a technique to create nanoemulsion that has often been described as a batch process. To the author's knowledge, only the group of Yoshizawa *et al.* have used a set-up that combined a microfluidic device and the phase inversion temperature emulsification in order to prepare monodispersed dodecane nanoemulsions continuously **[85]**. The following thesis reports an attempt to create a PIT emulsification machine working in continuous flow to reproduce the results of the batch method on food-grade oil emulsions. In order to identify the requirement for the building of the rig, it is essential to understand the process of PIT on the chosen emulsion system with the traditional batch method. Once the main parameters for a successful emulsification are gathered, an experimental set-up can be designed and built. Then, experiments are performed with the new continuous set-up to determine if the desired emulsions can be obtained.

Chapter 2 - Materials and Methods

2.1- Reagents

Hexadecane $CH_3(CH_2)_{14}CH_3$ (99 %, Aldrich) and soya bean oil from *Glycine max* (Fluka) were used without further purification as the oil phase. The major unsaturated fatty acids in soya bean oil triglycerides are linolenic acid, C-18:3; linoleic acid, C-18:2; and oleic acid, C-18:1.

Brij 30, Brij 97, Eumulgin B1, Eumulgin B2, Tween 80 and Tween 20 are non-ionic surfactants (Table 2.1). Brij 30 (Sigma) is a technical grade polyoxyethylene lauryl ether with an average of 4 mol of ethylene oxide (EO) per surfactant molecule, also referred as $C_{12}E_4$. Brij 97 (Sigma) is the name given to polyoxyethylene-10-oleyl ether. Eumulgin B1 and B2 (Cognis) were supplied by Unilever Corporate. They are polyethylene glycol of low toxicity with an average number of 12 and 20 ethylene oxides in the polyoxyethylene chain and are also known as Ceteareth-12 and Ceteareth-20. Tween 20 (Sigma) and Tween 80 (Acros Organics) are polyoxyethylene (20) sorbitan monolaurate and polyoxyethylene (20) sorbitan monooleate and are also called Polysorbate 20 and Polysorbate 80 respectively.

Table 2.1: Surfactants used and their characteristics

EO: ethylene oxide group, C: Carbon, HLB: Hydrophilic-lipophilic balance

Product Name	EO number	C chain	HLB value
Brij 30	4	C-12	9.7
Brij 97	10	C-18	12.4
Eumulgin B1	12	Mainly C-16 and C-18	13.4
Eumulgin B2	20	Mainly C-16 and C-18	15.4
Tween 20	20	C-12	16.7
Tween 80	20	C-18:1	15

The water phase consisted of reverse osmosis (RO) water or a sodium chloride solution at a concentration of 10^{-2} mol L^{-1} (purity: SigmaUltra, ≥99.5 %, Sigma-Aldrich).

2.2- Experiments

2.2.1- PIT determination

For each method, the final HLB temperature for a certain composition was taken as the average of two measurements.

2.2.1.1- Determination by conductimetry

Izquierdo *et al.* **[18]** determined the PIT of Hexadecane / $C_{12}E_4$ / Water emulsions using conductimetry measurements. The same method was used here, in order to make a duplicate of their results and test the experimental set-up. 200 mL of emulsion were prepared by simple shaking of the appropriate amounts of sodium chloride solution, hexadecane and Brij 30 at room temperature for 5 minutes.

.

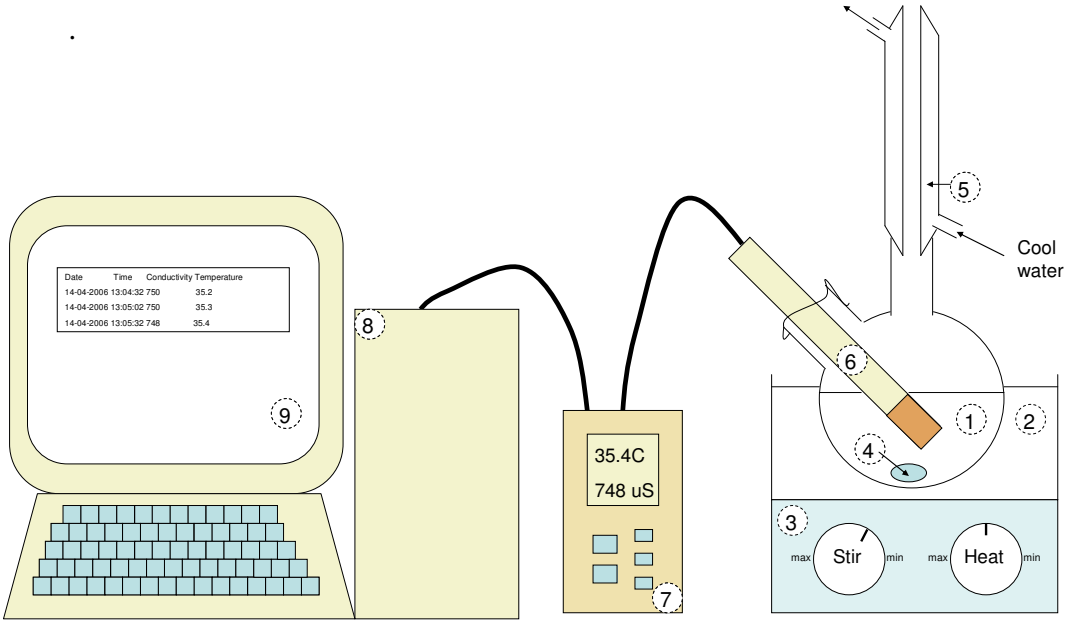

Figure 2.1: Diagram of the PIT determination apparatus

1- bicollar flask containing the emulsion, 2- water bath, 3- heating and stirring plate, 4- magnetic stirrer, 5- condenser, 6- conductivity electrode, 7- conductimeter, 8- computer base unit, 9- data acquisition software display

A conductivitymeter and a conductivity electrode Ultem / Stainless steel (Oakton Con 110 Conductivity / TDS / Meters, Cole-Parmer) were used to measure the conductivity of the emulsion as a function of temperature. The emulsion was stirred continuously with a magnetic stirrer and warmed up using a water bath, and the conductivity was measured simultaneously. To keep systems with the same compositions throughout the experiment, a condenser was used to prevent evaporation (Figure 2.1).

The evolution of the emulsion conductivity with temperature was followed using a Data Acquisition Software (Eutech Instruments). The software also saved the time data, from which the heating and cooling rate of the emulsions was calculated using the following equation:

$$\text{Heating rate at time t} = \frac{T_{t+1\,\text{min}} - T_{t-1\,\text{min}}}{2\,\text{min}} = \text{- Cooling rate at time t} \qquad \textbf{Equation 2.1}$$

where T_t is the measured temperature at time t.

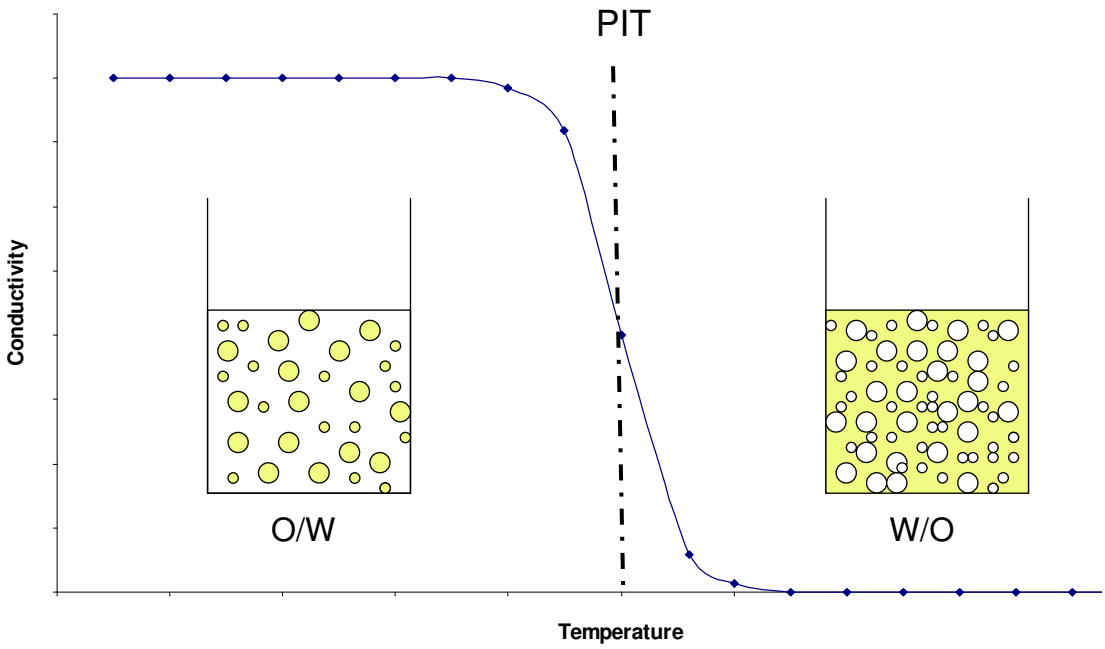

Figure 2.2: Conductivity of an emulsion as a function of temperature for the determination of the PIT

The conductimeter measures the conductivity of the continuous phase. At low temperatures, the emulsion type is oil-in-water (O / W). As a consequence, the conductivity displayed is the conductivity of the water phase. This latter value is rather high (around 800 μS) compared to RO water (around 200 μS) due to the addition of salt. After the Phase Inversion point, the emulsion turns into a W / O. The continuous phase is now the oil, and its low conductivity (approaching 0 μS) is displayed by the conductimeter. This change of conductivity around the PIT is recorded which makes it possible to determine the PIT by taking the average value between the maximum and the minimum values of conductivity (Figure 2.2).

A similar technique was applied to determine the PIT of emulsions Soya oil / Brij 97 / Water. These emulsions had to be stirred a few hours before reaching homogeneity.

2.2.1.2- Determination by turbidity

With this technique, the Phase Inversion Temperature of the emulsions Soya bean oil / Brij 97 / Water was determined by heating slowly the solutions and visually observing the start of turbidity.

2.2.2- Preparation of the nanoemulsions: Batch operation

The required amounts of RO water, soya bean oil and surfactant were stirred to reach homogeneity and then brought to a temperature near the PIT (± 2 °C) using the same experimental set-up as for the determination of the PIT (Figure 2.1) so that the temperature could be monitored versus time. Then, the emulsion was rapidly cooled by immersion in an ice bath or cooled down more slowly by just switching off the heating. During the cooling, the emulsions were continuously stirred. The influences of the heating and cooling rates and the highest and lowest temperatures reached on the appearance and size of the droplets are to be studied. Most of the samples were prepared at least 4 times, to ensure that the results were reproducible. Hexadecane / $C_{12}E_4$ / Water nanoemulsions were prepared similarly.

2.2.3- Preparation of the nanoemulsions: Continuous operation

A rig was designed to produce continuously nanoemulsions using the PIT method (Figure 2.3). It consisted of pumps, a copper coil immersed in an oil bath and a heat exchanger to cool down the emulsions. The rig will be described in more detail in Chapter 4.

Coarse emulsions were prepared with the required amounts of soya bean oil and Brij 97 solution. They were mixed with a magnetic stirrer for at least an hour to obtain an homogeneous mixture. For some experiments, they were homogenized using a rotor-stator homogenizer (T18 Basic Ultra-Turrax) for 10 minutes at 9500 tr min^{-1}.

The coarse emulsions were introduced in the experimental set-up and the resulting emulsions were collected and analyzed. Most of the emulsion samples were prepared at least 4 times, to ensure that the results were reproducible. Different settings of the rig were modified to study their influence on the resulting emulsions.

2.3- Analyses

2.3.1- Transparency measurements

A Unicam 5625 UV / VIS spectrophotometer was used to carry out transparency measurements. Before each use of the machine, a blank had to be done, i.e. RO water was placed in a cuvette and the spectrophotometer was then set on zero.

For the first use of the spectrophotometer, cuvettes were filled with different samples of emulsions prepared with Soya bean oil / Brij 97 / Water with appearances varying from white to transparent in order to find out the most suitable wavelength to work with. It was chosen as the one providing the widest range of absorbance values

for the tested solutions. The spectrophotometer was finally configured at λ = 540 nm in the visible range. It possessed the greatest ability to distinguish the samples.

All the samples were analyzed three times to check the accuracy and reproducibility of the transparency measurement.

2.3.2- Microscope observations

Drops of the different emulsions were placed on petri dishes and observed with a Microscope Diaphat 300 linked to a camera HV-C20. The images were recorded using the Software Image Pro-plus.

2.3.3- Droplet size determination

The mean droplet size and size distribution of the emulsions were determined by photon correlation spectroscopy (PCS) also called dynamic light scattering (DLS). A Zetasizer Nano Series 4S 0.31 Red (Malvern Instruments) was used to carry out the measurements.

Small particles in a suspension move in a random pattern known as Brownian motion. When a coherent source of light (such as a laser) with a known frequency is directed at the moving particles, the light is scattered and its frequency and intensity are changed. This shift in light frequency is related to the size of the particles causing this transformation. Indeed, under the same conditions, the smaller particles have a higher average velocity than the larger ones and as a consequence they cause different shift in the light frequency with the smaller particles producing greater shift than larger particles **[86]**. These short-term intensity fluctuations of the scattered light are used to determine the correlation function $G(\tau)$:

$$G(\tau) = \langle I(t) \cdot I(t+\tau) \rangle \qquad \textbf{Equation 2.2}$$

where $I(t)$ is the intensity of the scattered light at time t

and τ is the delay time.

Size is obtained from this correlation function by using different algorithms **[86]**. In the DTS (Dispersion Technology Systems) Software (Figure 2.3), the mean diameter (Z-average) and the width of the distribution also known as polydispersity index (PdI) were obtained from the cumulants analysis as described in the International Standard on DLS ISO13321 Part 8 **[87]**.

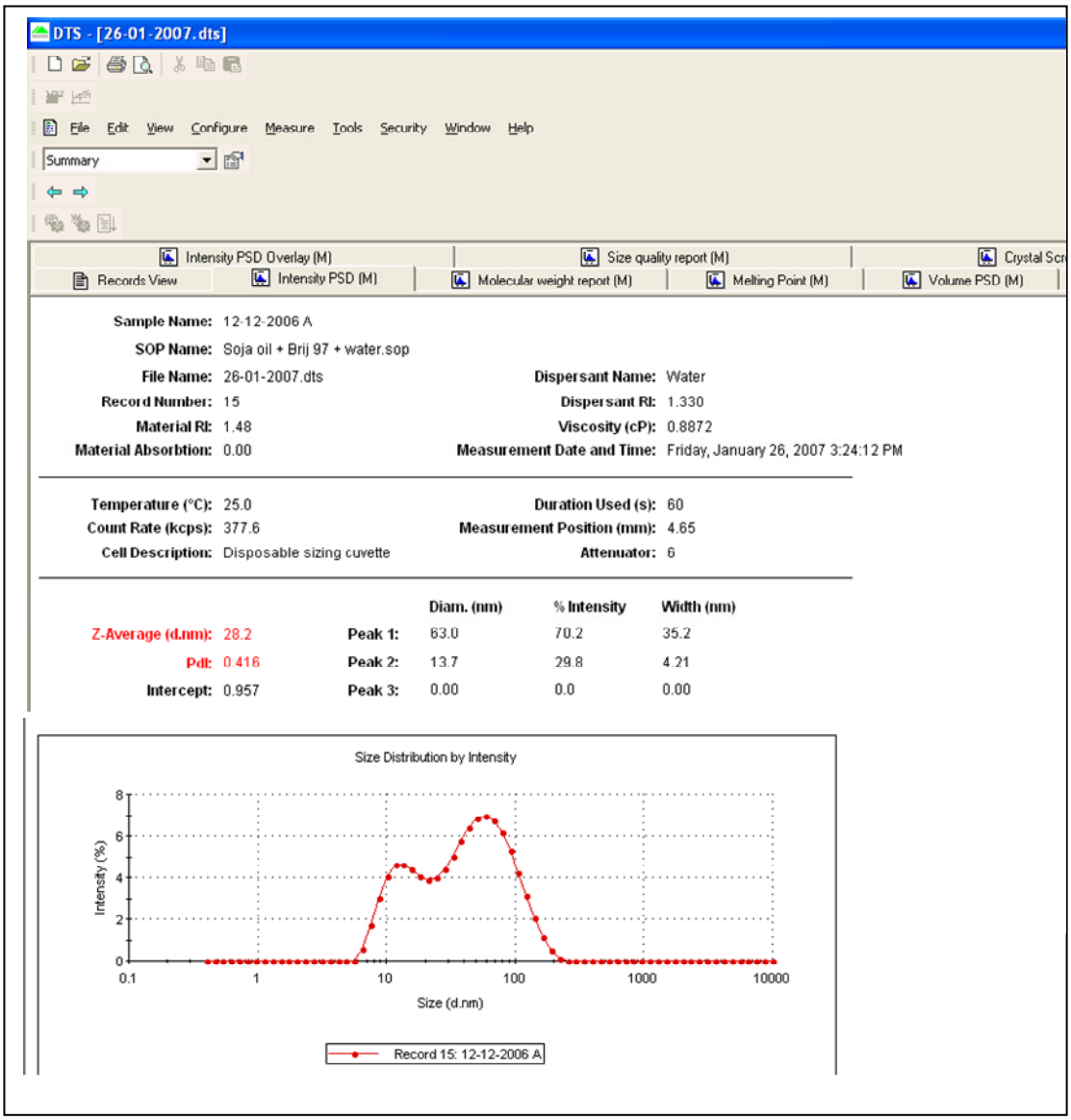

Figure 2.3: Data display of the DTS Data Software

The Z-average and PdI are the data kept for the evaluation of the size and size distribution determinations. The refractive index and viscosity of the dispersant **[88]** are data entered by the user**.**

Z-average and PdI are only comparable with results of other techniques if the sample is monomodal (PdI < 0.1), spherical and monodispersed. For PdI between 0.1 and 0.5, Z-average and PdI can be used to compare results measured in the same dispersant by DLS. For a PdI > 0.5, it is preferable to use another technique to determine the droplet size. It is also important to note that this mean size is an intensity mean and not a mass or number mean since it is calculated from the signal intensity **[87]**.

Dust in the samples is a common source of error, therefore it is very important to make clean samples. Furthermore, the concentration of the samples is also paramount for a successful measurement, as interferences appear when too many particles are present in the sample and the sizes given by the software consequently erroneous. To avoid making this mistake, all the samples were analysed several times with different dilutions to check the reproducibility of the measurements.

Also, the presence of strong interactions between the droplets or particulates can cause problems in interpreting the scattering data, especially in the case of concentrated systems. The studied systems were diluted several times consecutively to ensure that interactions between particles did not interfere with the results produced by the Zetasizer **[89]**.

The analysis was repeated at least 4 times for each sample. The error bars on the size measurement and polydispersity index were represented using the standard deviation of these measurements.

2.3.4- Stability

The emulsions were stored at ambient temperature after preparation. To check their stability, the different analyses presented previously were repeated on the samples 45 days later.

Chapter 3 - Batch emulsification

3.1- Introduction

Chapter 3 should enable to better understand the requirement of the Phase Inversion Temperature (PIT) emulsification. It also allows a first approach of the system that will be studied throughout the rest of this thesis. First tests will be performed with known systems to ensure that the set-up presented in Chapter 2 is functional. Then soya bean oil emulsions made with a selected surfactant are studied.

3.2- Test experiments

In a first attempt to prepare nanoemulsions using the Phase Inversion Temperature emulsification method, it was decided to duplicate the experiments made by Izquierdo *et al.*. **[18]**.

3.2.1- Determination of the HLB temperature

Izquierdo *et al.*. **[18]** conducted a study of emulsions made of Hexadecane / Brij 30 / Water. The following figure (Figure 3.1) shows the result of their conductivity experiments. They used these curves to determine the PIT of different compositions by taking the average value between the maximum and the minimum values of conductivity.

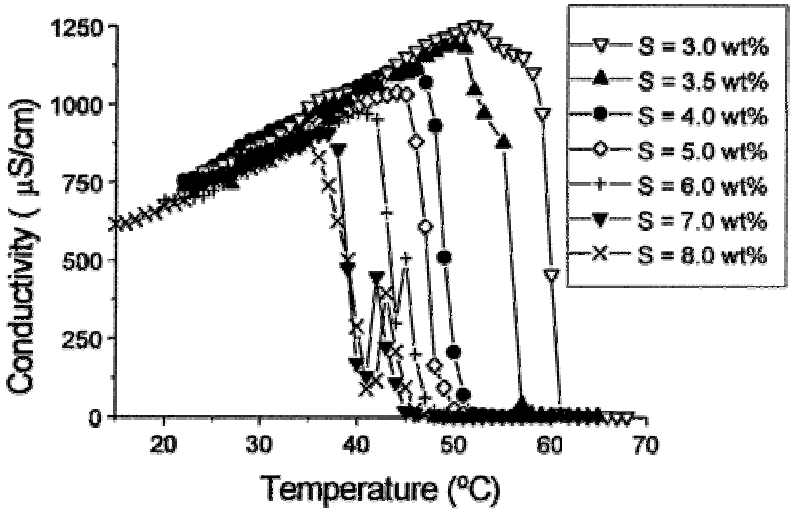

Figure 3.1: Conductivity as a function of temperature in the system aqueous 10^{-2} mol L^{-1} NaCl / $C_{12}E_4$ / hexadecane at different concentrations of surfactants, S, and constant oil concentration (20 % wt) extracted from [18]

Following this example, an emulsion composed of 20 % (w / w) Hexadecane, 5 % (w / w) Brij 30 and 75 % (w / w) 0.01 M NaCl solution was prepared. The following figure (Figure 3.2) presents the variation of the conductivity of this emulsion with temperature.

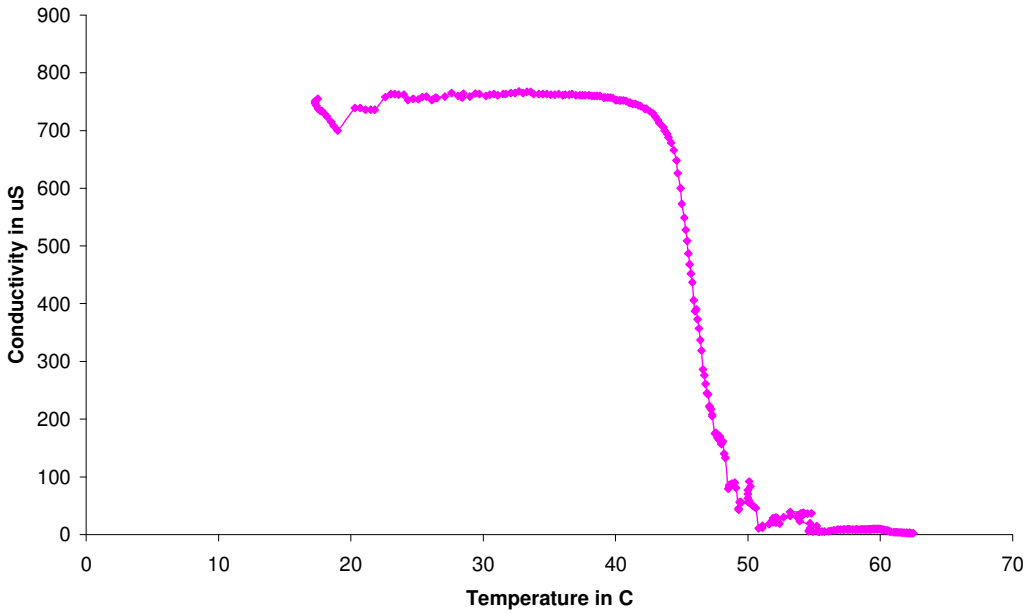

Figure 3.2: Conductivity as a function of temperature in the aqueous system: 20 % (w / w) Hexadecane / 5 % (w / w) Brij 30 / 75 % (w / w) 10^{-2} mol L^{-1} NaCl solution

The group of Izquierdo *et al.*. **[18]** determined for the same system a PIT temperature of 47 ºC. In this experiment (Figure 3.2), if the PIT is determined the same way (i.e. by taking the average value between the maximum and the minimum values of conductivity), the PIT is 46 ºC, one degree Celsius less than the result found by Izquierdo *et al.*. **[18]**. The results obtained with other compositions (Table 3.1) are also in good accordance with the PIT determined by Izquierdo *et al.*. **[18].**

However, the behaviour of the conductivity during the heating is different as there is no increase in conductivity in the present experiment. It could be due to the automatic temperature compensation operated by the Oakton conductimeter. The conductivity of a solution is dependent on the temperature: at high temperature, the electrolytes dissolve more and the ion mobility is more important. The conductivity of a solution therefore increases with temperature. The temperature compensation consists of calculating the conductivity value of a sample at a temperature known as the reference, usually 25 ºC, using the Temperature Coefficient (TC) **[90]**. In this case, this operation is done by the conductimeter automatically. The conductimeter of the group of Izquierdo *et al.*. **[18]** may not have done this compensation.

Table 3.1: Phase Inversion Temperature determined for a number of Hexadecane / Brij 30 / 0.01 mol L^{-1} NaCl solution emulsions

Composition of the emulsions Hexadecane / Brij 30 / NaCl Solution in % (w / w)	***Measured PIT in °C***	***PIT determined by Izquierdo et al.. [18]* in °C**
20 / 3 / 77	56	57
20 / 5 / 75	46	47
20 / 8 / 72	37	41

In this experiment (Figure 3.2), the conductivity measurements are not as smooth as for Izquierdo *et al.*. **[18]**. The formation of foam at the beginning of the heating altered the conductivity measurements up to 30 ºC. At about 50 ºC, the

conductivity is unstable and as a result the determination of the PIT temperature is not precise. Optically, no change was observed in the solution until 50 ºC. It stayed white but the stirring got very difficult around 47 ºC indicating an increase in the viscosity of the emulsion. At 50 ºC, the solution appeared clearly inhomogeneous with a separation in two different phases: one transparent and the other one white.

Figure 3.3: Emulsions 20 % (w / w) Hexadecane / 5 % (w / w) Brij 30 / 75 % (w / w) 0.01 mol L^{-1} NaCl solution

α) biphasic solution - slow heating up to 64 °C, slow cooling,

β) monophasic emulsion - slow heating up to 64 °C, fast cooling.

Above this temperature, the emulsion was divided into two sample bottles to observe the influence of the cooling rate on the appearance of the emulsion. The first half was slowly cooled down whereas the second one was quickly cooled down using an ice bath. The emulsion that was cooled down slowly stayed biphasic whereas the one cooled down quickly turned into a uniform white phase (Figure 3.3).

3.2.2- Droplet size determination

The system 20 % (w / w) Hexadecane / 5 % (w / w) Brij 30 / 75 % 0.01 mol L^{-1} NaCl solution was heated up slowly to 47 °C (Table 3.1) and cooled down rapidly to ambient temperature. The resulting emulsion was a uniform white phase,

similar to emulsion β in Figure 3.3. Its Z-average (mean diameter of the droplets) and polydispersity index (PdI which is a measure of the broadness of the size distribution) were found to be 222 nm and 0.299 respectively using Dynamic Light Scattering.

The group of Izquierdo *et al.*. **[18]** found a droplet radius of 47 nm in the case of the system 20 % Hexadecane / 5 % Brij 30 / 75 % water that had been warmed up to the PIT temperature and rapidly cooled down. These results are very different from the one obtained in the present study. This difference might be due to the batch of Brij 30 used.

3.2.3- Selection of surfactant

Investigation of soya oil emulsions was pursued in this study as this oil can be integrated into food and healthcare products. The continuous phase was water. In order to choose an interesting surfactant for the preparation of a soya bean oil emulsion, the following emulsifiers were tested:

-Eumulgin B1 and Eumulgin B2 (provided by Unilever),

-Tween 20 and Tween 80 (surfactants available in the lab),

-Brij 97 (already mentioned in the literature for its capacity to emulsify soya bean oil **[89, 91]**).

Each system were prepared using 20 % (w / w) of surfactant, 10 % (w / w) of soya oil and 70 % (w / w) water. The components were heated up until their boiling point in a water bath. Contrary to the other systems which remained white throughout the process, those prepared with Brij 97 went through a transparent phase. The emulsions were cooled down by either leaving the mixtures at ambient temperature or by quenching them in an ice bath. The resultant emulsions were unstable with exception of emulsions containing Brij 97. Even when soya oil proportions were lowered to 6 % (w / w), whilst keeping surfactant proportions at 20 % (w / w), no stable emulsions were obtained with any of the emulsifiers but Brij 97.

As for Brij 97 emulsions, those prepared with a slow cooling were stable white and those with a fast cooling were quite transparent. Success in making stable

soya bean oil droplets with Brij 97 probably resides in its structure. Indeed, its hydrophobic chain is comprised of 18 carbons, which confers it a similar chain length as the different triglycerides contained in soya oil **[2]**. As a consequence, Brij 97 is particularly appropriate for the preparation of emulsions with soya oil. However, Brij 97 is an ethoxylated surfactant that is not acceptable for use in food preparations. Even though, it has been used for the formulations of a few pharmaceutical microemulsions **[89, 91]**. Since the preparation of stable emulsions was achieved when using Brij 97, the mixture Soya bean oil / Brij 97 / Water was chosen as the system of study for the project.

3.3- Study of the system Soya bean oil / Brij 97 / Water

3.3.1- Determination of the HLB temperature

To determine the PIT, initial experiments similar to Izquierdo *et al.*. **[18]** were performed. However, the resulting conductivity curves did not always enable the determination of the PIT.

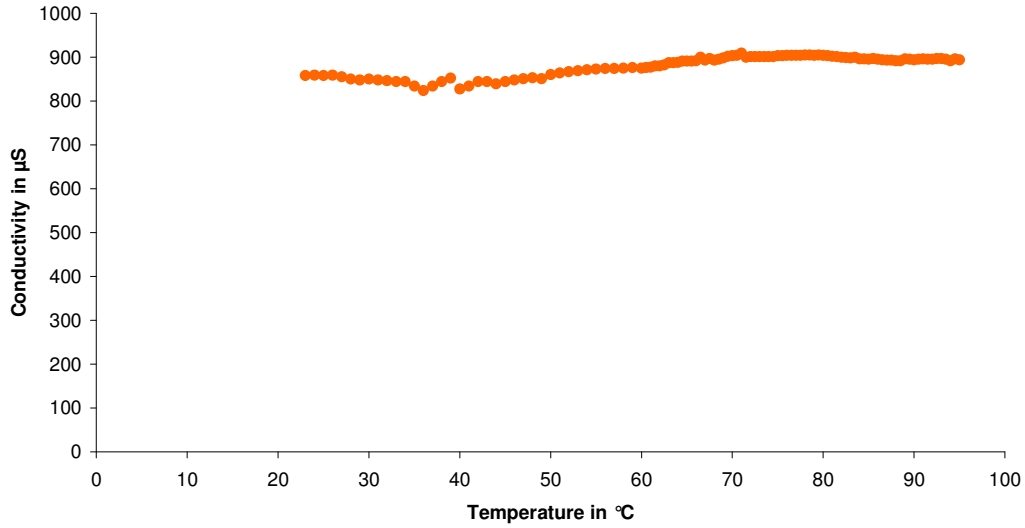

Figure 3.4: Conductivity in function of temperature for the system soya bean oil 5 % (w / w), Brij 97 7.5 % (w / w) and water 87.5 % (w / w)

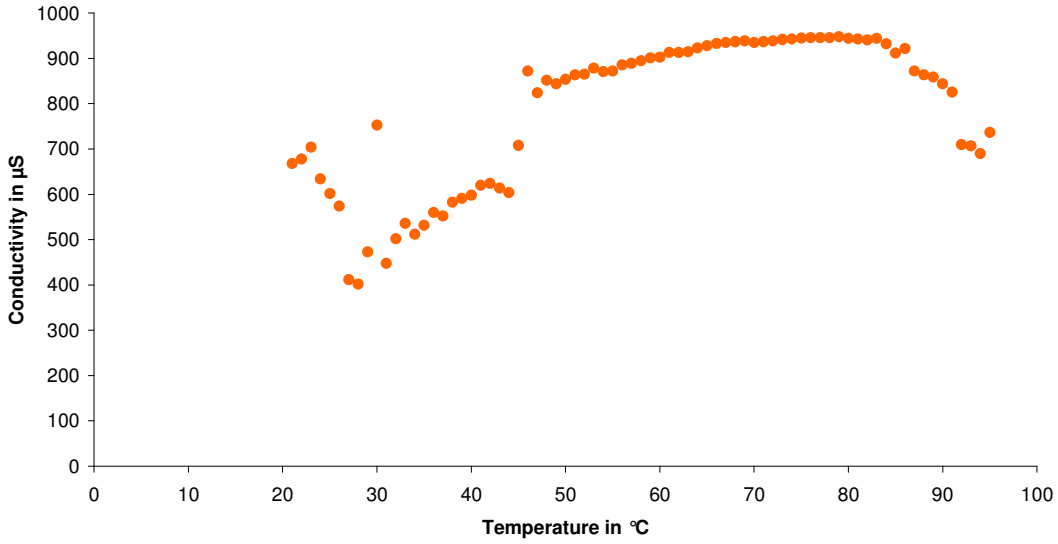

Figure 3.5: Conductivity in function of temperature for the system soya bean oil 10 % (w / w), Brij 97 15 % (w / w) and water 75 % (w / w)

Indeed, the system Soya bean oil / Brij 97 / Water had higher HLB temperatures than the system Hexadecane / Brij 30 / Water presented in Section 3.1. As a consequence, for some compositions, it is not possible to conclude if a HLB temperature exists or not, since the required temperature cannot be reached (Figure 3.4).

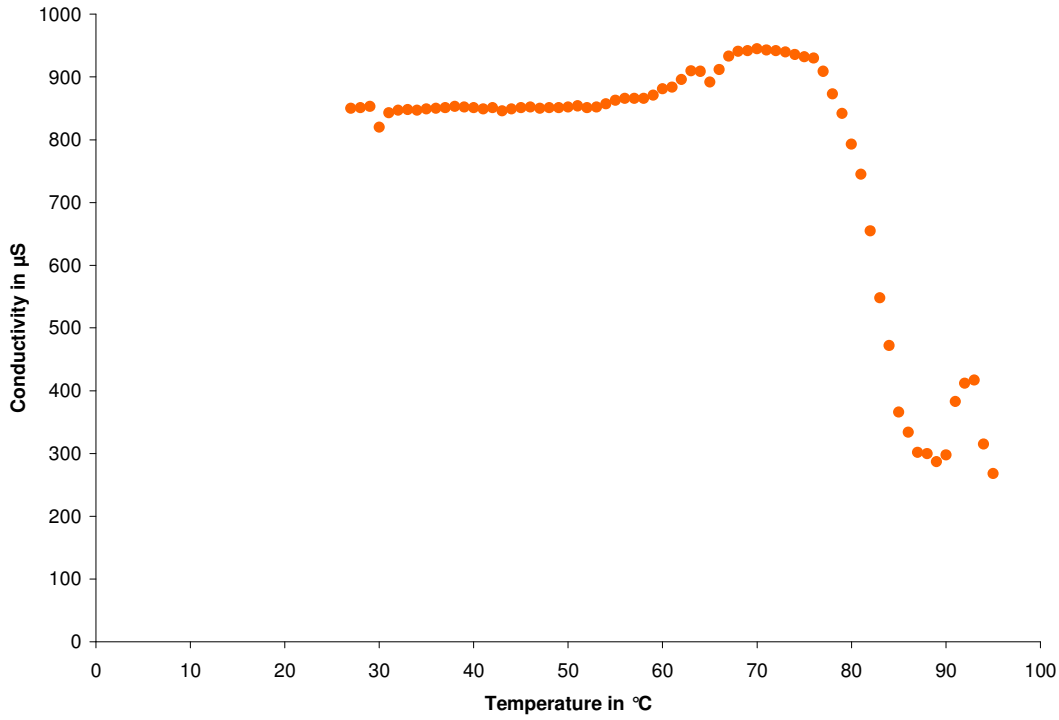

Figure 3.6: Conductivity in function of temperature for the system soya bean oil 5 % (w / w), Brij 97 15 % (w / w) and water 75 % (w / w)

In a few other cases, the fall in conductivity cannot be followed completely since the experiments were stopped at about 95 °C. As a result, an average value between the maximum and the minimum values of conductivity cannot be calculated (Figure 3.5).

Finally, the viscosity of the emulsions was not constant with temperature. Phases of different rheology are probably produced depending on the temperature. Due to this variation in viscosity, the stirring of the emulsions was not maintained constant, and became a source of instabilities for the measurement of the conductivity for some compositions. The beginning of the curve presented in Figure 3.5 illustrates this problem.

The only composition for which it was possible to determine the PIT using the method of Izquierdo *et al.*. **[18]** is presented in Figure 3.6. Its HLB temperature was estimated to be 82 °C. Conductivity experiments do not seem to be adapted for the system Soya bean oil / Brij 97 / Water in view of the low quantity of data obtained using this method.

Table 3.2: PIT evaluated by turbidity onset for different Water / Soya bean oil emulsions in presence of 20 % (w / w) of polyoxyethylene-10-oleyl ether

Soya bean oil concentration in % (w / w)	**PIT in °C evaluated by turbidity onset**	**PIT in °C determined by** [91]	**PIT in °C determined by** [92]
1	68	66.5	53.2
2	70	73	55.6
4	75	74.5	65.6
6	78	78	74

Malcolmson *et al.*. **[91]** and Warisnoischaroen *et al.*. **[92]** also used the PIT method to prepare Soya oil / Surfactant / Water emulsions. They determined the PIT by heating the solutions at a slow rate and noting the beginning of turbidity. Indeed, the HLB temperature is the temperature for which the affinities of the surfactant for

water and oil are balanced and for which the spontaneous curvature is zero **[19]**. Over this temperature, the surfactant is more soluble in the oil phase. As a consequence, the preparation separates in two phases: a W / O emulsion and a water phase. It is thought that the onset of turbidity marks this phase separation. A few experiments with compositions similar to the ones used by these groups were reproduced in order to check the feasibility of this method. The results are shown in the Table 3.2. It can be seen from this table that the HLB temperature increased with the content of soya bean oil.

Table 3.3: PIT determined with the onset of turbidity and the temperature reached at the start of the conductivity jump for different compositions.

- : no value was determined due to the impossibility to make a visual observation of the onset of turbidity

Emulsion composition in % (w / w) (Soya bean oil / Brij 97 / Water)	**Onset of turbidity in °C**
2.5 / 5.0 / 92.5	-
5.0 / 2.5 / 92.5	-
5 / 5 / 90	-
5.0 / 7.5 / 87.5	84
5 / 10 / 85	80
10 / 10 / 80	-
5 / 15 / 80	77
10 / 15 / 75	84
5 / 20 / 75	74
7.5 / 20 / 72.5	82
10 / 20 / 70	88

The results obtained are quite close to those from Malcolmson *et al.*. **[91]**. The significant differences observed when compared with Warisnoicharoen *et al.*. **[92]** might be explained by the inhomogeneities between surfactant batches. It is somewhat unexpected though since this kind of effect would have been more logical in the case of Malcolmson *et al.*. **[91]**. Indeed, Malcolmson *et al.*. prepared their emulsions with polyoxyethylene-10-oleyl ether Brij 96, a previous form of polyoxyethylene-10-oleyl ether Brij 97, not available anymore when the present results were produced. Polyoxyethylene-10-oleyl ether Brij 97 was used in Warisnoicharoen *et al.*. **[92]** and in the present work. After checking the good agreement with the other group researches, other compositions were studied (Table 3.3). From this table, it can be seen that the PIT temperature decreases with the addition of Brij 97.

3.3.2- Preparation of nanoemulsions Brij 97 / Soya bean oil / Water

Emulsions were prepared according to the method presented in Section 2.2.2. For some compositions, the PIT could not be determined. In these cases, the emulsions would be heated up until 95 °C, highest temperature that it was possible to reach.

3.3.2.1- Appearance of the emulsion

As seen in Section 3.2, the appearance of the Soya bean oil / Brij 97 / Water emulsion is sensitive to the rate of cooling. Even though the cooling process could not be controlled with accuracy, it was possible to make some qualitative experiments. It took on average 10 minutes with an ice bath to get an emulsion from the PIT temperature back to the ambient temperature; but without it, this time was increased to approximately 2 hours. The maximum cooling rate obtained for emulsions plunged into the ice-bath varied between 12 and 16 °C min^{-1} depending on the batch.

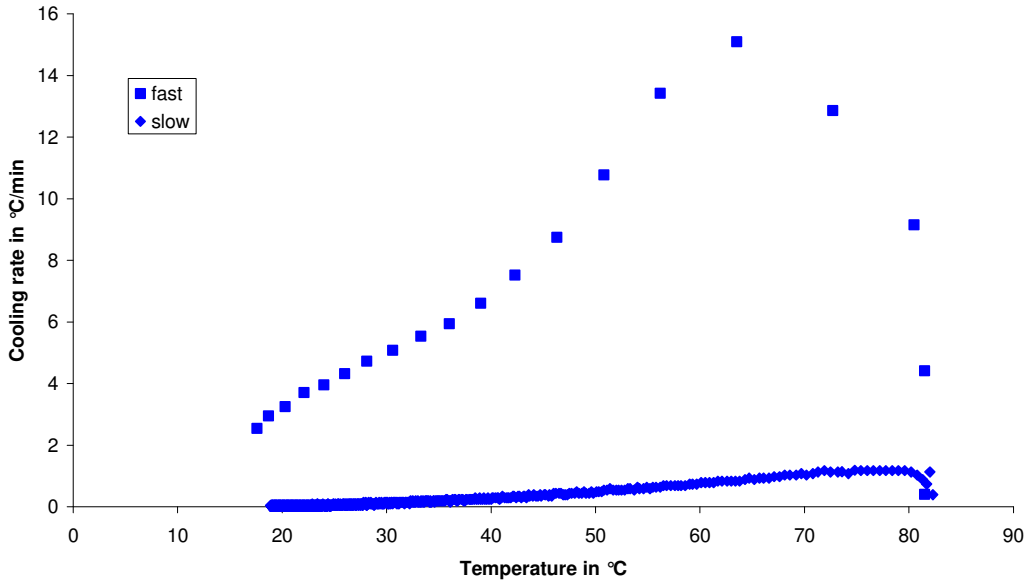

Figure 3.7: Cooling rates of the emulsion 7.5 % (w / w) Soya Bean Oil / 20 % (w / w) Brij 97 / 72.5 % (w / w) Water in function of its temperature

Note: fast for emulsion quenched in ice bath and slow for emulsion cooled down at ambient temperature

The cooling rates tended to be faster at the beginning of the immersion (Figure 3.7). This peak in the cooling rate happened in the PIT region. Less than 2 minutes were needed to obtain a shift of 20 °C away from the HLB temperature.

Table 3.4 presents the appearance and absorbance of emulsions made with different compositions using the PIT technique. The absorbance of the samples at λ=540 nm is a value in arbitrary unit (a.u.) that allows making a better distinction between the optical qualities of an emulsion than the human eye would do. The higher the number is, the more the solution is opaque. The smaller the number is, the closer it gets to the transparency of water. It must be noted that the use of absorbance values to compare the transparency of emulsions is qualitative; indeed, the standard deviation gets very important as the values diverge from 0. Examples of samples with different absorbance values are shown in Figure 3.8 and 3.9. Figure 3.8 shows transparent emulsions whereas in Figure 3.9, a non-stable emulsion is presented. Over time, it separated into 2 phases, at the top being the cream layer, whiter and richer in oil droplets that the underlying layer **[93]**. Coarse pre-emulsions (no thermal

treatment) and non-stable emulsions usually began creaming after a few minutes without stirring.

Table 3.4: Appearance and absorbance at λ= 540nm for emulsions of composition Soya bean oil / Brij 97 / Water subjected to two different cooling processes (slow heating)

Slow cooling: < 2 °C min^{-1}, Fast cooling: from 5-16 °C min^{-1}, Slow heating: 1-2 °C min^{-1}

The letters that appear next to some of the absorbance values refer to the reference of the corresponding sample pictures in Figure 3.8 and 3.9 and micrographs in Figure 3.12, 3.15 and 3.17.

Composition in % (w / w)	**PIT**	**Slow cooling**		**Fast cooling**	
		Appearance	**Abs. (a.u.)**	**Appearance**	**Abs. (a.u.)**
5.0 / 2.5 / 92.5	-	white / unstable	> 3 (**c**)	white / unstable	> 3 (**C**)
5 / 5 / 90	-	white / unstable	> 3 (**d**)	white / stable	> 3 (**D**)
5.0 / 7.5 / 87.5	84 °C	white / stable	> 3	transparent	0.12
5 / 10 / 85	80 °C	cloudy	0.35 (**e**)	transparent	0.11 (**E**)
10 / 10 / 80	-	white / unstable	> 3 (**g**)	white / unstable	> 3 (**G**)
5 / 15 / 80	77 °C	transparent	0.03 (**f**)	transparent	0.01 (**F**)
10 / 15 / 75	84 °C	white / stable	> 3 (**h**)	transparent	0.23 (**H**)
5 / 20 / 75	74 °C	transparent	0.01 (**b**)	transparent	0.08 (**B**)
7.5 / 20.0 / 72.5	82 °C	cloudy	0.22	transparent	0.04
10 / 20 / 70	88 °C	white / stable	1.40 (**a**)	transparent	0.14 (**A**)

From Table 3.4, the following observations can be made. A high quantity of surfactant is required to enable the preparation of stable emulsions. A high cooling rate also helps in order to obtain more transparent and stable emulsions for many compositions. For 20 % (w / w) of Brij 97, it was observed that 5 % (w / w)

Soya bean oil emulsions were transparent even with a slow cooling rate (< 2 °C min^{-1}) whereas with 10 % (w / w) Soya bean oil, the preparation of a bluish emulsion was only possible when the cooling rate was fast enough, i.e. when it was quenched in ice (Table 3.4). Emulsions containing 5 % (w / w) of soya bean oil requires a minimum of 5 % (w / w) Brij 97 to turn into stable emulsions, and must be accompanied with a fast cooling.

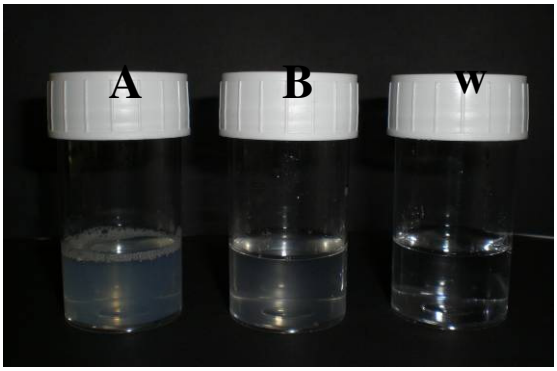

Figure 3.8: Transparency of emulsions compared to water

A- emulsion made of 10 % (w / w) Soya bean oil / 20 % (w / w) Brij 97 / 70 % (w / w) Water; fast cooling; Absorbance at λ=540 nm →0.14,

B- emulsion made of 5 % (w / w) Soya bean oil / 20 % (w / w) Brij 97 / 75 % (w / w) Water; fast cooling; Absorbance at λ=540 nm →0.08,

w- water; Absorbance at λ=540 nm →0.

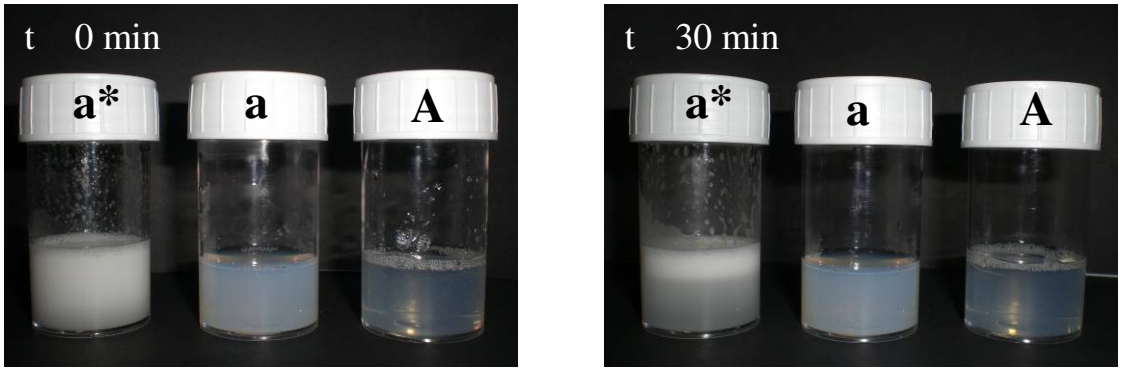

Figure 3.9: Pictures of 10 % (w / w) Soya bean oil / 20 % (w / w) Brij 97 / 70 % (w / w) Water emulsions.

a*- no thermal process; Absorbance at λ=540 nm →> 3

a- slow heating; slow cooling; Absorbance at λ= 540 nm →1.4

A- slow heating; fast cooling; Absorbance at λ= 540 nm →0.14.

The formation of a stable emulsion in this case is quite surprising since a HLB temperature was not determined either by turbidity or conductivity for this composition (Table 3.3). For the emulsion to be transparent, an even higher concentration of Brij 97 is required. For 10 % (w / w) soya bean oil, the content of surfactant needs to be at least 15 % (w / w) for the preparation of stable emulsion, and a fast cooling is required to obtain a transparent sample. The samples when stable tended to look bluish and when examined against the light, they appeared yellowish / red.

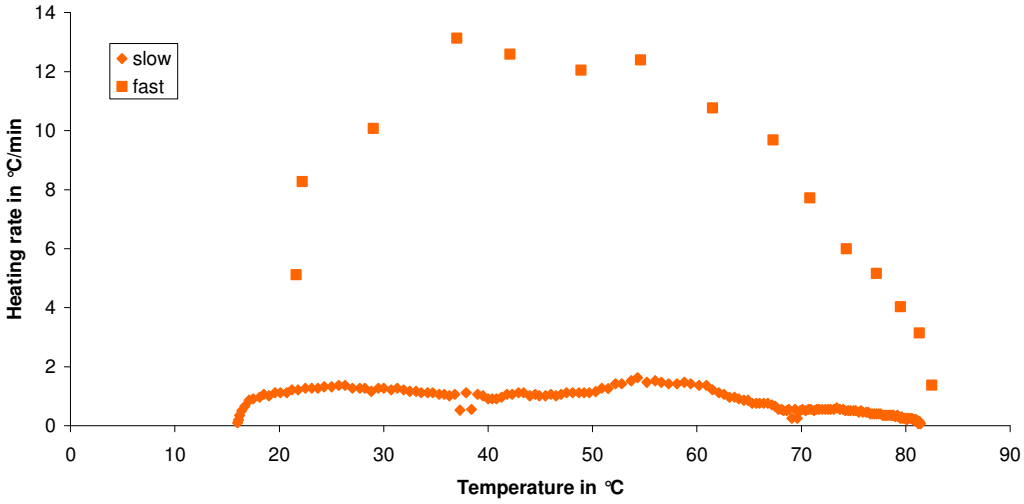

Figure 3.10: Heating rates of the emulsion 7.5 % (w / w) Soya Bean Oil / 20 % (w / w) Brij 97 / 72.5 % (w / w) Water in function of its temperature

Note: fast for emulsion immersed in bath at PIT temperature and slow for emulsion heated together with the water bath

The heating rate was also modulated in order to see the effect it could have on the appearance of the emulsions. Fast heating rates were obtained by plunging emulsions directly in a water bath at the PIT temperature whereas for slow heating rates, the emulsions were placed in a bath at ambient temperature and bath and emulsions would be heated together (Figure 3.10).

According to the results presented in Table 3.5, the heating rates do no seem to have an influence on the appearance of the emulsions. However, it is important to note that due to the equipment, the heating process can not be controlled with accuracy. Moreover, the extent of modulation of the heating rate is limited. Indeed, the area which could be particularly sensitive to this parameter is the PIT region, that is to say a high temperature region. But, contrary to the cooling rates, the highest heating rates do not occur in this zone since the temperature difference between the bath maximum temperature and the temperature of the emulsion are getting closer when approaching the PIT.

Table 3.5: Appearance and absorbance at λ= 540nm for emulsions of composition Soya bean oil / Brij 97 / Water subjected to two different cooling processes for slow and fast heating

Slow cooling: < 2 °C min^{-1}, Fast cooling: from 5-16 °C min^{-1};

Slow heating: 1-2 °C min^{-1}, Fast Heating: from 1-14 °C min^{-1}.

The letters that appear next to some of the absorbance values refer to the reference of the corresponding sample pictures in Figure 3.8 and 3.9 and micrographs in Figure 3.12, 3.15 and 3.17.

Conc. in % (w / w)	**Heating Rate**	**Slow cooling**		**Fast cooling**	
		Appearance	**Abs. (a.u.)**	**Appearance**	**Abs. (a.u.)**
5 / 2.5 / 92.5	Slow	white / unstable	> 3 (**c**)	white / unstable	> 3 (**C**)
	Fast	white / unstable	> 3	white / unstable	> 3
5 / 7.5 / 87.5	Slow	white / stable	> 3	transparent	0.12
	Fast	white / stable	> 3	transparent	0.16
10 / 10 / 80	Slow	white / unstable	> 3 (**g**)	white / unstable	> 3 (**G**)
	Fast	white / unstable	> 3	white / unstable	> 3
5 / 20 / 75	Slow	transparent	0.01 (**b**)	transparent	0.08 (**B**)
	Fast	transparent	0.03	transparent	0.16
7.5 / 20 / 72.5	Slow	cloudy	0.22	transparent	0.04
	Fast	transparent	0.18	transparent	0.11
10 / 20 / 70	Slow	white / stable	1.40 (**a**)	transparent	0.14 (**A**)
	Fast	white / stable	1.52 (**a^**)	transparent	0.15 (**A^**)

As a consequence, whatever the cooling and heating methods chosen, the emulsions would stay in the PIT range for at least 3 minutes (Figure 3.11). This might be enough to let the phase transition occur and as a result, would result in the preparation of similar final emulsions.

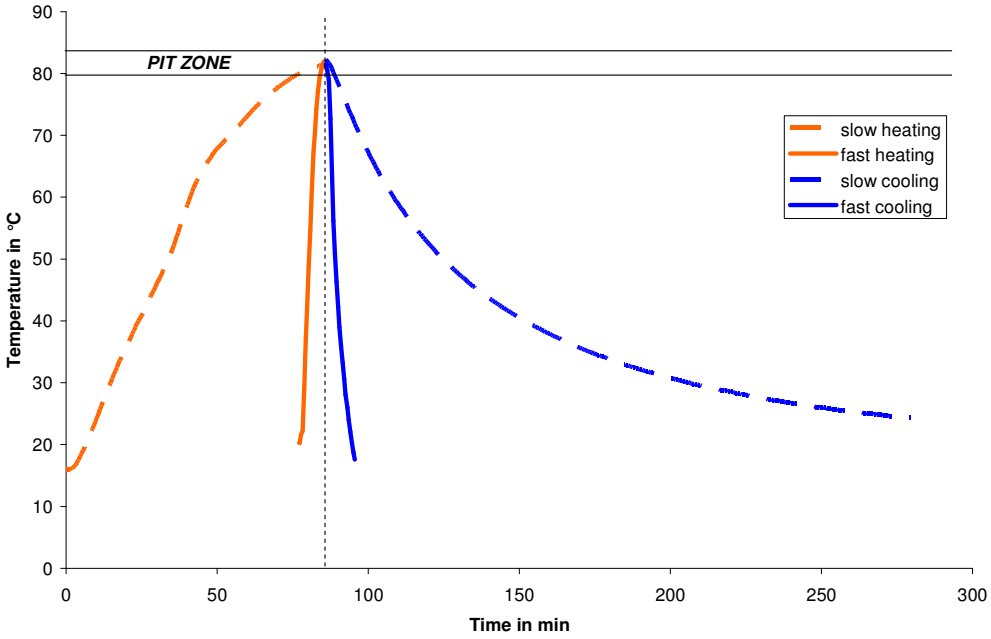

Figure 3.11: Time profiles of the different heating treatments for an emulsion 7.5 % (w / w) Soya Bean Oil / 20 % (w / w) Brij 97 / 72.5 % (w / w) Water

Note: The heating is fast for emulsion immersed in bath at PIT temperature and slow for emulsion heated together with the water bath. The cooling is fast for emulsion quenched in ice bath and slow for emulsion cooled down at ambient temperature.

3.3.2.2- Size analyses

As explained in Chapter 1, nanoemulsions can sometimes appear transparent since their droplets are so fine. Since some emulsions prepared previously presented this transparent characteristic, they might be made of nanodroplets. To check that hypothesis, micrographs were taken (Figure 3.12 and 3.15) and when possible, size was determined.

In Figure 3.12, emulsions containing 5 % (w / w) of soya bean oil are presented. Depending on the concentration of Brij 97, the droplets in emulsion

looked quite different. At the low concentration of 2.5 % (w / w) of surfactant (*c, C*), droplets were very numerous and clearly visible, in the micrometer range (up to 6 and 4 µm for respectively slow and fast cooling). Their polydispersity seemed high since their size varied significantly, especially in the case of slow cooling. Due to their large size droplets and high polydispersity, 2.5 % (w / w) Brij 97 emulsions are particularly unstable to creaming and cannot be successfully examined for size measurements with Light Diffraction Spectroscopy. Even though 5 / 2.5 / 92.5 emulsions presented no PIT at the scanned temperature and remained unstable after the thermal treatment (Tables 3.3 and 3.5), this latter has not been without effect. Indeed, from Figure 3.12, it is clear that the fast cooling had an important effect on the size of the droplets (*C*).

Less coalescence or Ostwald ripening seemed to have happened when the cooling was fast since the droplets in the micrograph C appear more uniform and with smaller size than the droplets in the micrograph c. Shinoda *et al.* **[70]** was underlining the importance of a rapid cooling in order to prevent the coalescence of the fine droplets formed near the PIT. Indeed, in the PIT region, the rate of coalescence is higher and the droplets growth is very quick. It seems that even in the absence of a PIT, rapid cooling is beneficial for the preparation of finer emulsions in presence of heat-sensitive surfactants.

In the micrographs with 5 % (w / w) of Brij 97 (*d, D*), the droplets appeared already much finer and more monodispersed than those made with less surfactant (*c, C*), despite the occurrence of a few larger droplets. Most of the droplets were so small that it was not possible to determine their size using the micrographs. They tended to flocculate which would result in a high instability to creaming **[11]**. However, the emulsions that were subjected to ice-bath quenching seemed to be stable against this creaming (Table 3.4). It was even possible to study their size using the Light Diffraction Spectrometer (Figure 3.13 and 3.14). Their Z-average was around 150 nm (*D*).

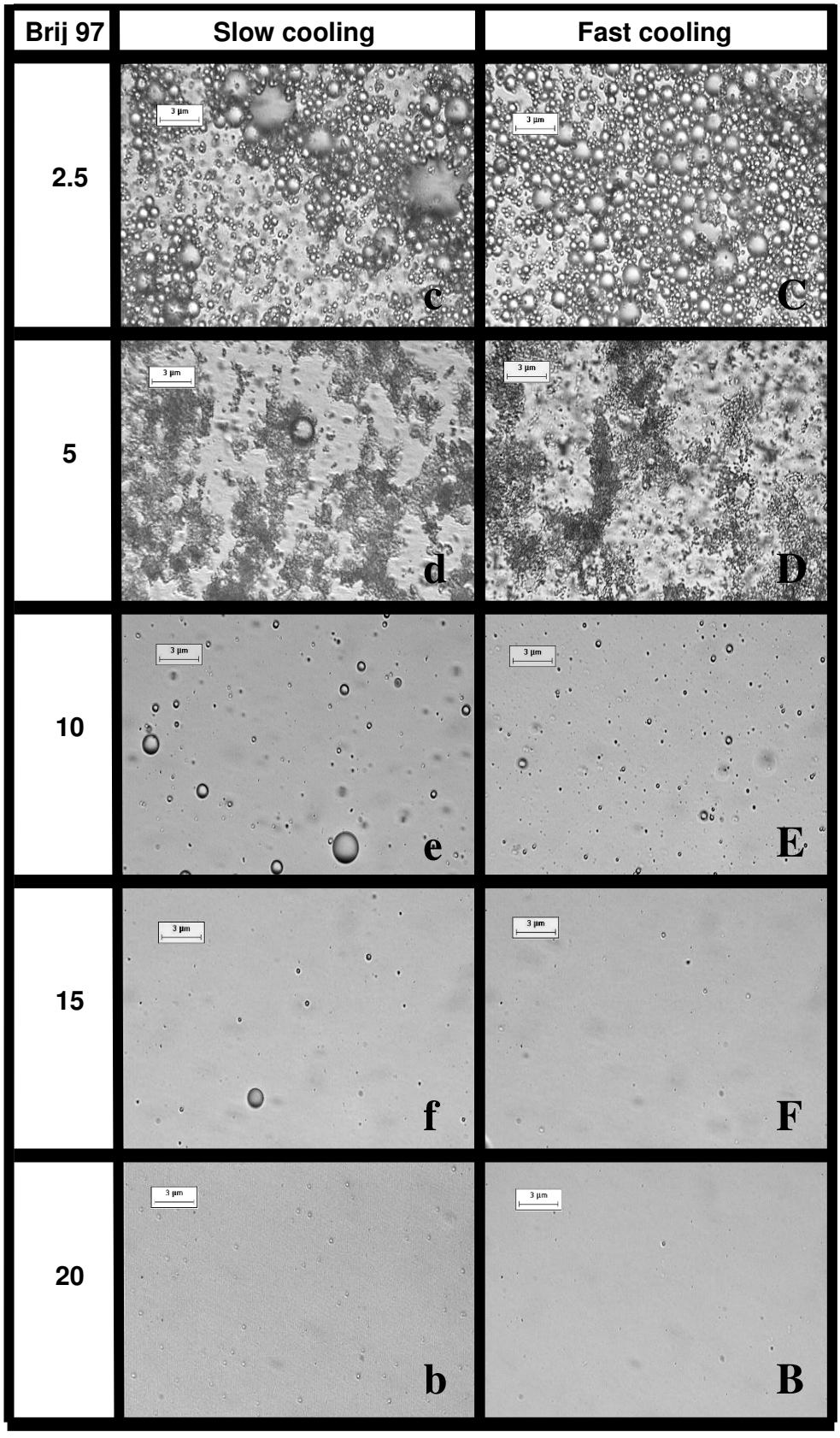

Figure 3.12 Micrographs of 5 % (w / w) soya bean oil emulsions with Brij 97 content in % (w / w)

Slow cooling: 0-2 °C min^{-1}, Fast cooling: 5-16 °C min^{-1}. The emulsions were heated up slowly (1-2 °C min^{-1}). Scale bar = 3 µm

For Brij 97 concentration of 10 % (w / w) and over (*e, E, f, F, b* and *B*), only a few droplets were visible. They were either present but too small to be observed with the microscope or the soya bean oil had simply dissolved into the water-surfactant solution. In each case, the fast cooling seemed to enable the preparation of finer and more monodispersed emulsions.

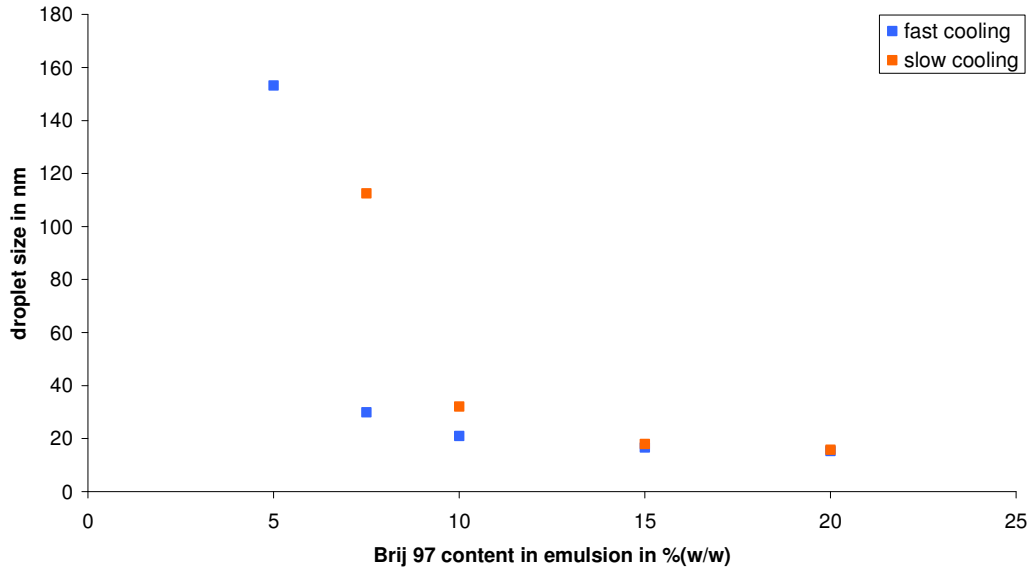

Figure 3.13 Evolution of the droplet size with the content of Brij 97 in O / W emulsions of concentration 5 % (w / w) soya bean oil

Slow cooling: < 2 °C min^{-1}, Fast cooling: from 5 °C min^{-1} up to 16 °C min^{-1}. The emulsions were heated up slowly (1-2 °C min^{-1}).

It was possible to measure with DLS the droplet size for emulsions with a content of 10 % (w / w) or more of Brij 97 (Figure 3.13). This probably means that the transparent emulsions contained very small oil droplets rather than solubilised oil. Emulsions that were white and stable (i.e. 5 / 5 / 90 with fast cooling and 5.0 / 7.5 / 87.5 with slow cooling) had a Z-average superior to 100 nm. All the others emulsions presented on the graph 3.13 had average size under 40 nm. These small sizes explain the transparency of these emulsions. However, it was observed that the slowly cooled 5 / 10 / 85 emulsions were cloudy whereas the quickly cooled 5.0 / 7.5 / 87.5 ones with a similar Z-average were transparent. This difference in appearance might be explained by Figure 3.14 where the polydispersity index of these emulsions was represented. Whilst all the emulsions had a PdI inferior to 0.3, the slowly cooled

5 / 10 / 85 emulsion showed a PdI close to 0.4. This polydispersity is higher than the other emulsions, and result in the presence of larger droplets that could prevent the emulsions to appear transparent. The formation of these larger droplets was probably promoted by the slow cooling since the phenomenon of coalescence is more important when the emulsion stays longer in the PIT zone.

Analysing the results in Figure 3.13, it seems that when the concentration of surfactant increases, the influence of the cooling rate on the size of the droplets decreases. The effects of the cooling rate and concentration of Brij 97 on the PdI are less clear (Figure 3.14).

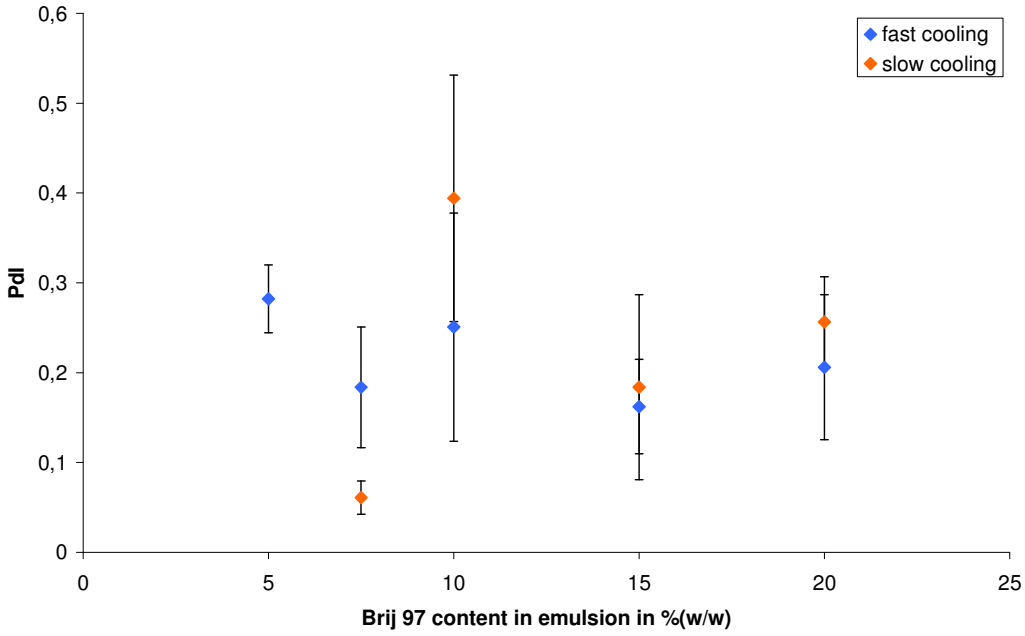

Figure 3.14: PdI of emulsions at 5 % (w / w) soya bean oil in function of the content in Brij 97
Slow cooling: 0-2 °C min^{-1}, Fast cooling: from 5 °C min^{-1} up to 16 °C min^{-1}. The emulsions were heated up slowly (1-2 °C min^{-1}).

Figure 3.14 presents very large error bars. They were estimated from the standard deviation after several repetitions of the analyses. The same sample, when measured twice, could be associated with two very different PdI values by the DLS device. Also, when two samples were prepared using the same conditions, the resulting Z-average would be very similar whilst the PdI could vary considerably.

These very large error bars make it difficult to conclude on the effect of both Brij 97 concentration and cooling rate on the PdI. The zetasizer might not be very sensitive to PdI when it is too high. Since the rate of coalescence is higher around the HLB temperature **[70]**, the PIT area is the zone where droplets are differentiating from one another if the cooling is not homogeneous. If the cooling process was improved so that all the emulsions could be subjected to the same rate of cooling throughout the batch, maybe the resulting emulsions could be more monodispersed compared to the emulsions obtained so far.

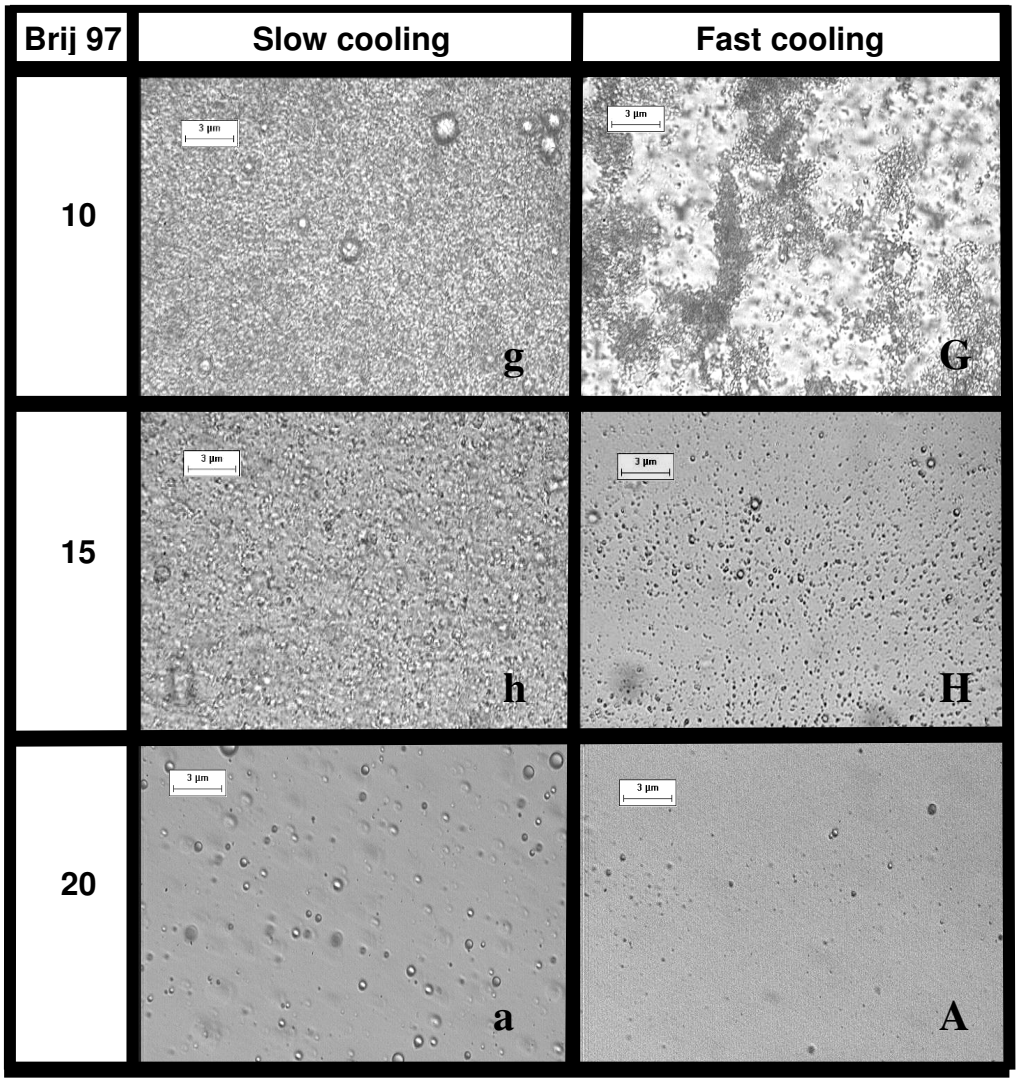

Figure 3.15: Micrographs of 10 % (w / w) soya bean oil emulsions in function of cooling rate and Brij 97 content in % (w / w)

Slow cooling: 0-2 °C min^{-1}, Fast cooling: from 5 °C min^{-1} up to 16 °C min^{-1}. The emulsions were heated up slowly (1-2 °C min^{-1}). Scale bar = 3 µm

Figure 3.15 and Table 3.6 present the micrographs and size measurements obtained for 10 % (w / w) soya bean oil emulsions. Even though it is only clearly visible for the quickly cooled 10 / 10 / 80 emulsion (*G*) in Figure 3.15, the flocculation phenomenon happened as well for the slowly cooled 10 / 10 / 80 (*g*) and 10 / 15 / 75 (*h*) emulsions. As seen previously with 5 % (w / w) soya bean oil emulsions, the size and polydispersity of the droplets decrease with the addition of surfactant and the use of fast cooling. The use of fast cooling seems advantageous; indeed, according to Table 3.6, the difference in the droplet size of the emulsions 10 / 15 / 75 slowly cooled (*h*) to quickly cooled (*H*) is as important as the droplet size reduction that would be obtained with an addition of 5 % (w / w) of Brij 97 (i.e slowly cooled emulsion 10 / 20 / 70 (*a*)).

Table 3.6: Size and PdI measurements of 10 % (w / w) Soya bean oil emulsions

The emulsions were heated up slowly (1-2 °C min^{-1}).

The letters that appear in the column Ref. refer to the corresponding pictures in Figure 3.8 and 3.9 and to the micrographs in Figure 3.15.

Brij 97 conc. in % (w / w)	**Slow cooling (0-2 °C min^{-1})**			**Fast cooling (5-16 °C min^{-1})**		
	Size in nm	**PdI**	**Ref.**	**Size in nm**	**PdI**	**Ref.**
15	190 (±12)	0.13 (±0.06)	h	45 (±6)	0.29 (±0.06)	H
20	63 (±21)	0.19 (±0.03)	a	24 (±5)	0.23 (±0.19)	A

In an attempt to study the effect of the soya bean oil concentration on the emulsions in more detail, more samples were prepared. The results obtained are presented in Figure 3.16. Not surprisingly, at constant concentration of surfactant, addition of soya bean oil results in an increase of the size droplets. The cooling rate seems to enable the production of slightly smaller droplets. However, interestingly, the error bars on these results are much larger than the error bars on the slowly cooled emulsion (apart for the emulsion slowly cooled with 10 % soya bean oil concentration).

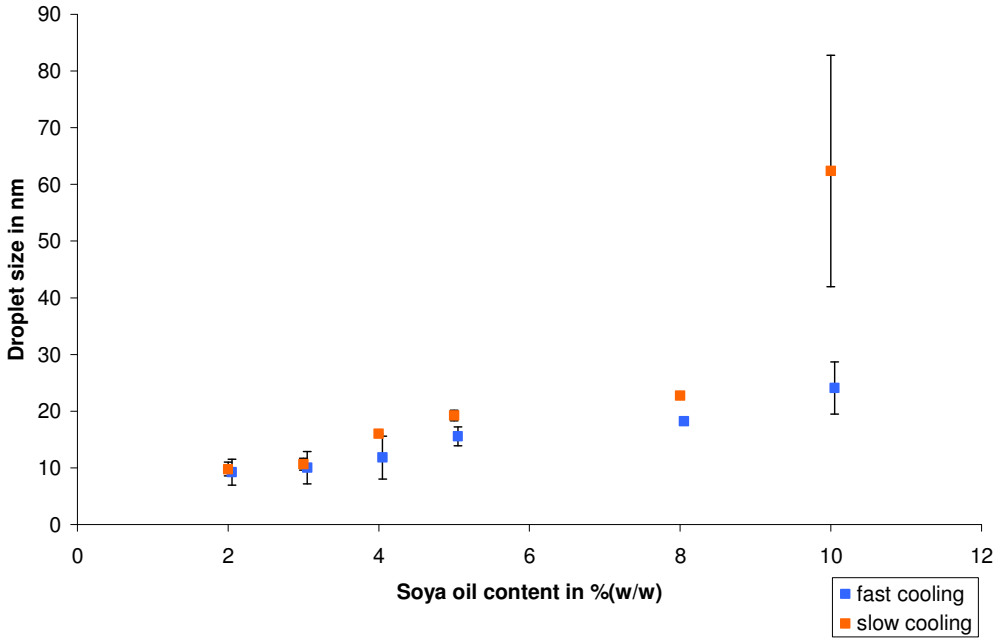

Figure 3.16 : Z-average of 20 % (w / w) Brij 97 emulsions in function of the rate of cooling and soya oil bean concentration

Slow cooling: 0-2 °C min^{-1}, Fast cooling: from 5 °C min^{-1} up to 16 °C min^{-1}. The emulsions were heated up slowly (1-2 °C min^{-1}).

These large error bars result from the disparity between the samples which were prepared under the same experimental conditions. This would suggest that reproducibility of the same conditions in the case of fast cooling was not obtained.

Previously in Section 3.3.2.1, observations led to the idea that the heating rate had no effect on the appearance of the resulting emulsions in the extent of the possible modulations offered by the equipment. However, this was not sufficient to conclude that it did not have any significant influence. Figure 3.17 presents two examples of composition subjected to different combinations of heating and cooling treatments. Within the same composition, emulsions which followed the same cooling process looked more alike.

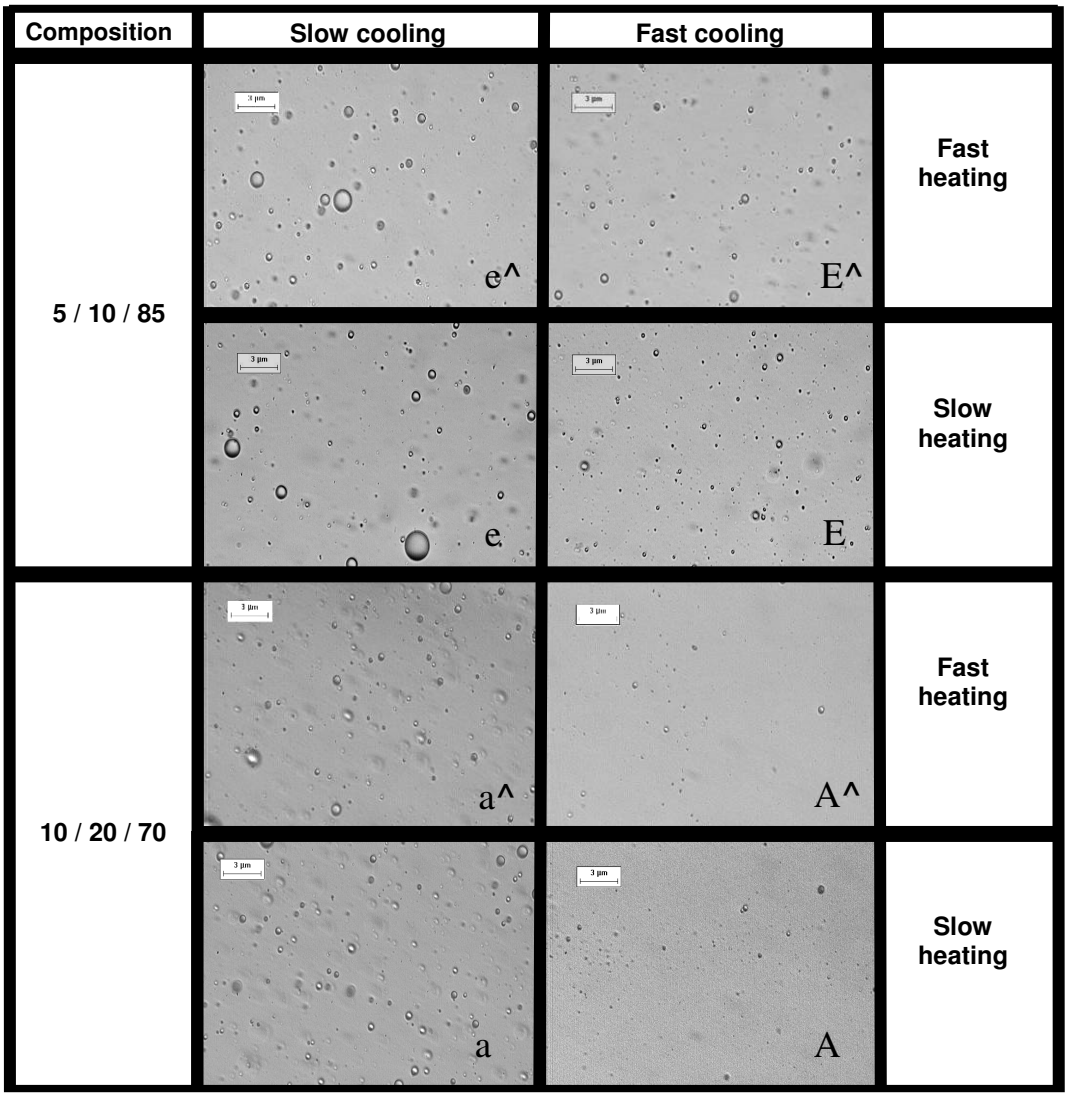

Figure 3.17: Micrographs of two different Soya bean oil / Brij 97 / Water compositions subjected to different thermal processes

Slow cooling: < 2 °C min^{-1}, Fast cooling: from 5-16 °C min^{-1}, Slow heating: 1-2 °C min^{-1}, Fast Heating: from 1-14 °C min^{-1}

Scale bar = 3 µm

Moreover, when comparing the size analyses from slow and fast heating in Table 3.7, it seems that the heating process does not play a role in the Z-average and polydispersity of the droplets. According to these results, the rate of cooling appears to be the only thermal factor that influences on the droplet. However, these results are relative since the modulation of heat could only be done to a certain extent as explained in 3.3.1.2.

Table 3.7: Size analyses of different Soya bean oil / Brij 97 / Water compositions subjected to different thermal processes

The letters that appear in the column Ref. refer to the corresponding sample pictures in Figure 3.8 and 3.9 and micrographs in Figure 3.12, 3.15 and 3.17.

Conc. in % (w / w)	Slow cooling (0-2 °C min^{-1})			Fast cooling (5-16 °C min^{-1})		
	Size in nm	PdI	Ref.	Size in nm	PdI	Ref.
Slow heating (1-2 °C min^{-1})						
5 / 10 / 85	32 (±3)	0.40 (±0.14)	e	21 (±3)	0.25 (±0.13)	E
5 / 15 / 80	18 (±2)	0.19 (±0.10)	f	17 (±1)	0.17 (±0.06)	F
10 / 20 / 70	63 (±21)	0.19 (±0.03)	a	24 (±5)	0.23 (±0.19)	A
Fast heating (up to 14 °C min^{-1})						
5 / 10 / 85	34 (±2)	0.34 (±0.18)	e^	19 (±4)	0.21 (±0.10)	E^
5 / 15 / 80	21 (±4)	0.30 (±0.16)		19 (±2)	0.14 (±0.05)	
10 / 20 / 70	40 (±5)	0.18 (±0.12)	a^	22 (±8)	0.26 (±0.09)	A^

At least 3 other groups studied the droplet size for emulsions Soya bean oil / Brij 97 / Water **[2, 89, 94]**. They all allowed the emulsions to cool down at ambient temperature under constant stirring, which corresponds with the slow cooling method of the present work.

The measurements of Flanagan *et al.* **[2]** only represented a very narrow range of compositions: the successive dilutions of the system 6 / 30 / 64. They obtained droplet sizes between 12.6 and 6.4 nm. No experiment with such a high concentration of surfactant (30 % (w / w)) was performed in the present work, but comparison can still be made with compositions such as 5 / 20 / 75 (b on Figure 3.12) for which the resulting droplet size after slow cooling treatment was 17 nm, a value which is quite close from the size range found by Flanagan *et al.*.

Malcolmson *et al.* **[89]** did not work either with the same compositions as presented in this work. They also did experiments with low concentrations of soya bean oil and high concentrations of surfactant and found droplet sizes in the range 10 to 20 nm. Again, their results seem in agreement with the present ones when

compared with the slowly cooled emulsion of composition 5 / 20 / 75 prepared in this work (Z-average of droplets = 17 nm).

Finally, Warisnoicharoen *et al.* **[94]** experimented with two compositions that were studied in the present work. As a consequence it is possible to make direct comparisons between both results (Table 3.8). There is a good agreement between the droplet sizes measured by Warisnoicharoen and the results found in the present work.

Table 3.8: Comparison between droplet sizes found by Warisnoicharoen *et al.* [94] for the system Soya bean oil / Brij 97 / Water containing 20 % (w / w) of Brij 97and results of the present work

Soya bean oil content in % (w / w)	**Droplet size in nm by** [94]	**Measured droplet size in nm in the present work**
2	10.1	9 (±2)
4	11.8	11 (±1)

Warisnoicharoen *et al.* **[94]** performed light diffraction spectroscopy on undiluted emulsions whereas for the present study, this operation was impossible with the available apparatus. The dilutions made for measuring the droplet size with the available DLS equipment seemed to not affect the size of the droplets, since the results were in very good accordance with those of Warisnoicharoen *et al.* who did not dilute their samples. No change of property under dilution is one of the characteristics of a nanoemulsion. As seen in Chapter 1, by definition, nanoemulsions are dominated by the kinetics of a system and not by thermodynamic aspects such as the composition. This stability on dilution is advantageous. Indeed, this means that the emulsion could be made less viscous and that it could possibly be added to formulations without alteration of its size and transparency properties.

3.4- Conclusion

Different emulsions were prepared using the PIT method introduced by Shinoda *et al.* **[70]**. The first set of results with emulsions made of hexadecane, Brij 30 and a centimolar solution of NaCl enabled to check if it was possible to measure the phase inversion temperature of a system containing a non-ionic ethoxylated surfactant using a conductimeter. However, this method was later tested on the system Soya bean oil / Brij 97 / Water and did not seem appropriate for the determination of its PIT. A visual method was then chosen to obtain the PIT of different compositions. The HLB temperature seemed to increase with the concentration of oil and the decrease of surfactant.

Soya oil / Brij 97 / Water nanoemulsions were prepared using the PIT method in a batch. They were brought to the PIT temperature of the chosen compositions and then cooled down at either fast or slow cooling rate. The appearance of the resultant emulsions varied from unstable white to stable transparent mixtures. Emulsions with a high proportion of soya bean oil and low content of Brij 97 tended to be whiter and less stable, especially if the cooling rate was slow. White emulsions presented in most cases a higher droplet size than the more transparent ones. The heating rate did not seem to have an influence on the appearance and droplet size of the nanoemulsions.

Chapter 3 also showed that without accuracy and control of the temperature, reproducible results were difficult to obtain. The construction of a rig, which would allow the continuous manufacture of emulsions using heat exchangers might allow a more precise control of the heating and cooling processes than the batch operations. If the conditions were more reproducible, emulsions with well determined size droplets could be produced. Also, a more homogeneous heat treatment i.e. where all the drops of liquid are processed under the exact same conditions might lead to the preparation of more monodispersed emulsions than the batch method where there could be a gradient of temperatures through the bulk despite the continuous stirring.

Chapter 4 – Continuous set-up

4.1- Introduction

In Chapter 3, different Soya oil / Brij 97 / Water nanoemulsions were prepared using the PIT method introduced by Shinoda *et al.* **[70]** in a batch system. It was shown that the thermal treatment could have an important influence on the size of the final droplets. When cooled down rapidly, droplets would tend to be smaller than when cooled down at a slower pace. The equipment used for batch emulsion preparation did not allow a good control of parameters such as heating and cooling rates or highest temperature reached. This might have an effect on the polydispersity of the samples obtained but also on the reproducibility of the same emulsion from one batch to the other.

Designing a continuous rig with heat exchangers might help in controlling more accurately these factors and as a consequence, could improve the quality of the resulting emulsions. Moreover, a faster cooling rate could be obtained; this might allow the preparation of even finer droplets and more stable emulsions. Using heat exchangers for the heat treatment of the emulsion is an opportunity to move from a batch to a continuous production. This could have the advantages of improving the time efficiency and reducing the cost of production.

This chapter deals with the design and construction of a continuous PIT emulsification rig. In a first part, the requirements of the rig are identified. Then, from this basis, the rig is built using the available pieces of equipment needed to get as close as possible to these specifications. The second section describes the different components used in the rig. Finally, the first tests on the experimental set-up are presented. Subsequently, a number of modifications are made to improve it.

4.2- Identification of the rig requirements

4.2.1- Temperature requirements

In Chapter 3, it was shown that the cooling rate is extremely important to obtain small droplet size. To prevent coalescence of the emulsions as much as possible and obtain very fine droplets, it could be useful to work with even faster cooling rates than the one obtained with the batch apparatus in Chapter 3. It was possible to get a maximum cooling rate of 16 °C min^{-1} in the region of the PIT. A heat exchanger would allow higher cooling rate. A continuous source of refrigerant fluid is necessary to maintain a continuous cooling on the emulsion side.

A source of heat is necessary to heat up the coarse emulsion. According to results from Chapter 3, it seemed that the heating rate did not have much importance for the preparation of the nanoemulsions. However, special attention must be taken to ensure that the emulsions get in the region of the HLB temperature. The system Soya Bean Oil / Brij 97 / Water emulsions was studied in Chapter 3 and it was shown the highest temperature necessary is 88 °C in the case of the emulsion of composition 10 % (w / w) of soya bean oil, 20 % (w / w) of Brij 97 and 70 % (w / w) of water.

Finally, elements to measure the temperature at specific points in the rig are required to check that both heating and cooling processes meet design specifications.

4.2.2- Modulation requirements

The rig is designed to enable the continuous preparation of nanoemulsions. It would be interesting if it could be used on a wide range of different compositions. As a consequence, the rig parameters need to be adjustable according to the kind of nanoemulsions being made.

First, it would be interesting to be able to vary the emulsion compositions online. For this purpose, two pumps with variable flow rates should be used: one delivering the oil and the other the aqueous surfactant solution as it enables to modify the ratio of the ingredients. To ensure the formation of a coarse emulsion before the entrance in the heat exchangers, the two feeds require to be mixed.

The HLB temperature is specific to a composition. As a result, when the ratio of ingredients is changed, the temperature that needs to be reached for emulsification also varies. Therefore, it would be useful to be able to modulate parameters such as cooling and heating rates and maximum temperature reached by the emulsion in the rig. This probably could be achieved by choosing appropriately the temperature of the heating medium and the flow rates of emulsion delivery as well as the heating and cooling fluids.

The continuous experimental set-up as is schematically shown in Figure 4.1.

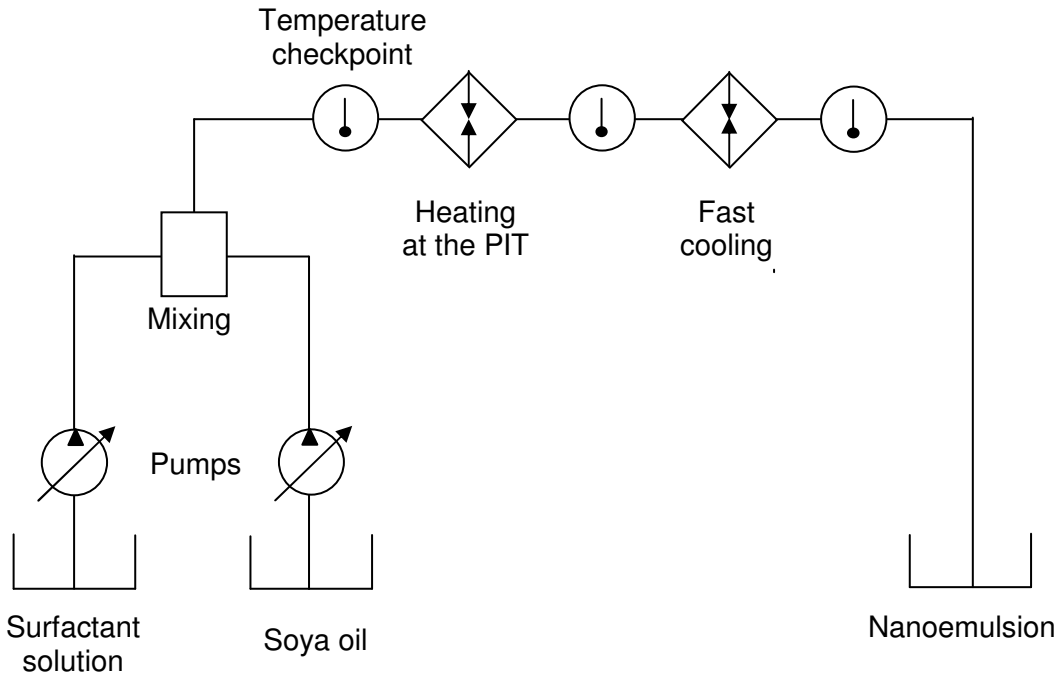

Figure 4.1: Sketch of the continuous rig for the preparation of nanoemulsions using the PIT emulsification technique

4.3- Construction of the preliminary rig

Some expensive equipment that could fulfil the requirements stated in Section 4.2 was lent by Unilever Corporate: a heat exchanger, two precision pumps and a micromixer. The remaining of the components needed for the assembling of the rig was chosen to fit around these first pieces; their size determined the dimensions of the other components of the rig.

4.3.1- Pre-emulsion (coarse emulsion preparation at the start of the rig)

Two micro annular gear pumps mzr-4605 from HNP Mikrosysteme GmbH (Figure 4.2) were provided by Unilever Corporate. They are very precise and can function for very small flow rates. These pumps can deliver between 0.012 up to 72 mL min^{-1}.

Figure 4.2: From left to right, pumps mzr-2905 / mzr-4605 / mzr-7205 [95]

A mzr-Pump controller software was used to control the different flow rates of the emulsion components (Figure 4.3) **[95]**.

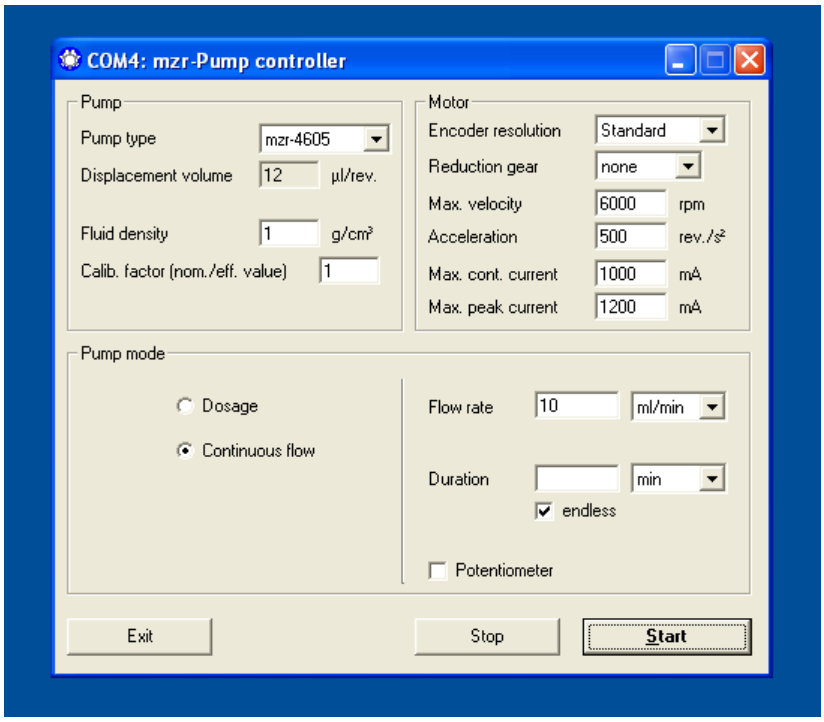

Figure 4.3: Display of the Software mzr-pump controller

The tubing chosen for the pumping of the constituents was made of polytetrafluoroethylene (PTFE) and had an outer diameter of 1 / 8" and an internal diameter of 1 / 16". Glass bottles topped with a screw cap containing two inserts for the tubings were used as feed bottles for the constituents of the emulsion. The extremity of the tubing was tied to a solid filter that protected the pump from particles and contamination; it also prevented from sending particles into the rest of the rig. Magnetic stirrers (Bibby HB502) were used to ensure homogeneity of the feeds at all times (***s*** on Figure 4.14). After each pump, a plastic valve was used to direct the fluid either back to the feed tank or to the rest of the rig.

Figure 4.4: Micromixer [96]

Then, the two phases were mixed in a slit interdigital micromixer SSIMM (IMM Institut für Mikrotechnik Mainz GmbH) (Figure 4.4). The tubings were held secure onto the micromixer with pieces of Teflon tubing (internal diameter: 1 / 16", outer diameter: 1 / 4"). According to the manufacturer, the flow rate in the micromixer cannot exceed 25 mL min^{-1} **[96]**.

4.3.2- Cooling of the emulsion with a microheat exchanger

A gas phase microreactor (GPMR) that could be used as a heat exchanger for liquids was provided by Unilever Corporate (Figure 4.5). It was decided to use it on the cooling side since it was shown that the speed of cooling was an important factor for the quality of the resulting emulsions.

A heat exchanger is a device built for efficient heat exchanges from one medium to another **[97]**. Here the two media were separated by a solid wall made of thin stainless steel plates so that the two liquids did not mix.

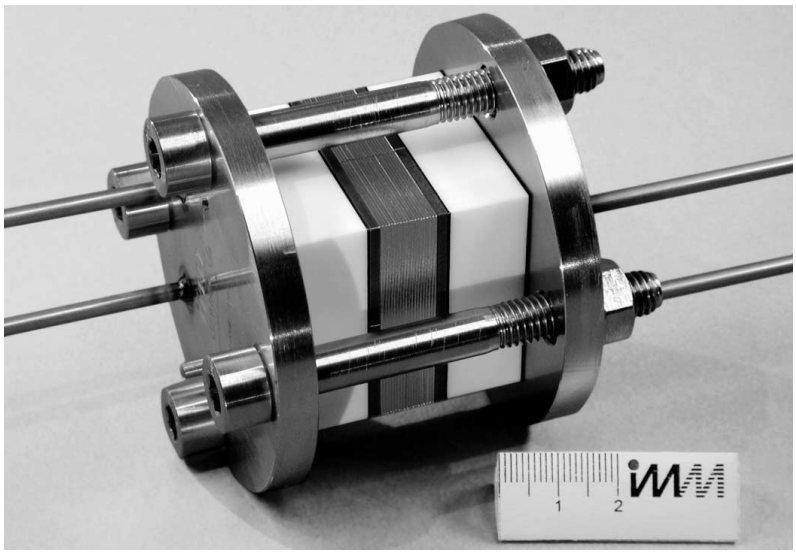

Figure 4.5: Gas phase Microreactor [98]

The GPMR comprised a stack of 20 plates that were arranged for counter-flow practice so that the emulsion and the cooling stream flowed in opposite directions (Figure 4.6). Each plate consisted of 34 parallel microchannels of 300 μm width and

200 µm depth. This heat exchanger admits a maximum flow rate of 120 mL min^{-1} **[98]**.

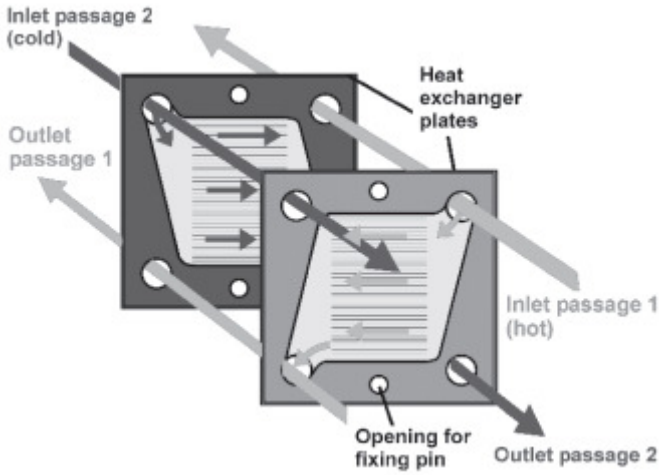

Figure 4.6: Counter-flow principle in plates of the GPMR [98]

A pump was used to circulate ethylene glycol in the microheat exchanger (***h-e*** on Figure4.14) to cool down the warm emulsion. The ethylene glycol was kept in a bottle topped with a screw cap and insert for soft tubing to ensure that no dust or particles went inside the heat exchanger and provoked a clogging. It was maintained in a cold bath (***c*** on Figure 4.14) refrigerated with a cooler Grant C2G.

The temperature was controlled at the inlets and outlets of the heat exchanger using mineral insulated thermocouples. These thermocouples fixed in copper tubing with araldite were inserted in the rig using T-junctions (10 cm away from the inlets and outlets of the heat exchanger) and were connected to the computer via a USB-based channel thermocouple input module USB-TC purchased from Measurement Computing Corp (Figure 4.7).

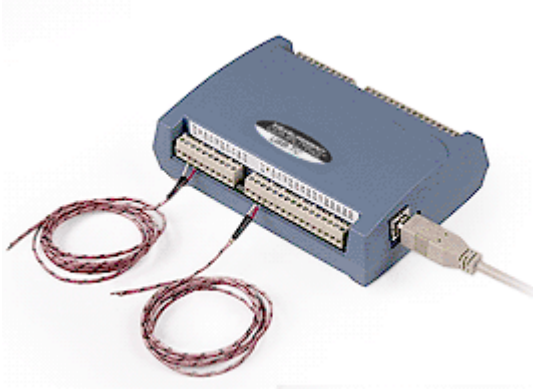

Figure 4.7: USB-TC [99]

The temperatures could be recorded and checked in real time with the measurement software TracerDAQ.

Using some heat transfer calculations **[100]**, it is possible to evaluate the requirements of the pump for the cold source. The general equation to calculate heat transfer across a surface is:

$$Q = U \times A \times \Delta T \qquad \textbf{Equation 4.1}$$

where Q is the heat transfer by unit time, U the overall heat transfer coefficient, A the area available for the heat flow, and ΔT is the difference in temperature between the two fluids. ΔT is taken as θ_m, the logarithmic mean temperature difference over the length of the exchanger:

$$\theta_m = \frac{\theta_1 - \theta_2}{\ln \frac{\theta_1}{\theta_2}} \qquad \textbf{Equation 4.2}$$

where θ_1 is the difference of temperature on one side of the exchanger i.e. $\theta_1 = T_1 - T'_1$ and θ_2 is the difference of temperatures on the other side i.e. $\theta_2 = T_2 - T'_2$ (Figure 4.8).

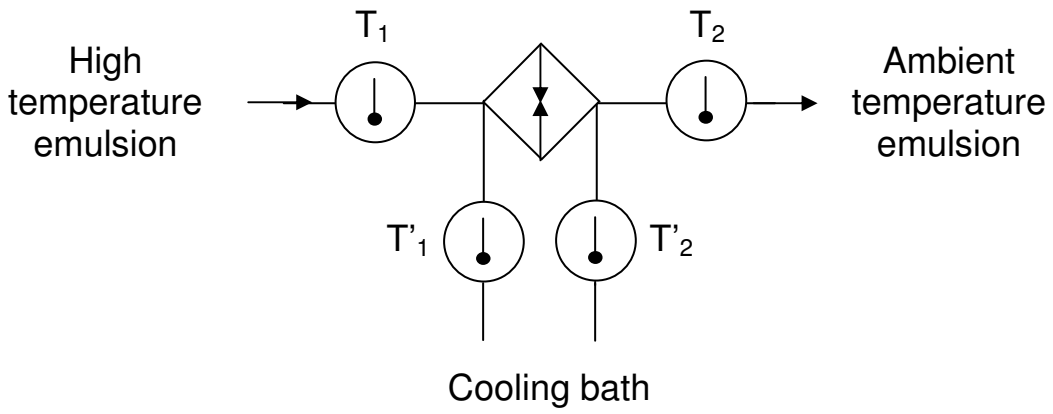

Figure 4.8: Heat exchanger temperatures

The lost or gained heat between two points on the same side (i.e on the cool or hot side) can be expressed using the following equation:

$$dQ = G \times C_p \times dT$$ **Equation 4.3**

where G is the mass flow rate and C_p is the specific heat at constant pressure. If this equation is integrated on the length of the tube (Figure 4.8):

$$Q = G \times C_p \times (T_o - T_i)$$ **Equation 4.4**

With T_o and T_i being respectively the outlet and inlet temperature of the tube.

The calculations were performed for the maximum energy demand:

- T_1= 88 °C as it is the highest HLB temperature that was determined for the system Soya bean oil / Brij 97 / Water
- T_2= 20 °C since the emulsions need to be cool down to ambient temperature

The microheat exchanger will be set up with a counter-flow current:

-T'_2 is the inlet temperature of the cooling fluid and T'_2= 10 °C

-T'_1 is the outlet temperature of the cooling fluid

- C_p = 4.18 J g^{-1} K^{-1} **[88]** on the emulsion side (the emulsion specific heat value is chosen as the maximum between the two values of $C_{p\ water}$= 4.18 J g^{-1} K^{-1} and $C_{p\ soya\ oil}$= 2.44 J g^{-1} K^{-1} in order to determine the highest flow rate that could be required in the rig).
- $C_{p\ ethylene\ glycol}$= 2.51 J g^{-1} K^{-1} **[101].**
- $\rho_{ethylene\ glycol}$ = 1.11 g cm^{-3} **[101].**
- $G_{emulsion}$ = 25 g min^{-1} as the maximum rate on the emulsion side is imposed by the use of the micromixer as stated in Section 4.3.1.
- $A_{heat\ exchanger}$= 0.00408 m^2 **[102].**
- $U_{heat\ exchanger}$ = 4000 W m^{-2} K^{-1} **[102]**. The chosen overall heat transfer coefficients used in the present work are broad approximations. These values depend on many variables such as the fluid velocities, their viscosity, the temperature differences.

Using the applied parameters and equations presented previously, it is possible to calculate the maximum flow rate necessary on the refrigerant side. First, Equation 4.4 is utilized to evaluate the total heat lost by the emulsion side (Q_{lost}= 118 J s^{-1}). Then, by combining Equations 4.1 and 4.2, the outlet temperature of the refrigerant can be deduced (T'_1= 83 °C). Finally, using Equation 4.4 again but this time for the heat gained by the cooling side, the maximum flow rate necessary for the antifreeze can be determined: $\dot{V}_{max\ refrigerant}$= 36 mL min^{-1}.

A peristaltic pump Watson Marlow 101U (with a maximum flow rate of 13mL min^{-1}) was used to start with. That might not be sufficient to cool down the emulsion efficiently. However, since all the calculations were done considering the maximum values, the flow rates of the peristaltic pump could be enough to match the requirements of the rig. Preliminary tests will be done to check whether or not a replacement needs to be found.

4.3.3- Heating up of the emulsion

In order to heat up the emulsions at their HLB temperature, it was chosen to have them circulate in a copper coil plunged in an oil bath at high temperature. The oil used was a special silicon oil for oil bath obtained from Sigma-Aldrich produced to be used at temperatures up to 180 ºC. The main features of the coil were imposed by the rest of the equipment i.e. the size of the incoming pipe from the micromixer and the size of the tubing connected to the heat exchanger. As a consequence, the copper coil (Cole-Parmer) was chosen with an internal diameter (ID) of 1 / 16" and an outer diameter (OD) of 1 / 8".

Calculations were done in order to estimate the length of copper coil L needed to heat the emulsions at the phase inversion temperature. The assumptions were as follows:

- T_{bath}= 95 °C
- T_0 is the temperature of the emulsion at the coil entrance and T_0 = 20 °C
- T_L is the temperature of the emulsion at the coil outlet and T_L = 88 °C as it is the highest HLB temperature that was determined for the systems Soya bean oil / Brij 97 / Water
- $G_{emulsion}$ = 25 g min^{-1} as the maximum rate is imposed by the use of the micromixer as stated in Section 4.3.1.
- C_p = 4.18 J g^{-1} K^{-1} **[88]** (the emulsion specific heat value is chosen as the maximum between the two values of $C_{p\ water}$= 4.18 J g^{-1} K^{-1} and $C_{p\ soya\ oil}$= 2.44 J g^{-1} K^{-1} in order to determine the highest flow rate that could be required in the rig).

- U_{copper}= 400 W m^{-2} K^{-1} **[101]**. The chosen overall heat transfer coefficients used in the present work are broad approximations. These values depend on many variables such as the fluid velocities, their viscosity, the temperature differences.

$$A_{coil} = L \times \pi \times ID$$ **Equation 4.5**

By combining Equations 4.1, 4.2, 4.4 and 4.5:

$$L = \frac{G_{emulsion} \times C_p \times \ln\left(\frac{T_0 - T_{bath}}{T_L - T_{bath}}\right)}{\pi \times ID \times U_{copper}}$$ **Equation 4.6**

According to the calculations, a length of 2.07 m was necessary for the emulsion to reach the required temperature. As a result, a total length of 2.20 m was chosen, from which 2.08 m were submerged into an oil bath (MGW Lauda) with a capacity of approximately 3 litres. The rest of the copper tubing was used to make connections with the rig on each side: 5.5 cm for the inlet and 6.5 cm for the outlet. Thermocouples were placed at each extremity of the coil using T-junctions as done previously in Section 4.3.1.

4.4- Preliminary experiments and subsequent rig corrections

All the calculations and assumptions presented previously were done using many approximations. As a consequence, results may differ significantly from what was estimated. A few experiments were carried out to check the rig met the design specifications and to see how experiments could differ from theory.

4.4.1- Micromixer efficiency

The channels of the micromixer had very fine dimensions (45 by 200 μm) **[96]**. As a consequence, there was an important pressure build-up at the entrance of the mixer. The connections made with Teflon tubing were too weak to be subjected

to high pressure. Therefore, even though the provider suggested that the micromixer could be used up to 25 mL min^{-1}, the connections popped out if the total flow rate exceeded 8 mL min^{-1}, which decreased significantly the range of flow rates the rig could be used at.

In order to evaluate the efficiency of mixing with the maximum flow rate possible, experiments were done with soya bean oil on one side (A) and a solution of Brij 97 at 22.2 % (w / w) on the other (B) at different flow rates:

- 1: $\dot{V}_A$ =0.86 mL min^{-1} and $\dot{V}_B$ =7.14 mL min^{-1} (emulsion with 10 % (w / w) of soya oil)
- 2: $\dot{V}_A$ =0.43 mL min^{-1} and $\dot{V}_B$ =7.57 mL min^{-1} (emulsion with 5 % (w / w) of soya oil)

The resulting emulsions were collected after their passage in the micromixer i.e. they were not subjected to any thermal treatments. For both combinations of flow rates, the micromixer was not efficient for the preparation of good pre-emulsions. The mixtures settled into 2 different phases within a few minutes: soya oil on top (clear yellow), and solution of Brij 97 at the bottom (transparent). Their appearance were very different from the coarse emulsions prepared in Chapter 3 (Figure 3.9), for which even when the emulsions were highly unstable the cream layer was white due to the partitioning of the surfactant between the aqueous and oil phase.

The preliminary experiments with the micromixer demonstrated that the latter did not enable the rig to work optimally. It did not fulfil its function at mixing and also hindered the overall performance of the rig by limiting the range of possible flow rates. The acquisition of a micromixer allowing work at high pressures being too expensive, it was decided that it would be replaced by a T-junction in stainless steel from Swagelok. Using this strategy, the panel of possible flow rates could be enhanced.

4.4.2- Heat transfer – heating side

In order to check that the copper coil length calculated previously was sufficient to heat the emulsions at the required temperature, tests were carried out (these experiments were performed before the replacement of the micromixer, hence the use of a maximum flow rate of 8 mL min^{-1}). Water at room temperature was circulated in the coil at different flow rates and the oil bath temperature was set at 95 °C. Then, the water temperature after passage in the oil bath was measured at the copper coil outlet, located 4.5 cm away from the oil surface (See experiments 1, 3, 5 and 7 in Table 4.1). The measurements were collected after a circulation of at least 4 minutes as it was observed that around 2 min 30 sec were necessary for the system to reach steady state whichever flow rate was chosen (Figure 4.9).

Table 4.1: Water temperature after passage in the copper coil

The tip of the thermocouple was placed in the rig tubing at 4.5 cm above the oil bath surface at an average temperature of 95 °C. Experiments 1, 3, 5 and 7 were performed without insulation and *experiments 2, 4, 6 and 8 with the Armaflex protection*.

Experiment	$\dot{V}_{water}$ in mL min^{-1}	T_{water} in °C	T_{water}-T_{bath} in °C
1	8	91.28	3.48
2	*8*	*93.26*	*1.39*
3	4	89.15	5.55
4	*4*	*92.41*	*2.09*
5	2	84.94	9.27
6	*2*	*90.42*	*4.89*
7	1	72.91	12.33
8	*1*	*87.07*	*7.77*

The water temperatures at the coil outlet in experiments 1, 3, 5 and 7 of Table 4.1 were all very inferior to the oil bath temperature. What is more, the slower the water flow was, the more important was the difference between these two

temperatures. As a consequence, it was deduced that the water probably reached the temperature of the oil bath through its circulation in the copper coil. However, it lost a significant amount of heat as soon as the copper coil emerged from the oil.

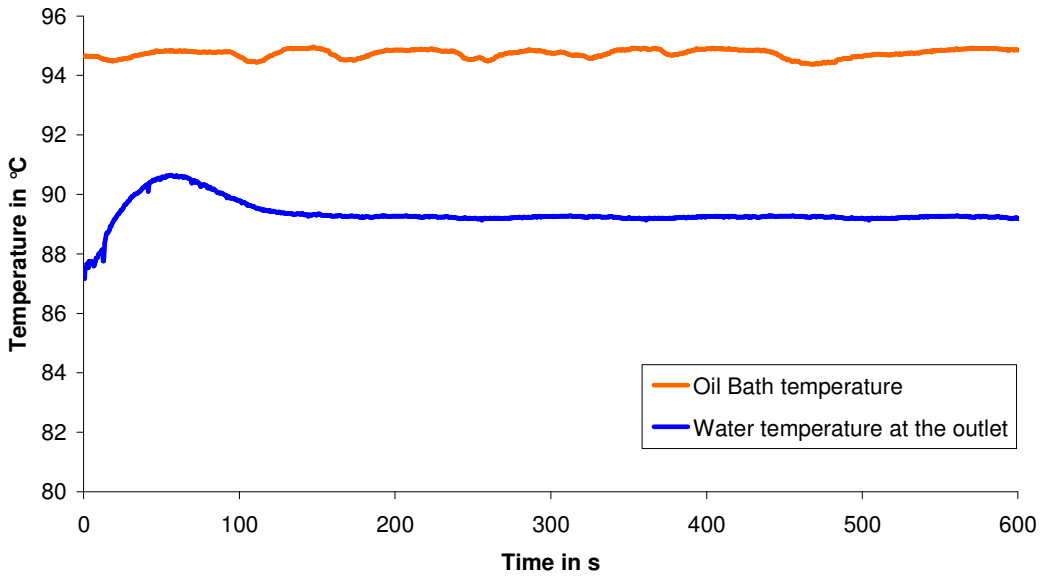

Figure 4.9: Illustration of the time required to reach equilibrium.

An example with a flow rate of 4 mL min^{-1}.

t=0s corresponds with the start of the pumps.

To reduce this heat loss as much as possible, insulating tape Armaflex (Armacell) was wrapped around the part of copper coil that was not immersed in oil and around the connectors that led to the heat exchanger. To check the effectiveness of the insulation, the tests were repeated and compared with the previous results (See experiments 2, 4, 6 and 8 in Table 4.1). The Table 4.1 shows that the addition of the lagging tape reduced the initial heat loss between 36 and 62 %.

Table 4.2: Water temperature measurements and estimations with an oil bath at 95 °C

h represents the height above the oil surface.

$\dot{V}_{water}$ in mL min^{-1}	T_{water} (measured) in °C (h = 4.5 cm)	T_L (calculated) in °C (h = 0 cm)	T_L-T_{water} in °C
5	92.93	95	2.07
10	93.69	94.80	1.11
15	92.67	93.58	0.91

After these experiments, the micromixer was replaced by a simple T-junction. As a consequence, higher flow rates could be tested (Table 4.2). Also, soon after starting the experiments with the rig, the oil bath was replaced by a stirred bath GD120-S5 from Grant (***h*** on Figure 4.14). The copper coil and lagging disposition were not modified.

In Table 4.2, it can be observed that for 5 and 10 mL min^{-1}, the temperature at the outlet increased with the flow rates as it was seen previously in Table 4.1. However, the temperature obtained for 15 mL min^{-1} did not follow this trend. Actually, this behaviour can be explained by the fact that the water does not reach the oil bath temperature above a certain flow rate. Indeed, using Equations 4.1 and 4.4, it was possible to estimate the water temperature just before it emerges from the oil bath in function of the flow rate:

$$T_L = \frac{T_{bath}\left(e^{\frac{U_{copper}\times A_{coil}}{G_{emulsion}\times C_p}} - 1\right) + T_0}{\left(e^{\frac{U_{copper}\times A_{coil}}{G_{emulsion}\times C_p}}\right)}$$

Equation 4.7

The difference between the estimated temperature at the oil surface and the temperature measured by the thermocouple (that is to say 4.5 cm above the oil surface) tended to decrease with the increase of flow rate (Table 4.2). Thus, a slow flow rate would generate more heat loss than a fast one during the passage of water in the 4.5 cm of tubing above the oil surface. The loss of heat outside the oil bath is immediate and the drop of temperature can be noticed even after passage in a very small section of the tubing. When the flow rate is slow, this drop is more important.

Using the same equations, it was possible to determine the residence time of the liquid above a certain temperature depending on its flow rate. For example, if this temperature was chosen as one of the HLB temperatures, the combination of Equations 4.1 and 4.4 could enable to estimate the area of copper coil necessary to reach that temperature:

$$A_{HLB} = \frac{G_{emulsion} \times C_p \times \ln\left(\frac{T_{bath} - T_0}{T_{bath} - T_{HLB}}\right)}{U_{copper}}$$ **Equation 4.8**

Then A_{HLB} can be used to get $t_{T \geq HLB}$, the time spent above the HLB:

$$t_{T \geq HLB} = \frac{(L - \frac{A_{HLB}}{ID \times \pi}) \times \pi \times \left(\frac{ID}{2}\right)^2}{\dot{V}_{emulsion}}$$ **Equation 4.9**

In Table 4.3, the time spent above the highest and lowest HLB temperatures found in Chapter 3 for different flow rates is presented in the case of 2 different oil bath temperatures. It can be seen that for the same flow rate, the time of residence above the HLB is more important when the oil bath is set at a high temperature. As a consequence, when working with the same flow rate, it can be deduced that the heating rate is faster when the oil bath is at higher temperature.

Table 4.3: Estimation of the time spent above the PIT for different flow rates.

T_{Bath} in °C	$\dot{V}_{water}$ in mL min^{-1}	$t_{T \geq 74\,°C}$ in s	$t_{T \geq 88\,°C}$ in s
80	5	40	0
	10	15	0
	15	7	0
95	5	44	40
	10	19	15
	15	11	7

4.4.3- Heat transfer – cooling side

Water was run through the microheat exchanger to check that it behaved as predicted in the Section 4.3.2. The peristaltic pump delivered ethylene glycol around 10 °C at its highest capacity i.e. 13 mL min^{-1}. Figure 4.10 and 4.11 represent the evolution of the temperature at the outlet of the cooler for flow rates being respectively 8 and 15 mL min^{-1}.

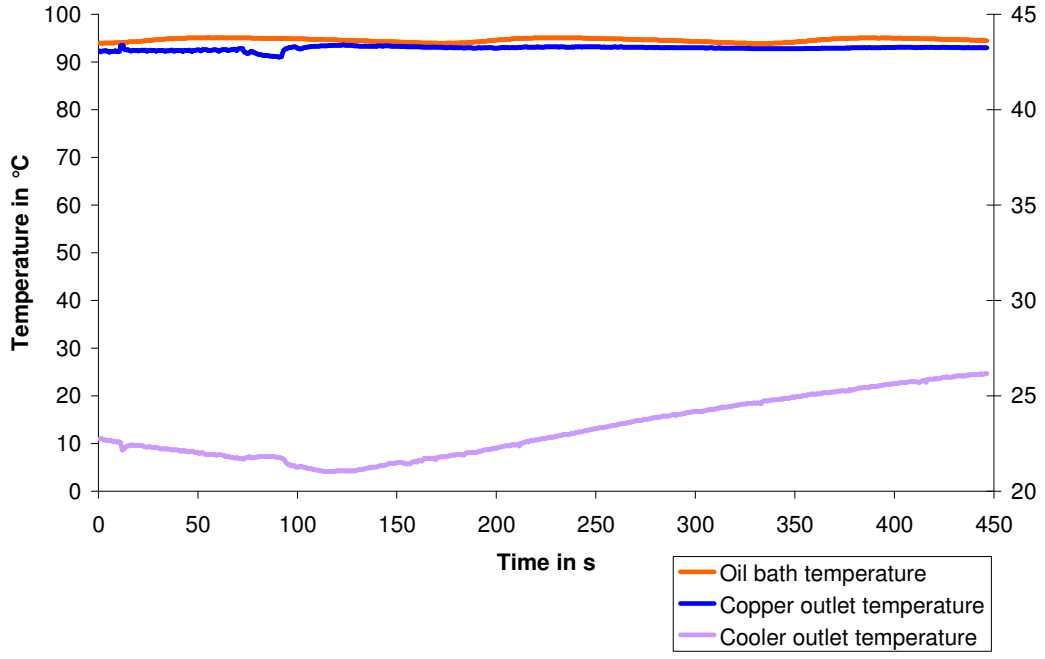

Figure 4.10: Temperature at the outlet of the heat exchanger for 8 mL min^{-1}

The secondary axis (on the right side) is used for the cooler outlet temperature in °C

The results presented in Figure 4.10 show that cooling was achieved. However, the cooler outlet temperature did not seem to reach a steady state and slowly increased. As a consequence, in order to cool down the emulsion efficiently around 20 °C with a fast rate, experiments needed to be done not long after the start of the rig. As the goal of the rig development is to prepare emulsions continuously, this solution reveals to be a great contradiction. For higher flow rates such as 15 mL min^{-1} (Figure 4.11), the problem was even more acute. The cooler outlet temperature went quickly

above 40 °C, which would prevent the preparation of emulsions under steady conditions.

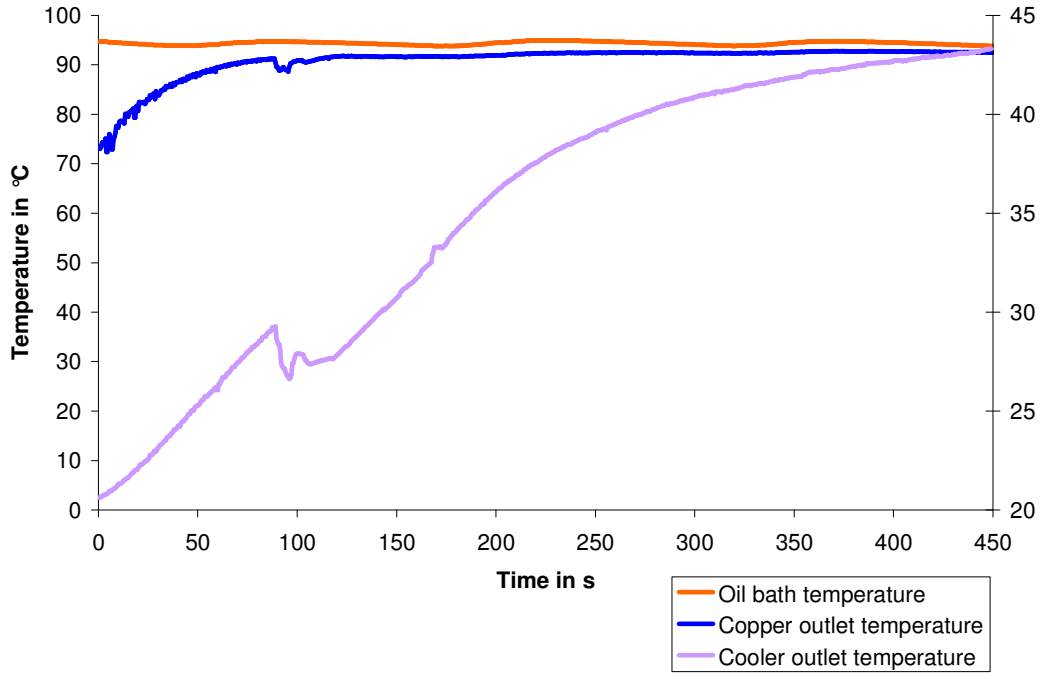

Figure 4.11: Temperature at the outlet of the heat exchanger for 15 mL min^{-1}
The secondary axis (on the right side) is used for the cooler outlet temperature in °C

The heat exchanger (***h-e*** on Figure 4.14) was not able to function properly due to the poor flow rates provided by the peristaltic pump. The use of a more powerful pump was paramount to solve this problem. The peristaltic pump got replaced by a gear pump (Verder) with a maximum flow rate of 15 L hr^{-1} (***p3*** on Figure 4.14). It enabled an efficient cooling of the water as shown in Figure 4.12. It presents the evolution of the temperature at the cooler outlet which quickly stabilised around 15 °C. Since the inner volume of the heat exchanger was small (32 mm^3 per layer **[98]**), the time required to get from the initial temperature to a temperature close to ambient temperature was very short: around 20s for a flow rate of 1 mL min^{-1} and only one second for a flow rate of 15 mL min^{-1}.

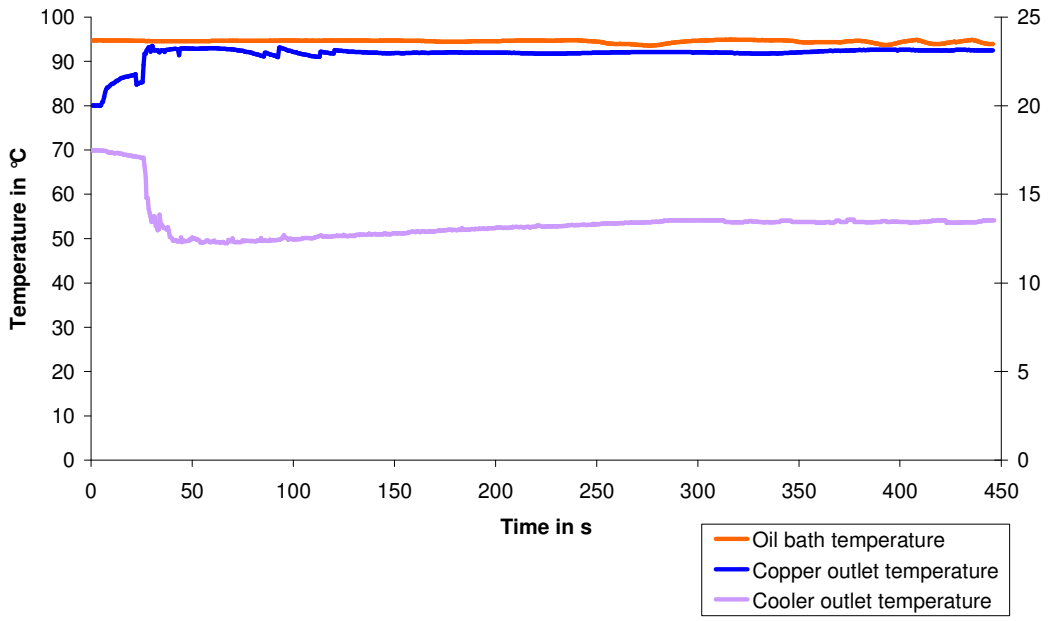

Figure 4.12: Temperature at the outlet of the heat exchanger for 15 mL min^{-1} using the gear pump

The secondary axis (on the right side) is used for the cooler outlet temperature in °C, the gear pump was used at a flow rate of 40 mL min^{-1}.

4.4.4- Tests with pre-emulsion

As explained previously in Section 4.4.1, without micromixer, the premixed emulsions could not be prepared online. Pre-emulsion needed to be made before using the rig and were introduced directly in one of the feed bottles (***p-e*** on Figure 4.14). When these coarse emulsions were used for the first time, a few problems occurred.

A coarse emulsion with a composition 10 % (w / w) Soya bean oil / 20 % (w / w) Brij 97 / 70 % (w / w) Water was pumped into the rig with a flow rate of 5 mL min^{-1}. The oil bath (***h*** on Figure 4.14) was heated up at 95 °C. Shortly after starting, the rig quickly stopped functioning due to a clogging in the copper tubing and heat exchanger. The rig also appeared to have leaked from the plastic valves, probably because of the increasing pressure provoked by the blockage. The rig had to be opened and cleaned.

As a consequence of these problems, the experimental rig was modified. First, a water backflush / flush system was set in order to clean the rig without having to dismantle it and prevent its clogging by the gelation of emulsions inside the tubing. A valve was added before the copper coil to allow a cleaning of the pipes without having to change the content of the feed tanks (considering the use the second pump in the eventuality of the acquisition of an adequate micromixer). A peristaltic pump Watson Marlow 101U was used for flushing (***p4*** on Figure 4.14). The protocol consisting in flushing water for at least 4 minutes before putting the emulsion constituents in circulation might help reduce the time of equilibration and decrease the risk of clogging. From that point onwards, all experiments would follow this principle.

Then, a pressure gauge (Figure 4.15) was placed before the copper coil. It would permit to check the occurrence of a pressure build-up and allow a quick reaction in the case of the onset of clogging. The plastic valves that had leaked were exchanged for Stainless steel valves (Swagelok). Finally, a valve was added between the copper coil and the microheat exchanger (***h-e*** on Figure 4.14). It would enable to take samples of the emulsions and check on their apparent viscosity before opening the whole rig. It also could give the opportunity to look at the effect of a slower cooling rate compared to the one provided by the heat exchanger (Figure 4.13).

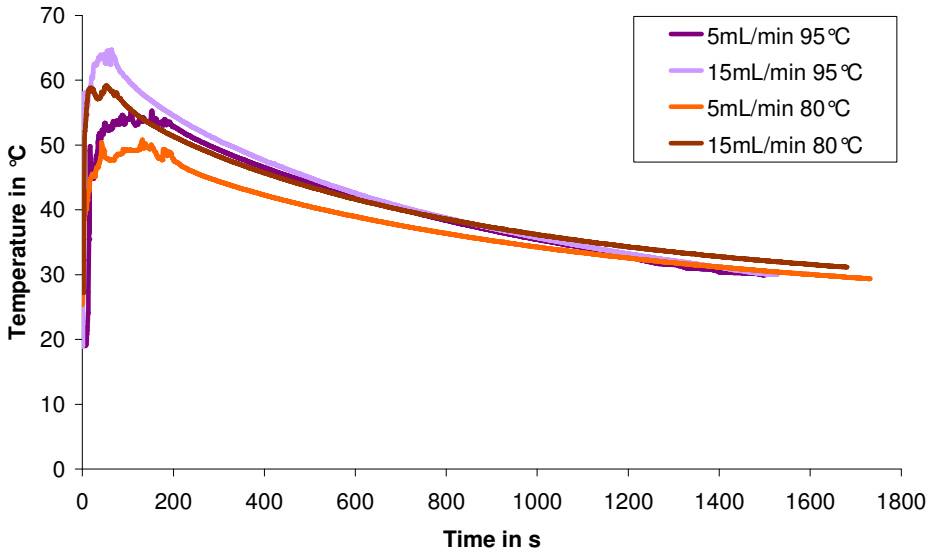

Figure 4.13: Cooling of 15 mL of water collected using the valve after the copper coil

In Figure 4.13, the flow rates and the oil bath temperature were changed to see the influence of these parameters on the temperature of the resulting samples. It can be observed that the loss of heat was very quick, especially at the beginning of the experiment. When the samples at 15 mL min^{-1} were collected, they had already lost more than 20 °C compared to the corresponding oil bath condition and the samples at 5 mL min^{-1} up to 40 °C. This means that the cooling rate was still very high at the start of the collection even though the heat exchanger was not used. However, the samples resided around 10 minutes in the region 50 to 40 °C and took around an hour to get to ambient temperature which was definitely slower than the heat exchanger that brought samples down to ambient temperature in less than 20 s.

Figure 4.14: Final version of the PIT emulsification rig

c: cooling bath, ***cl***: feed bottle for cleaning, ***h***: heating bath, ***h-e***: microheat exchanger, ***m-p1***: micropump for coarse emulsion, ***m-p2***: micropump for cleaning, ***p3***: gear pump, ***p4***: peristaltic pump for flushing, ***s***: magnetic stirrer, ***TrD***: TracerDaq softaware used to determine the evolution of temperatures with time

4.5- Summary

A rig was designed in order to be able to prepare emulsions continuously with the PIT technique. When the initial plans were drawn, a prototype was built and tested. After the preliminary experiments, changes were made, the most important being the suppression of the micromixer. As a consequence, the machine lost the function of preparing unique compositions by the way of modulating the velocity of the pumps but higher flow rates could be explored. Also, since the micromixer did not get replaced during the different series of experiments, it was possible to use one of the tanks for the cleaning of the rig (***cl*** on Figure 4.14). Finally, the unexpected clogging of the rig led to the introduction of a valve between the two heat transfer components. Additional emulsion samples with a slower cooling rate could be collected using this path. A picture and a schematic of the final version of the rig are presented in Figure 4.14 and 4.15.

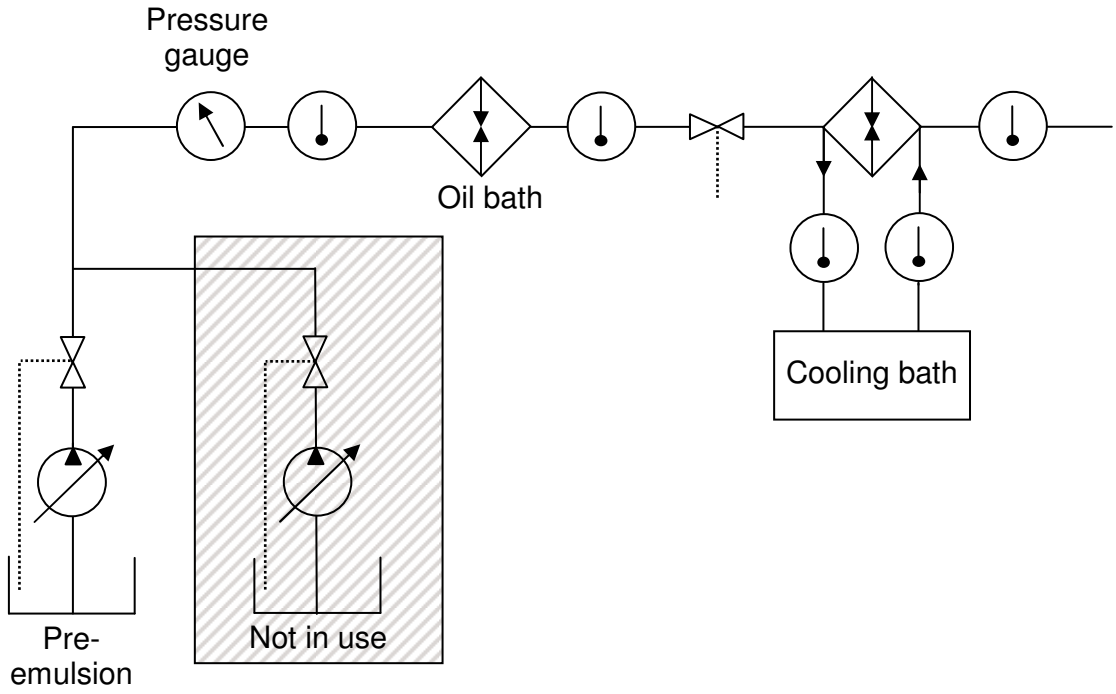

Figure 4.15: Schematic of the final rig

Chapter 5 – Continuous emulsification

5.1- Introduction

After the rig described in Chapter 4 had been built, it was important to understand how the experimental conditions influenced the characteristics of the resulting emulsions. Experiments were performed in order to find the best factors to make the machine work optimally.

The rig parameters which were examined are:
- the composition of the coarse emulsion and the preparation methods,
- the flow rate of the emulsion in the tubing,
- the cooling treatment which was modulated using two different outlets to collect the treated emulsions, one after the heating coil to allow slow cooling and one after the heat exchanger in which the emulsions were rapidly cooled down.
- the heating treatment which could be modified according to the flow rates used and the temperature of the heating fluid.

The resulting variables that were analysed are:
- the size of the treated emulsion droplets using microscopy and DLS,
- the emulsion appearance using the spectrophotometer and visual observation,
- the stability by repeating the tests on 45-day-old emulsions.

All these factors, parameters and variables were closely linked together. In order to present the results in the clearest way as possible, the parameters are introduced using the following protocol. At the beginning, all but one are kept constant. The importance of the one parameter will be discussed briefly and the influence of the others will be temporarily ignored to be dealt with only later, i.e. when they are modified themselves. Tackling with the second parameter, all but the second and first parameters will be kept constant and the discussion will broaden on the cross-influence of the two studied conditions. Analysing the experiments following this method, parameter after parameter, should enable to understand the combined actions that the different factors may have on each other.

The last section of this chapter is a short comparison between the experiment results obtained with the batch and the continuous processes. It enables to check if the expectations for the rig were met.

5.2- Pre-emulsion preparation

Before starting the analyses of the influence of the different parameters, the pre-emulsion preparation will be presented. Indeed, as explained in Chapter 4, due to problem with the mixer, it was decided that the coarse emulsions would not be processed online: only one of the pumps was used to pump emulsions in the rig and pre-emulsions were prepared in advance. In order to explore the parameters of the machine, the range of compositions was narrowed down to 3 (5, 7.5 and 10 % (w / w)).

A solution of Brij 97 in water was prepared with 22.2 % (w / w) of surfactant and as a consequence, the ratio of Brij 97 to water remained unchanged in all the samples. Only the concentration of soya bean oil was varied: 5, 7.5 and 10 % (w / w). The coarse emulsion was prepared this way in order to reproduce the same compositions when using the micromixer online (i.e. with the Brij 97 solution at 22.2 % (w / w) pumped on one side and the soya been oil on the other). However, due to the change in the building of the rig explained in Section 4.4.4, this latter experiment was not pursued.

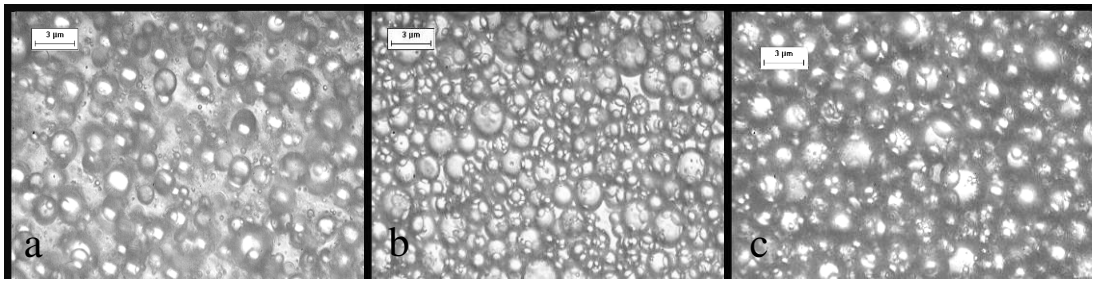

Figure 5.1: Micrographs of the coarse emulsions made with the solution of Brij 97 at 22.2 % (w / w)

Content of soya bean oil in % (w / w): a→5, b→7.5 and c→10. Scale bar = 3 µm

Micrographs of the pre-emulsions were taken (Figure 5.1). They show very polydispersed droplets with a size up to 2 µm for 5 and 7.5 % (w / w) (*a* and *b*) and up to 3 µm in the case 10 % (w / w) of soya bean oil (*c*). These big droplets began to cream very fast after preparation, i.e. within the first 20 minutes. Two phases were clearly separated after an hour (Figure 5.2).

Figure 5.2: Creaming of the coarse emulsions made with the solution of Brij 97 at 22.2 % (w / w)
Content of soya bean oil in % (w / w): A and D→10, B and E→7.5 and C and F→5.

The PIT values for these three emulsions were evaluated with the turbidity method as described in Chapter 3 (Table 5.1). They were very close to the HLB temperatures found for the emulsions made previously with a content of 20 % (w / w) of Brij 97. They were 73, 82 and 88 °C for soya bean oil concentration of 5, 7.5 and 10 % (w / w) respectively (Table 3.3). More than the small change in compositions, the visual inaccuracy inherent to the determination of the start of turbidity could be taken into account to explain the slight difference observed between the two sets of experiments.

Table 5.1: PIT of 3 different emulsions made with an aqueous solution at 22.2 % (w / w) of Brij 97

Content of soya bean oil in % (w / w)	PIT in °C
5	74
7.5	83
10	88

5.3- Influence of different factors on size and polydispersity index

5.3.1- Influence of the oil content

Pre-mixed solutions were prepared at concentration 5, 7.5 and 10 % (w / w) of soya bean oil with a solution of Brij 97 at 22.2 % (w / w) by simple stirring with a magnetic stirrer as described in Section 5.1. The oil bath was first set up at 95 ºC. This temperature was chosen since it is above the Phase Inversion Temperature of each of the 3 different compositions being studied (Table 5.1). The rig was left running at constant flow rate (7.5 mL min^{-1}) for at least 4 minutes to let it reach a thermal steady state, then 15 mL samples were collected from the outlet after the copper coil. Analyses were performed on the samples once they reached ambient temperature. The results of the analyses of droplet size with DLS are presented in Figure 5.3 and 5.4.

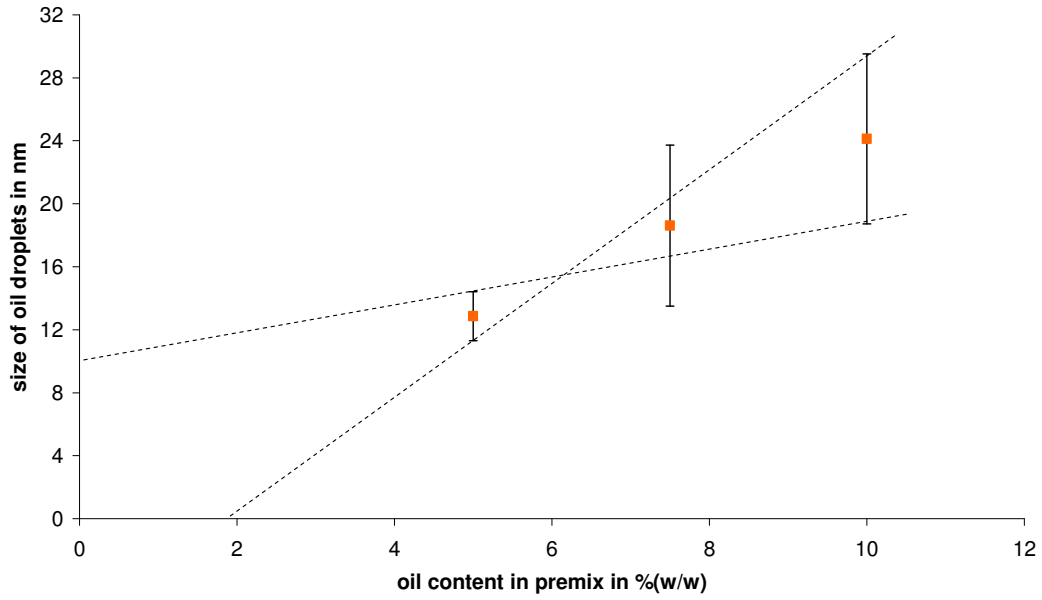

Figure 5.3: Evolution of the droplet size of nanoemulsions prepared with the rig at constant flow rate (7.5 mL min^{-1}) with soya bean oil content

The dotted lines present the estimation of the standard error on the slope value.

The coarse emulsions were prepared using an aqueous solution at 22.2 % (w / w) of Brij 97. The ratio of Brij 97 to water is kept constant.

The error bars in Figure 5.3 and 5.4 and in the next graphs involving the size of nanoemulsion droplets and polydispersity index have been estimated using the standard deviation between all the experiment results (as mentioned previously, at least 4 samples were prepared for each set of conditions and the measurements with the DLS were repeated a minimum of 4 times).

As expected from the results of the batch experiments described in Chapter 3, Figure 5.3 shows that the droplet size increased with the oil content. The PdI in Figure 5.4 did not present a clear trend. Again, as observed in the previous chapters, the DLS apparatus does not seem to give accurate measurements of this value.

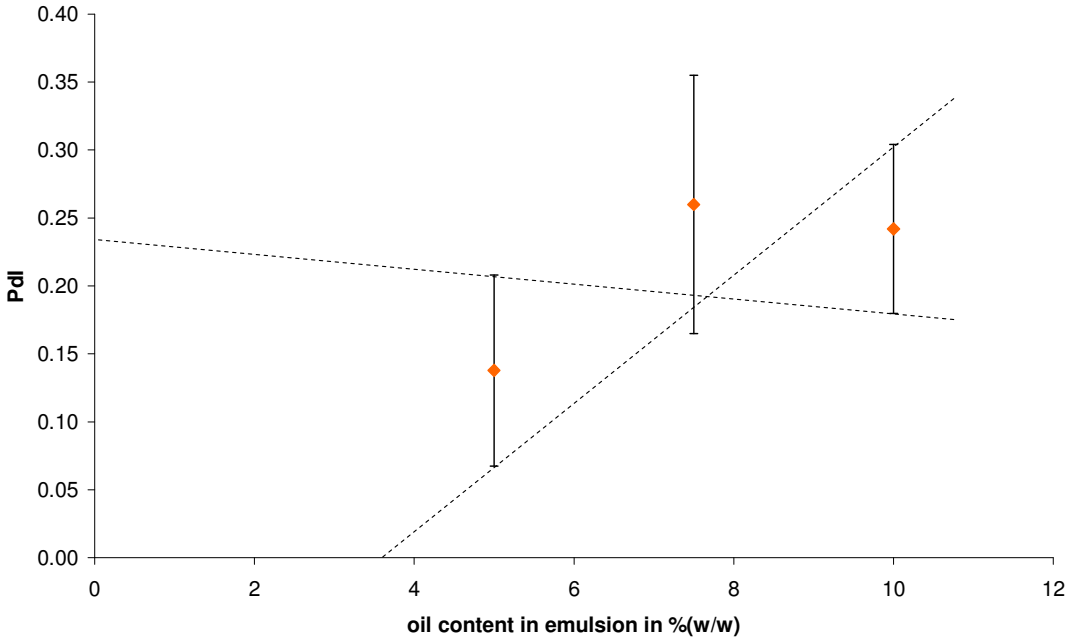

Figure 5.4: Evolution of the polydispersity index of nanoemulsions prepared with the rig at constant flow rate (7.5mL min^{-1}) with soya bean oil content

The dotted lines present the estimation of the standard error on the slope value.

The premixed emulsions were prepared using an aqueous solution at 22.2 % (w / w) of Brij 97. The ratio of Brij 97 to water is kept constant.

5.3.2- Influence of the flow rate

The flow rate of the coarse emulsions in the rig was varied between 2 and 15 mL min^{-1}. It was observed that the viscosity of 10 % (w / w) soya bean oil pre-emulsion increased when it went through the heating part at 2 mL min^{-1} causing not

only a pressure build-up in the tubing visible on the pressure gauge (Figure 4.15) but also the formation of gel. As a consequence, a very inhomogeneous liquid-gel system was obtained when collection of samples was performed after the heating coil. The gel parts inside the emulsion would liquefy within a few hours or days after formation. This gelation of the emulsion might be the consequence of the long residence time at 95 °C.

For flow rates between 5 and 15 mL min^{-1} and compositions with 7.5 and 10 % (w / w) of oil, even though the heated pre-emulsions were liquid at the outlet of the heating coil, a layer of gel sometimes appeared at the surface of the liquid when it was left to cool down at ambient temperature. This gel might have been produced because of the surface dehydration of the samples. In order to measure the size of the droplets using the DLS, this layer was allowed to dissolve back into the rest of the liquid, usually making the liquid less transparent in appearance.

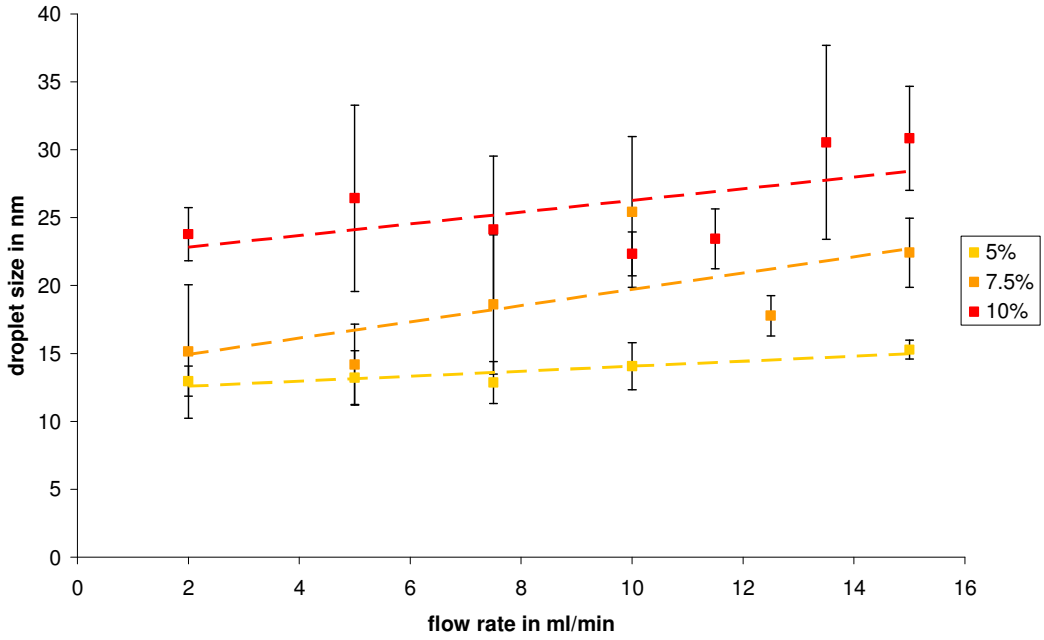

Figure 5.5: Influence of the flow rate on the droplet size of emulsions containing 5, 7.5 and 10 % (w / w) of soya bean oil

The coarse emulsions were prepared using an aqueous solution at 22.2 % (w / w) of Brij 97. The ratio of Brij 97 to water is kept constant.

The same protocol was followed for the emulsions at 10 % (w / w) oil produced at 2 mL min^{-1}. For all the other compositions and flow rates, the samples collected at the outlet would remain liquid during their cooling.

Figure 5.5, 5.6 and 5.7 present the results obtained from these experiments. A few observations can be made. First, the influence of the oil concentration in the emulsions can be highlighted once more; the oil droplets were bigger at high concentration as can be seen on Figure 5.5.

Then, the droplet size error bars for 5 % (w / w) oil emulsion were smaller than for the two other oil content emulsions. This might be due to the gelation at surface that sometimes appeared on samples with 7.5 and 10 % (w / w) concentration. On melting, the gel layer might generate droplets with a different size than the ones in the bulk. This would introduce a source of inhomogeneity in the data since the average value was taken from all the samples prepared under the same conditions, independently of the fact that a gel layer had appeared or not.

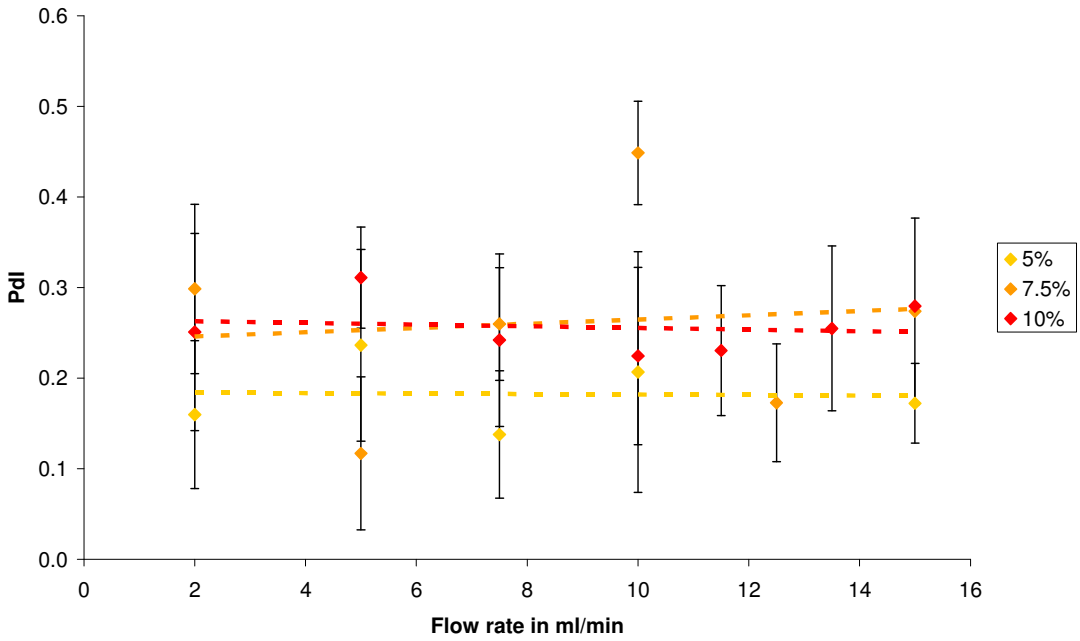

Figure 5.6: Influence of the flow rate on the polydispersity index for emulsions containing 5, 7.5 and 10 % (w / w) of soya bean oil

The coarse emulsions were prepared using an aqueous solution at 22.2 % (w / w) of Brij 97. The ratio of Brij 97 to water is kept constant.

As a consequence, these experiments were certainly less reproducible than those at 5 % (w / w) of soya bean oil. Actually, emulsions with a concentration of 7.5 % (w / w) of soya oil were the most sensitive to gelation at surface after passage in the heating coil. This could explain why the trends of both its PdI and droplet size as a function of flow rate for this concentration in Figure 5.5 and 5.6 were not as clear as for the two other compositions. Besides, its different behaviour compared to 5 % (w / w) and 10 % (w / w) oil emulsions was particularly evident on Figure 5.7 where the measurements for 7.5 % (w / w) soya oil were more spread-out than for the two other compositions.

The error bar on the droplet size of the emulsion at 10 % (w / w) of soya bean oil made at 2 mL min^{-1} (Figure 5.5) is quite small (±2 nm) even though it was explained beforehand that it was subject to gelation. Two reasons can be given to explain this observation. All the samples created under these conditions were subjected to the gelation; hence, the experiments were more reproducible and no discrepancy was noticed in the data. The second reason could be that the gelation phenomenon is different from the gelation at the surface of the sample. Indeed, the gel is produced somewhere in the tubing of the set-up, during or just after the heating treatment, whereas the gelation at surface is only happening post-operation. The bulk itself was subjected to the changes provoked by the formation of the gel. For the polydispersity index (Figure 5.6), the error bars are important irrespectively of the experimental parameters i.e. flow rate and oil content. This leads to think that they were arising not only from the lack of reproducibility of the experiments due to the gelation phenomenon but also from the measuring instrument itself.

Finally, the results in Figure 5.5 and 5.6 seem to imply that the effects of the flow rate on the droplet size were very small. The trend lines are linear and even though they tend to go slightly upwards in Figure 5.5, all of them are very close to horizontal. To confirm this trend, t-tests were performed for emulsions of the same concentration prepared at 2 and 15 mL min^{-1}. For emulsions at 5 % (w / w) in soya bean oil, the P-value is 0.25. That indicates there's no significant difference between the size of emulsions prepared at 2 mL min^{-1} and those at 15 mL min^{-1}. However, as the concentration in soya bean oil increases, the P-value decreases (the P-values of emulsions at 7.5 and 10 % (w / w) in soya bean oil prepared at 2 and 15 mL min^{-1} are

respectively 0.04 and 4 10^{-9}). This shows that the flow rate gets a more significant influence on the size of the droplets as the oil concentration increases. This leads to the conclusion that the residence time of the emulsion above the HLB temperature has also an effect on their droplet size. For example, according to the calculations shown in Chapter 4 and making the approximation that $C_{p\ water}$ is equal to $C_{p\ pre\text{-}emulsion}$ since the pre-emulsions' main compound was water, the difference in droplet size between a mixture at 10 % (w / w) of soya bean oil heated for only 7 s above its Phase Inversion Temperature with a flow rate of 15 mL min^{-1} and for 40 s with a flow rate of 5 mL min^{-1} (Table 4.3) is 3 nm (Figure 5.5).

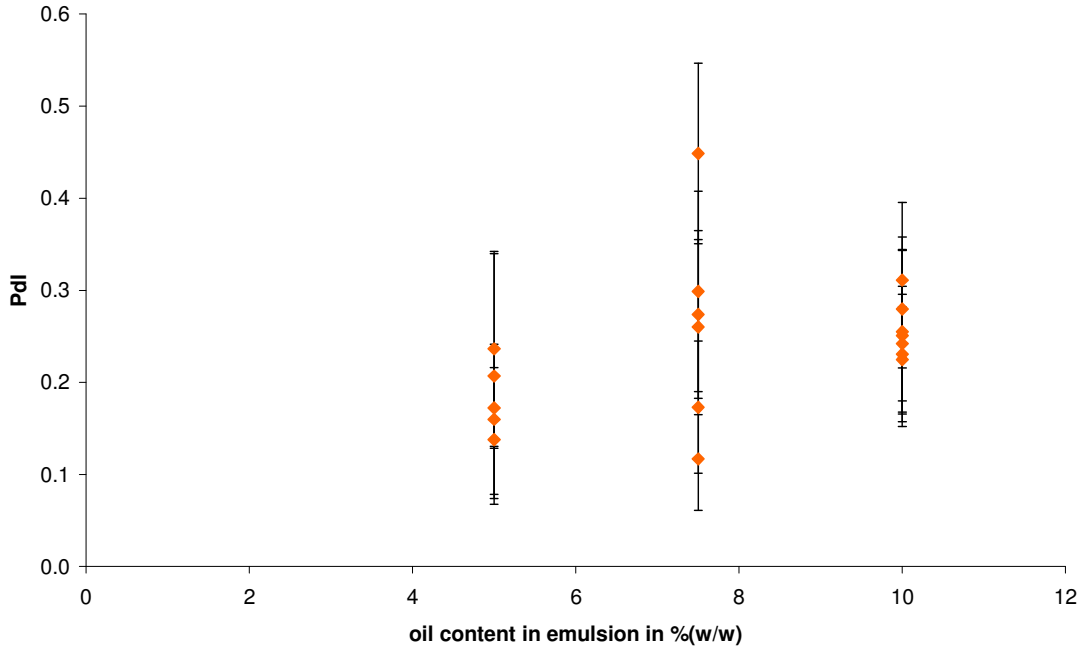

Figure 5.7: Evolution of the polydispersity index of nanoemulsions prepared with the rig at different flow rates (2-15 mL min^{-1}) with the soya bean oil content of the coarse emulsions

The coarse emulsions were prepared using an aqueous solution at 22.2 % (w / w) of Brij 97. The ratio of Brij 97 to water is kept constant.

Figure 5.7, which is a more detailed version of Figure 5.4, since more data have now been gathered, helps to answer to the question remained opened in Section 5.3.1, i.e. the influence of the oil concentration on the polydispersity of the emulsion. It seems from Figure 5.7 that the PdI increased with the oil concentration.

5.3.3- Influence of the cooling treatment

Rapid cooling was obtained using the second part of the rig: the microheat exchanger. The results are shown in three different figures (Figure 5.8, 5.9 and 5.10), one figure for each composition. The data from the slow cooling experiments shown previously in Section 5.3.2 is also presented in each diagram in order to draw a comparison between the two cooling modes and determine if the droplet size and polydispersity of nanoemulsions produced with the rig are dependent on the cooling treatment. For 10 % (w / w) of soya oil in emulsion, rapid cooling was only performed for flow rates above or equal to 10 mL min^{-1}. Indeed, under that threshold, the risk of clogging of the rig was high, and the results were quite irreproducible. The formation of gel, already mentioned in Section 5.3.2, blocked the cooling part, and resulted in the clogging of the experimental set-up.

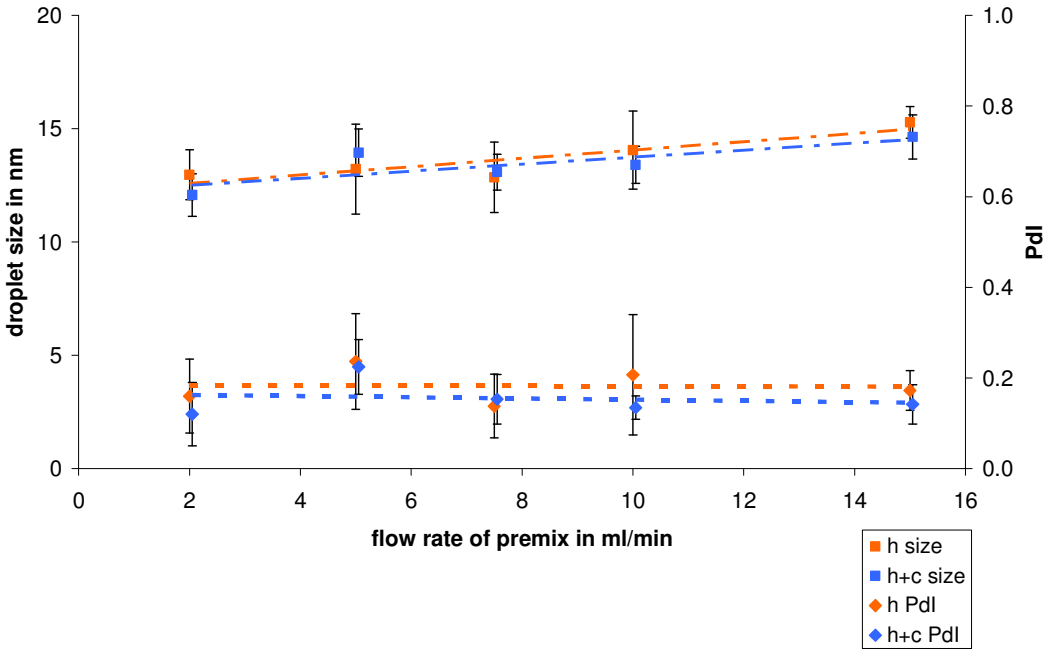

Figure 5.8: Comparison of the cooling treatment effects on 5 % (w / w) soya bean oil emulsions
h= slow cooling, h+c= fast cooling
The coarse emulsions were prepared using an aqueous solution at 22.2 % (w / w) of Brij 97.

In the Section 5.3.2, the gel was produced in the heating part of the rig for a flow rate of 2 mL min^{-1} only. As a consequence, it is supposed that when the rig was used at 5

and 7.5 mL min^{-1} with the heat exchanger, the gel was produced during the transfer from the heating part of the system to its cooling part or in the microheat exchanger itself.

On the three graphs, the standard deviations on both PdI and size droplets were smaller for the samples that went through the heating and cooling parts than that for the samples that went only through the heating part. As a result, it seems that the samples were more reproducible when they underwent a rapid cooling. It must also be noted that samples prepared using the cooling part of the rig presented a lower droplet size and polydispersity index on Figure 5.8, 5.9 and 5.10. The effect of the cooling treatment was more important as the oil concentration increased.

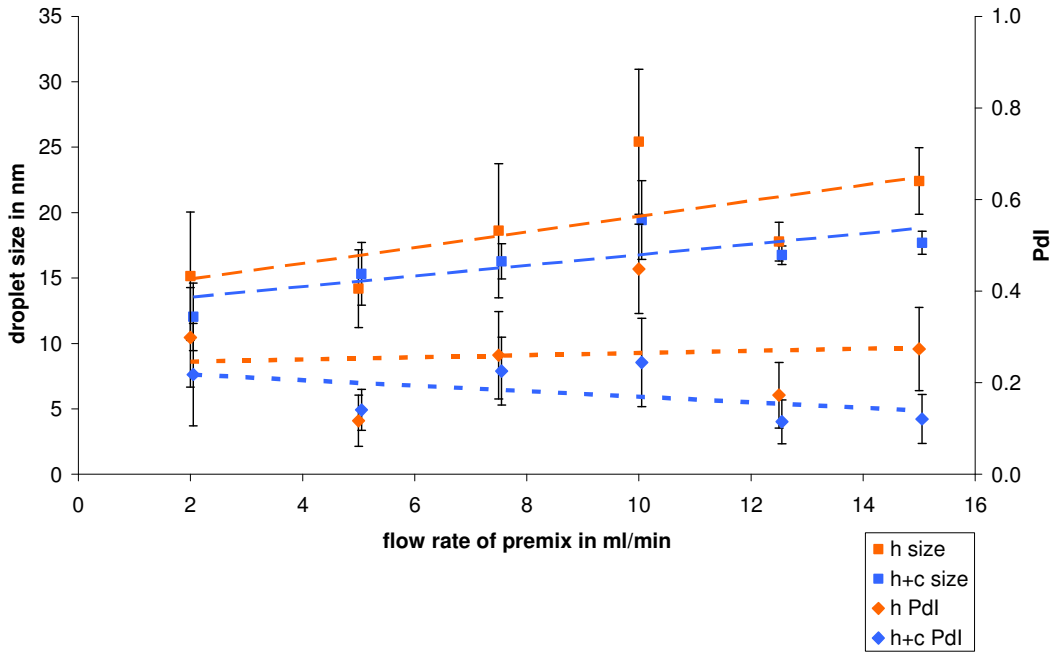

Figure 5.9: Comparison of the cooling treatment effects on 7.5 % (w / w) soya bean oil emulsions

h= slow cooling, h+c= fast cooling

The pre-emulsions were prepared using an aqueous solution at 22.2 % (w / w) of Brij 97.

When this size reduction was merely a few tenth of nm in the case of the 5 % (w / w) oil concentration emulsions (Figure 5.8), it went down of nearly ten nm with the 10

% (w / w) soya oil samples (Figure 5.10). This improvement in the emulsion characteristics might be the consequence of two factors.

First, in the same way as the batch experiments seen in Chapter 3, the rapid cooling allows the emulsion to get more rapidly out of the PIT zone where the droplets are very sensitive to Ostwald ripening. Another reason to explain this improvement might be the cooling homogeneity brought by the use of heat exchanger. Indeed, as already mentioned in Section 5.3.2, when the samples were left to cool at ambient temperature, the temperature at the surface got down quicker than in the bulk and a gel sometimes appeared on the surface. On the contrary, when using the heat exchanger system, it was noted that there was no gel layer formation at the surface of any samples. Indeed, when passing through the heat exchanger, it can be considered that the temperature of each emulsion drop decreased at the same rate until reaching ambient temperature. In Section 5.3.2, the gel formation was already thought to be a cause for high polydispersity index. The present results seem to confirm this hypothesis.

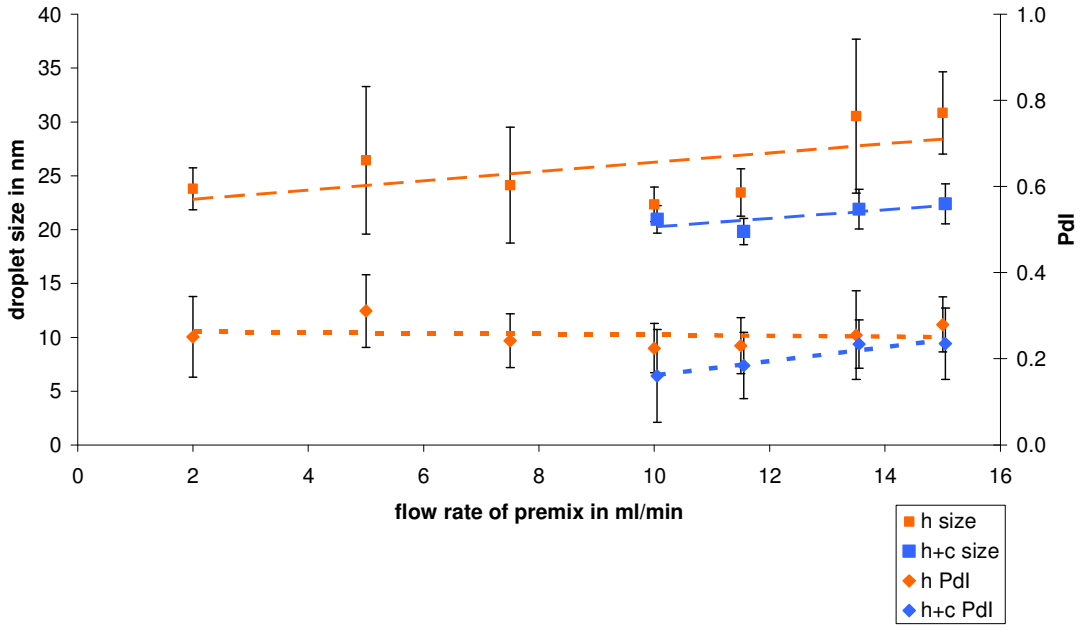

Figure 5.10: Comparison of the cooling treatment effects on 10 % (w / w) soya bean oil emulsions

h= slow cooling, h+c= fast cooling

The coarse emulsions were prepared using an aqueous solution at 22.2 % (w / w) of Brij 97.

5.3.4- Influence of the pre-emulsion mixing

It was decided to consider the importance of the pre-mixing on the quality of the resulting nanoemulsions. Two types of emulsions were used for this purpose: the simply stirred pre-emulsions described in Section 5.2 and the homogenized pre-emulsions prepared using a rotor-stator homogenizer Ultra-Turrax.

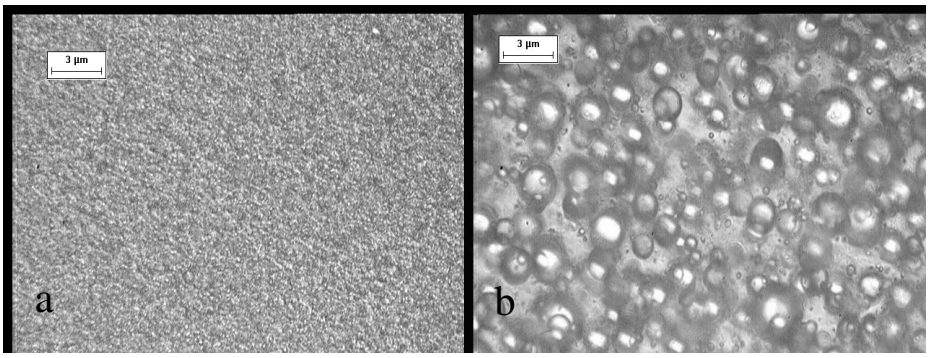

Figure 5.11: Micrographs of emulsions at 5 % (w / w) of soya bean oil

a) homogenized with ultra-turrax, b) mixed with a magnetic stirrer.

Pre-emulsions prepared using an aqueous solution at 22.2 % (w / w) of Brij 97. Scale bar = 3 µm.

The use of the homogenizer decreased the size of the pre-emulsion droplets greatly as observed on the micrographs in Figure 5.11. The size of these emulsion droplets (~0.2 µm) was 10 times smaller than that of the simply stirred coarse emulsions (~2 µm). Despite their better characteristic in term of size, they were still very unstable and the systems creamed very fast. The behaviour of these samples in term of creaming was very different to the simply stirred emulsions (Figure 5.12).

The simply stirred system did not show a clear boundary between the water and oily phase since it can be noted that the colour of the water phase got more transparent with time. On the contrary, the creaming boundary of the homogenized pre-emulsion was sharp (the colour of the water phase is very clear from the start of the creaming phenomenon) and its height increased with time. This indicates that the emulsion had a tendency to flocculate **[103]**.

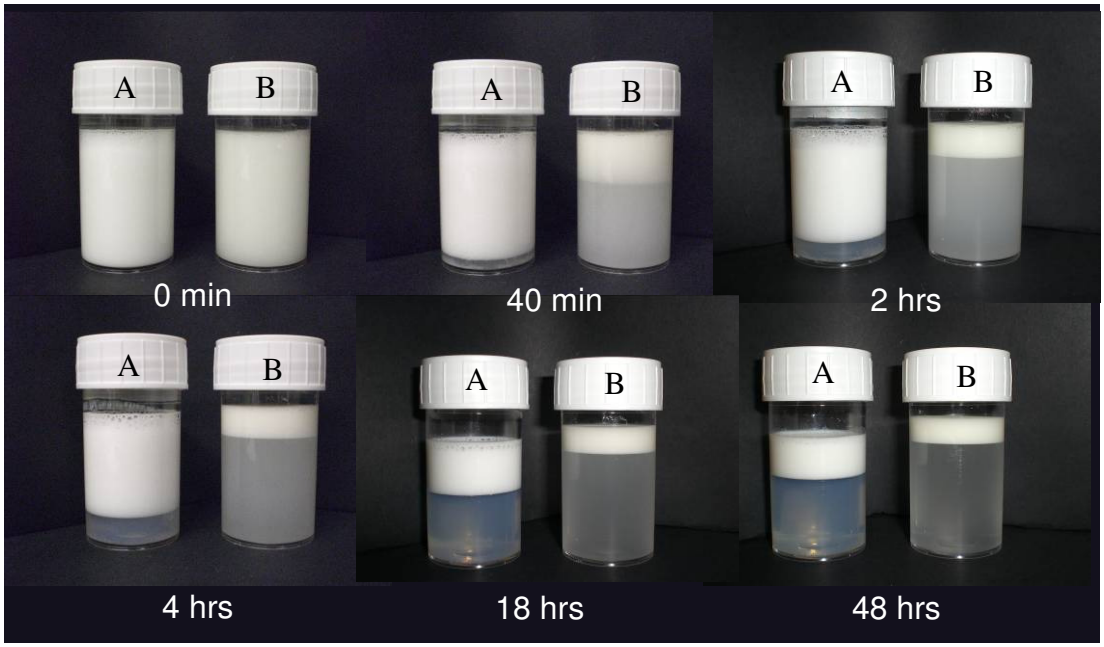

Figure 5.12: Evolution of creaming with time for two emulsions at 10 % (w / w) of soya bean oil

A) homogenized with ultra-turrax, B) mixed with a magnetic stirrer.

The coarse emulsions were prepared using an aqueous solution at 22.2 % (w / w) of Brij 97.

When the emulsion was observed using the microscope over time, this phenomenon was clearly visible (Figure 5.13). The emulsion made with simple stirring and the one made with the homogenizer seem to have a different final volume of oily phase on Figure 5.12. However, it is difficult to confirm it since the preparation of the emulsions caused in both cases the formation of foam, which is not discernable on the figure above.

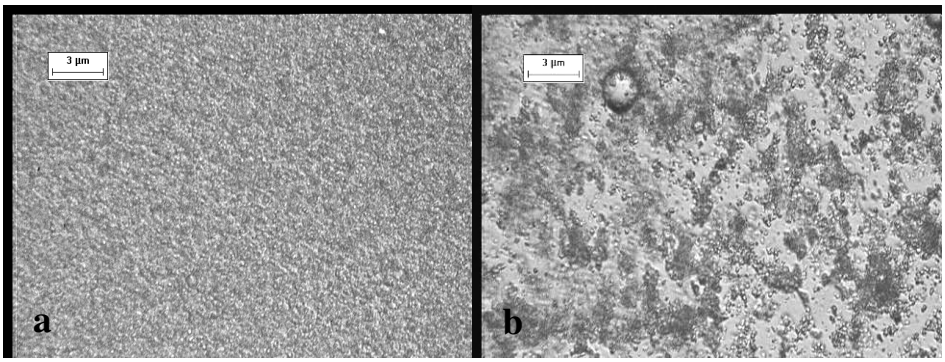

Figure 5.13: Micrographs of homogenized emulsion with 5 % (w / w) of soya bean oil

a) at time t=o; b) at t=10min. Scale bar = 3µm

The pre-emulsions were prepared using an aqueous solution at 22.2 % (w / w) of Brij 97.

Because of time constraints, tests with homogenized pre-emulsions were only done for a restricted number of conditions:

- oil bath temperature: 95 ºC
- flow rate: 10 mL min^{-1}
- cooling using the microheat exchanger

Since rapid cooling was chosen for these experiments, it was decided to present the results only after the section about the cooling rate influence to allow analyses of the fast cooling emulsions to be developed first. It can be seen on Figure 5.14 than the use of homogenized pre-emulsions seemed to improve the reproducibility of experiments since the error bars were smaller in that case. The droplet size and PdI tend to be smaller with the homogenized pre-emulsions. However, the reduction in size is not major: in the best case i.e 7.5 % (w / w) of soya oil, less than 2 nm are gained through the use of the homogenizer. The polydispersity trendline seems to be decreasing for the homogenized emulsion. The observation of this trend that had not appeared in the previous sections could be due to the better reproducibility of the experiments made with homogenized before.

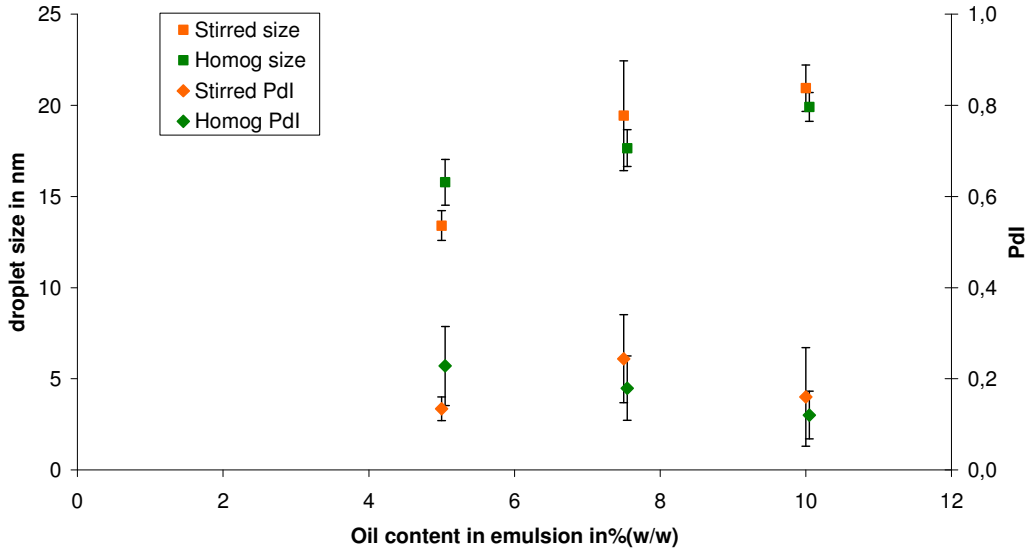

Figure 5.14: Comparison of the droplet size and PdI in function of the soya bean oil content for two types of pre-emulsions

The pre-emulsions emulsions were prepared using an aqueous solution at 22.2 % (w / w) of Brij 97

The use of a homogenizer prior to the thermal treatment seemed to enable the preparation of more reproducible nanoemulsions with the PIT technique. This should be taken into account when building the micromixer online. However, in the present work, it was not possible to prepare all the pre-emulsions using the homogenizer. Therefore, the experiments were pursued with simply stirred pre-emulsion.

5.3.5- Influence of the heating treatment

Changing the oil bath temperature results in the variation of 3 factors concerning the heating treatment:

- the highest temperature reached,
- the rate of heating,
- the time of residency above the PIT.

Whilst the influence of the time of residency has already been looked into in Section 5.3.2 through the modulation of the pre-emulsion flow rate and thought to be not very significant on the resulting droplet size and PdI of the nanoemulsions especially if the concentration in soya bean oil of the emulsion was small, the two other parameters have yet to be investigated. Experiments were performed to determine the influence of these factors. Samples were prepared with emulsions of concentration 5 and 10 % (w / w) of soya bean oil at 5 and 10 mL min^{-1} while setting the oil bath at different temperatures: 80, 85, 90 and 95 ºC (Figure 5.15).

No stable emulsions were obtained with an oil bath at 80 °C; the resulting dispersions were too cloudy to be analysed with the DLS apparatus, hence this temperature does not appear in the Figure 5.15. These emulsions contained large and polydispersed droplets for both types of cooling as can be seen on Figure 5.16 for emulsions with 5 % (w / w) of soya oil. Even though they were not stable, the micrographs prove that the heating process still had an impact on their appearance since they are very different from the one presented in Figure 5.1 (*a*).

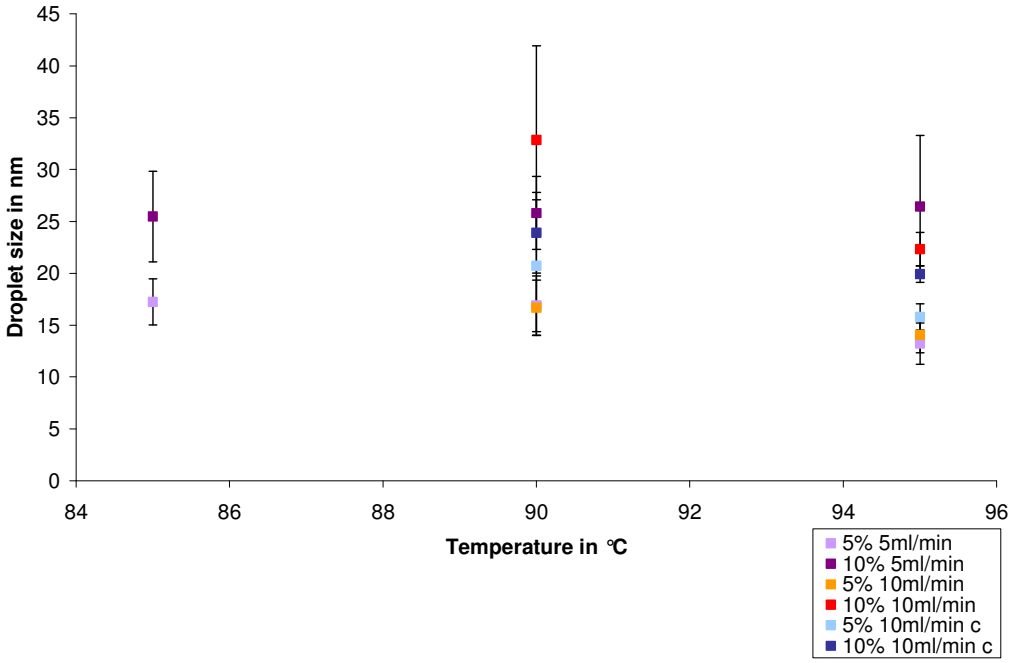

Figure 5.15: Influence of the oil bath temperature on the droplet size of different emulsions

The legend presents the oil content of the coarse emulsion, and the flow rate and cooling technique used (the 'c' stands for cooling i.e. use of the heat exchanger).

While not obtaining a stable nanoemulsion with an oil bath at 80 °C seemed quite normal with a pre-emulsion containing 10 % (w / w) of soya bean oil whose PIT was determined as 88 °C, it was a bit unexpected for the emulsions at 5 % (w / w) since their PIT was determined equal to 74 °C (Table 5.1). The temperature near the outlet of the copper coil was measured. It was around 76 °C when the flow rate was 5 mL min^{-1} and 77 °C when it was 10 mL min^{-1} which proved that the coarse emulsions were brought slightly above the PIT temperature determined for emulsions at 5 % (w / w) of soya bean oil.

According to the calculations presented in Chapter 4, with an oil bath at 80 °C the 5 % (w / w) soya bean oil emulsions at 5 and 10 mL min^{-1} were heated above the HLB temperature for 40 and 15 s respectively. Table 5.2 recaps these time duration calculated in Chapter 4, with some additional values for 85 and 90 °C. Despite earlier conclusions about the relative independency of flow rate on the resulting droplet size for emulsions with a low oil content (Section 5.3.2), an additional assay at 80 °C was done with the 5 % (w / w) soya bean oil pre-emulsion

at 2 mL min^{-1}, which corresponds to a residence time of the emulsion above the PIT of 114 s.

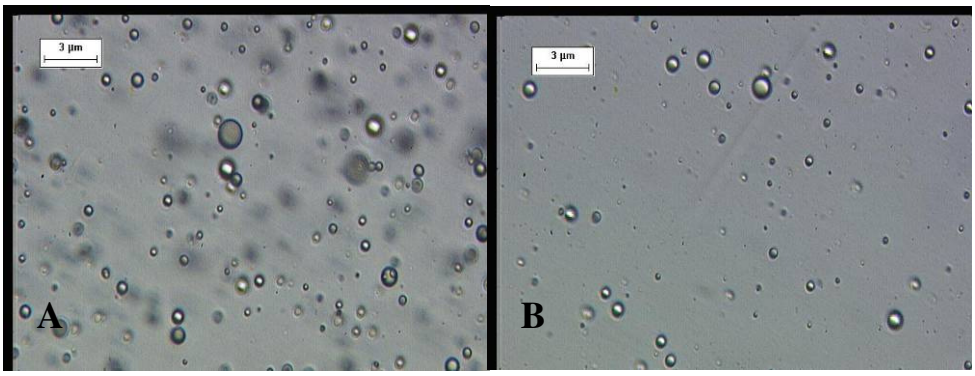

Figure 5.16: Micrographs of emulsions at 5 % (w / w) soya bean oil that were circulated in the rig at 5 mL min^{-1}, with the oil bath at 80 °C

A) the emulsion was sampled after the copper coil; B) the heat exchanger was used to cool down the emulsion rapidly.

The pre-emulsions were prepared using an aqueous solution at 22.2 % (w / w) of Brij 97.

Scale bar = 3 µm

It allowed the preparation of an inhomogeneous liquid-gel as previously described in Section 5.3.2. After dissolution of the gel, the droplet size of the emulsion could be measured in this case and was determined to be 16(±2) nm. This result was in the same order of magnitude as those presented for the same composition and made at different temperatures in Figure 5.15.

Table 5.2: Estimation of the residence time above the PIT for different flow rates

T_{Bath} in °C	$\dot{V}_{water}$ in mL min^{-1}	$t_{T\geq74\,°C}$ in s	$t_{T\geq88\,°C}$ in s
80	2	114	0
	5	40	0
	10	15	0
85	5	42	0
	10	17	0
90	5	43	35
	10	19	10
95	5	44	40
	10	19	15

With these observations, it would appear that in order to obtain stable nanoemulsions with an oil bath temperature close to the PIT of an emulsion, the time of residence of the emulsion above the PIT required to be longer than with an oil bath set on a higher temperature. Such effect of the flow rate was not noticed before since the experiments done so far were performed with an oil bath at 95 °C. However, these long times of residency could also result in the formation of a gel.

According to Figure 5.15, it was possible to prepare a stable 5 % (w / w) soya bean emulsion at 85 °C with a flow rate of 5 mL min^{-1}. The residence time above 74 °C at 5 mL min^{-1} was determined to be 42 s, only two seconds more than in the case of the bath at 80 °C. The difference between the highest temperatures reached in these cases was 5 °C. Stable emulsions at 5 % (w / w) in soya bean oil could be prepared with a flow rate of 10 mL min^{-1} with an oil bath at 90 °C, which means that the emulsions were subjected only for 19 s at a temperature above its PIT. These observations seem to confirm the previous hypothesis that time of residency matters more at low temperature.

In the literature, for some rare systems such as Kerosene / Tween blend / NaCl brine, a delay in the temperature-driven phase inversion phase was observed **[104]**. In the present case, this hysteresis phenomenon could explain the need of the system for a minimum residency time to change phase. However, according to Marquez *et al.* **[104]**, the delay increased with the rate of heating. This is not the case with the Soya bean oil / Brij 97 / Water system. Indeed, with the present apparatus, the heating rate is slower when the oil bath is set on 80 °C rather than 95 °C. As a consequence, the delay in the inversion phase should have been even longer for higher oil bath temperatures, but that is not what happened. Experimentally, the higher the oil bath temperature was, the shortest time the coarse emulsion needed to be heated in order to obtain successful nano-emulsification. When higher temperatures are reached, more energy is given to the system. This might help reducing the delay in the phase change. That may be the reason why it was observed in the literature that more stable nano-emulsions were obtained when prepared some distance away from the optimum state i.e. away from the Phase Inversion Temperature **[66]**.

Another interesting result from Figure 5.15 was the successful nanoemulsification of the 10 % (w / w) soya bean oil pre-emulsion for the flow rate of 5 mL min^{-1} with the oil bath set at temperature 85 °C. This latter value was inferior to the PIT of the studied emulsion estimated at 88 °C. This observation appears to be a bit in contradiction with the previous statements since the 5 % (w / w) soya bean oil pre-emulsion required longer residency time around its HLB temperature than the 10 % (w / w) one which was further away from it. It might be because the phase change in the case of 5 % (w / w) emulsion requires more energy than with 10 % (w / w) since it contains less oil. The emulsion at 5 % (w / w) would need more time to gather the latent heat it requires to get from one phase to another. Because of its higher content in soya bean oil, the 10(w / w) % emulsion might reverse more readily when it gets in the PIT zone than the 5 % (w / w) pre-emulsion.

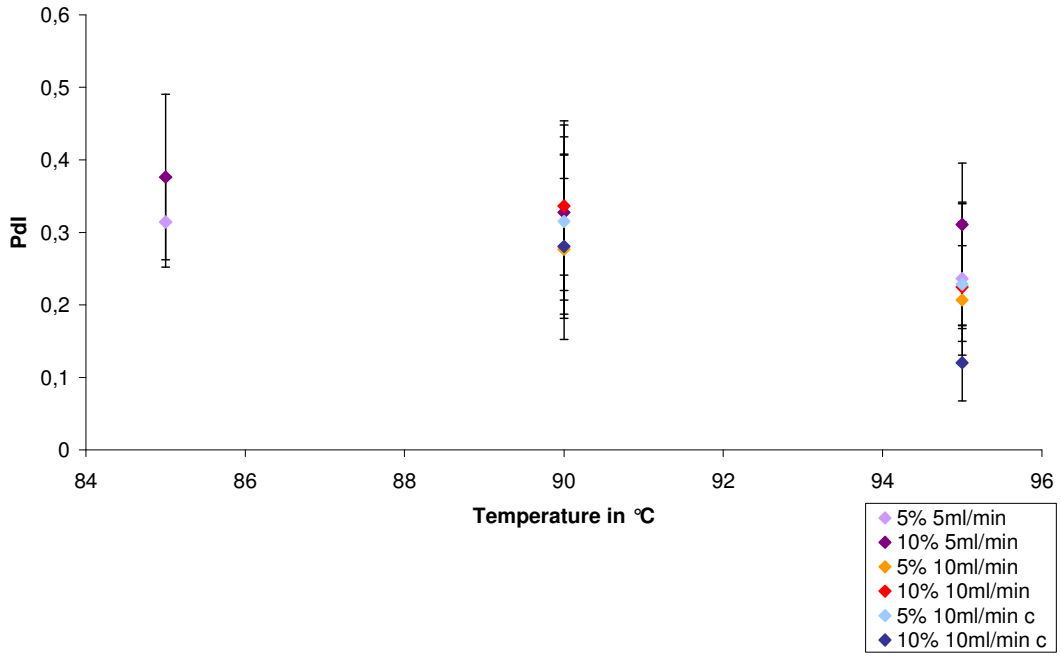

Figure 5.17: Evolution of the polydispersity index of different emulsions with the oil bath temperature

The legend presents the oil content of the pre-emulsion, and the flow rate and cooling technique used (the 'c' stands for cooling i.e. use of the heat exchanger). The coarse emulsions were prepared using an aqueous solution at 22.2 % (w / w) of Brij 97.

In Figure 5.15, error bars appeared to get smaller at high temperature, which means that the experiments were more reproducible when the oil bath is set on a high temperature. Also, it was observed that a slight decrease of the size with the increase of the oil bath temperature occurred. Although observations on PdI were quite inconclusive so far, this time it seems possible to draw a conclusion. Indeed, in Figure 5.17, the PdI decreased with increasing temperature. The systems are more polydispersed when prepared at lower temperature. This could explain why the emulsions made at these temperatures were less stable.

5.3.6- Influence of the time of storage

The prepared nanoemulsions were kept for 45 days. After this period, the size analyses were repeated. Figure 5.18 shows the droplet size of 5 % (w / w) soya bean oil emulsions after preparation and 45 days later. Droplet size increased with time. However after 45 days of storage at ambient temperature, the emulsions still presented very small droplet size and it was still possible to use the DLS to do the measurements.

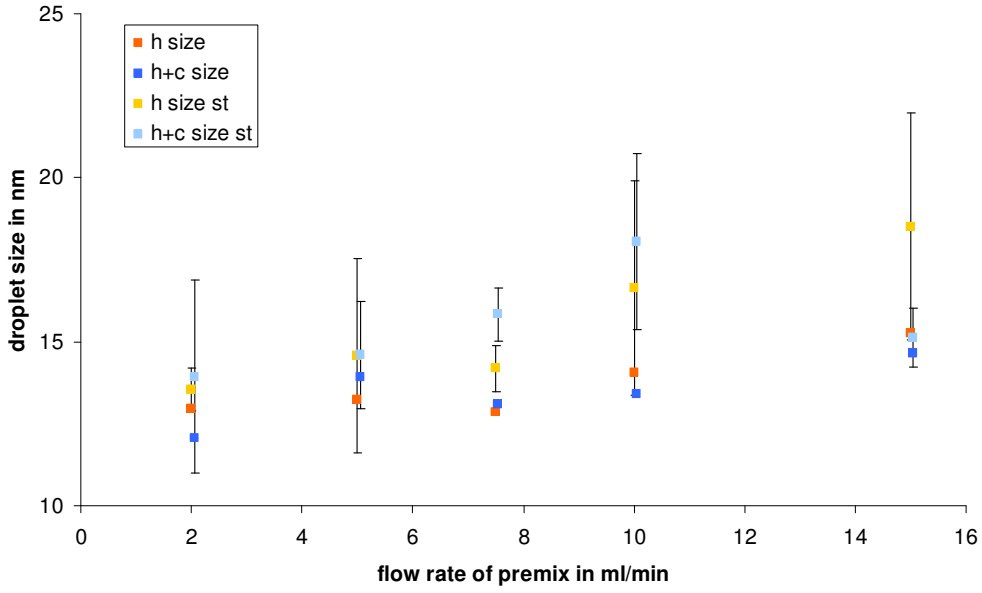

Figure 5.18: Droplet size of emulsions at 5 % (w / w) in soya bean oil in function of flow rate

h= slow cooling, h+c=fast cooling and st=stability i.e. the measurements made after 45 days of storage. For reason of clarity, standard deviations are only presented on the stability measurements.

The oil bath was set at 95 °C. The coarse emulsions were prepared using an aqueous solution at 22.2 % (w / w) of Brij 97

From the analysis of results shown in Figure 5.18, it seems that the droplets tended to grow more with time when the emulsions were prepared at high flow rates. Also, the fast cooling appeared to be less efficient at producing stable emulsions than slow cooling. However, these trends might be coincidental. Indeed, the graph presented in Figure 5.19 uses the same parameters except for the oil content, which is at 10 % (w / w) in this case, but this time, the flow rate did not seem to have an impact on the size of the droplets after 45 days. Similarly, the cooling method chosen did not seem to have an action on the growth of the droplets over time. As a consequence, it is difficult to conclude whether or not the flow and cooling rates have a role in the long-term stability of the nanoemulsions.

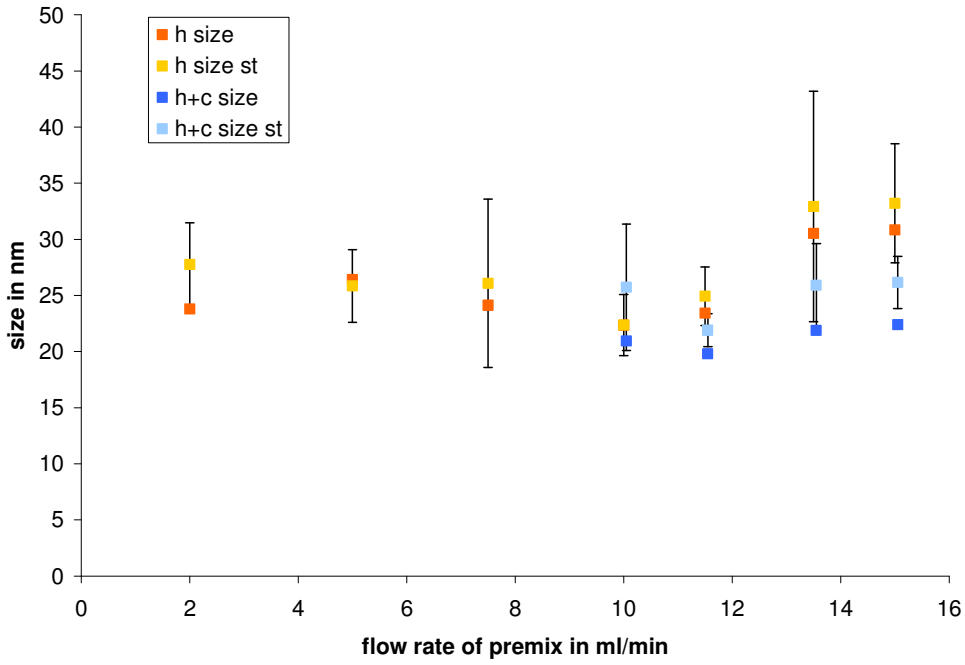

Figure 5.19: Droplet size of emulsions at 10 % (w / w) in soya bean oil in function of flow rate

h= slow cooling, h+c=fast cooling and st=stability i.e. the measurements made after 45 days of storage, T_{bath}=95 °C. For reason of clarity, standard deviations are only presented on the stability measurements. The coarse emulsions were prepared using an aqueous solution at 22.2 % (w / w) of Brij 97.

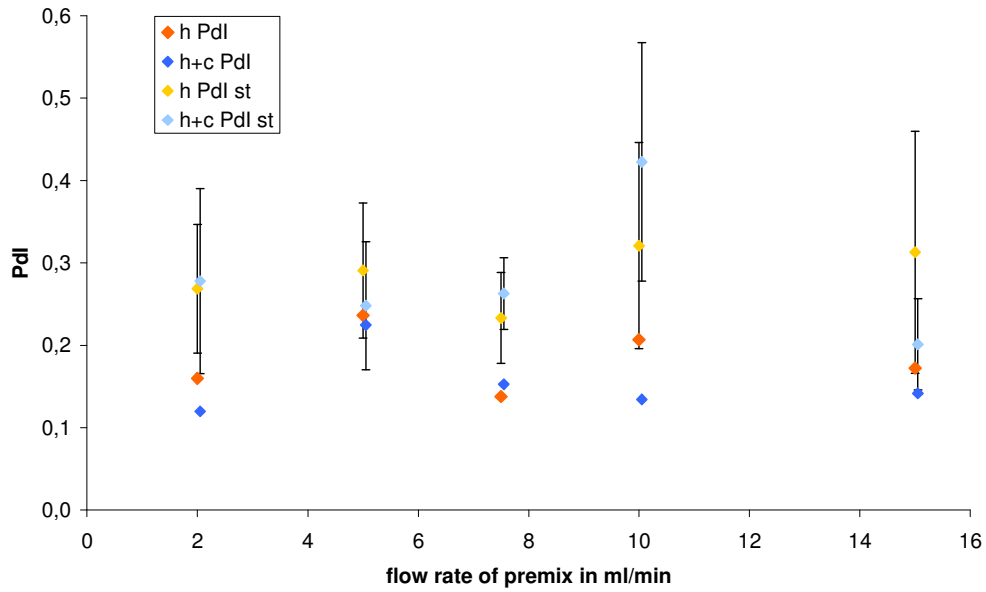

Figure 5.20: Polydispersity index of emulsions at 5 % (w / w) in soya bean oil in function of flow rate

h= slow cooling, h+c=fast cooling and st=stability i.e. the measurements made after 45 days of storage, T_{bath}= 95 °C. For reason of clarity, standard deviations are only presented on the stability measurements. The pre-emulsions were prepared using an aqueous solution at 22.2 % (w / w) of Brij 97.

No process parameter in the preparation of the emulsions seems to specifically induce the widening of the droplet size distribution with time (Figure 5.20). After 45 days, the nanoemulsions got more polydispersed. Indeed, the polydispersity for fresh emulsions at 5 % (w / w) in soya bean oil were around 0.2 (Figure 5.8). After 45 days, this average had shifted towards 0.3 (Figure 5.20). But, these size distributions could still be considered quite narrow. Because of time constraints, the effect of the bath temperature on the degradation of the nanoemulsions was not studied. The analyses of the results did not enable to determine a particular factor that would improve the stability of the nanoemulsions over time.

5.4- Influence of the different factors on the emulsion transparency

5.4.1- Relationship between size / PdI and transparency

Figure 5.21 presents the transparency of an emulsion (here as the absorbance value at λ = 540 nm) in function of its average droplet size. It regroups data analyses gathered from all the previous rig experiments.

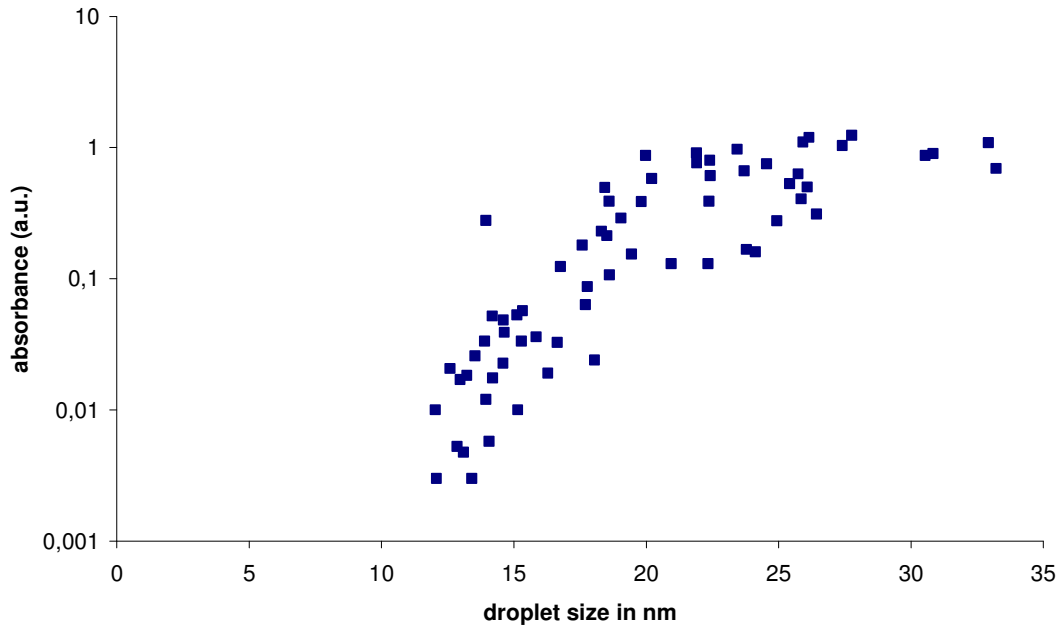

Figure 5.21: Absorbance value at λ = 540 nm of emulsions prepared using the rig in function of their droplet size

Whereas it could have been thought that the droplet size of a nanoemulsion was directly related to its transparency, this relationship did not appear so clear. Indeed, some samples with similar droplet size could present various degrees of transparency and two samples with the same absorbance values could have different droplet sizes. However, a trend appears in favour of a more transparent emulsion when the droplet

size was small. As for the polydispersity index presented in Figure 5.22, there was not much correlation with the transparency of the emulsions; it might be due the low quality of the PdI measurements underlined previously.

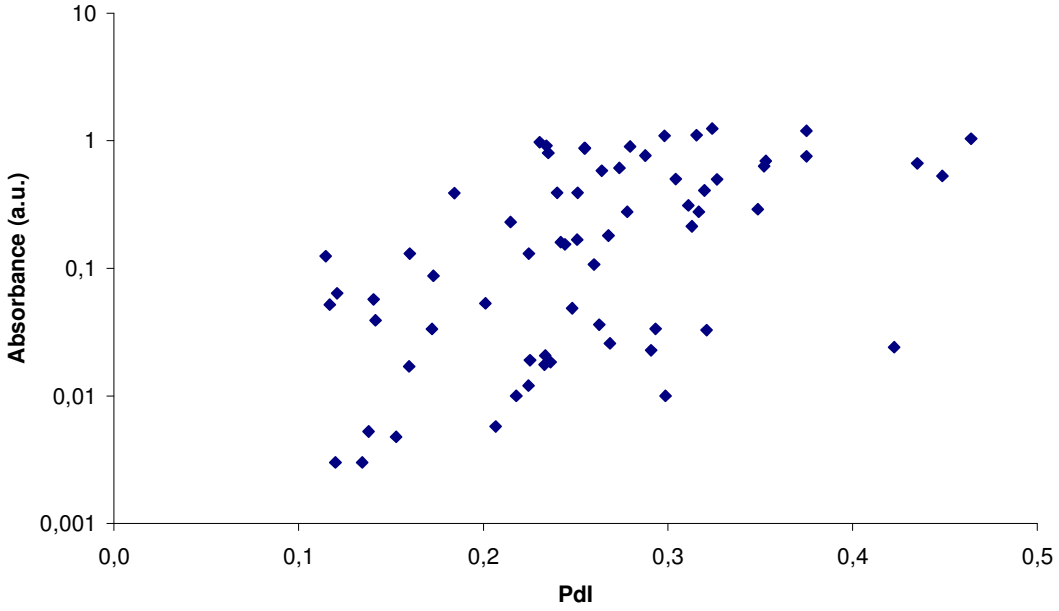

Figure 5.22: Absorbance value at λ = 540 nm of emulsions prepared using the rig in function of their polydispersity index

Despite these non-conclusive results, the transparency of the emulsions was still an important element for the size analyses of the experiments. Indeed, it was more difficult to use the Diffraction Light Spectroscope on a cloudy emulsion. Sometimes, the quality criteria were not met with this kind of emulsion no matter how much it got diluted. As a consequence, it was thought that the more transparent the emulsion was, the more accurate the measurements performed on it would be.

5.4.2- Influence of the oil content on the emulsion transparency

The transparency of emulsions made with the rig could be influenced by the following experimental conditions: oil content, flow rate, cooling rate and oil bath temperature.

Figure 5.23 presents the absorbance of nanoemulsions as a function of different oil contents. Emulsions with values of 0.15 and under were transparent to the eye. All the nanoemulsions made with the coarse emulsions at 5 % (w / w) of soya bean oil were clear with their absorbance values under 0.1. Figure 5.23 leads to the conclusion that transparent emulsions were more easily produced using a low oil concentration; a similar conclusion was drawn for the batch emulsions analysed in Chapter 3. In Figure 5.23, most of the emulsions which were cooled quickly displayed lower absorbance values than their slowly cooled counterparts. This implies that a high cooling rate was favourable to obtain more transparent emulsions.

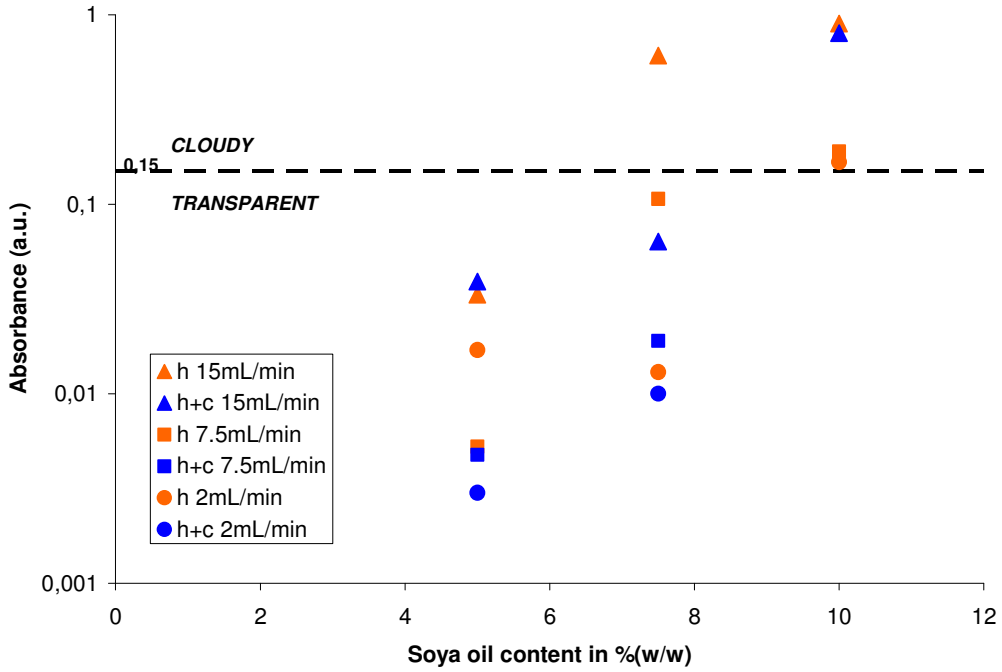

Figure 5.23: Absorbance value at λ = 540 nm of emulsions prepared using the rig under different flow rates in function of their oil content

h= slow cooling; h+c= fast cooling, oil bath temperature= 95 °C

Figure 5.24 represents the absorbance values of nanoemulsions as a function of flow rates. The concentration of soya bean oil of 7.5 % (w / w) was chosen because it resulted in larger range of absorbance values on Figure 5.23. As previously, it can be seen that the rate of cooling had an impact on the transparency of the resulting emulsions. They tended to be more transparent when the cooler was used.

Figure 5.24 shows that emulsions prepared at low flow rates were more transparent that emulsions prepared at high flow rates. Emulsions that stayed a long time above the PIT had clearer appearance than emulsions with short times of residency in the oil bath set at the same temperature. This trend is particularly clear for the slowly cooled emulsions. Previously, it was thought with respect to the size measurements that the flow rate did not matter much as long as the product was prepared at a high temperature.

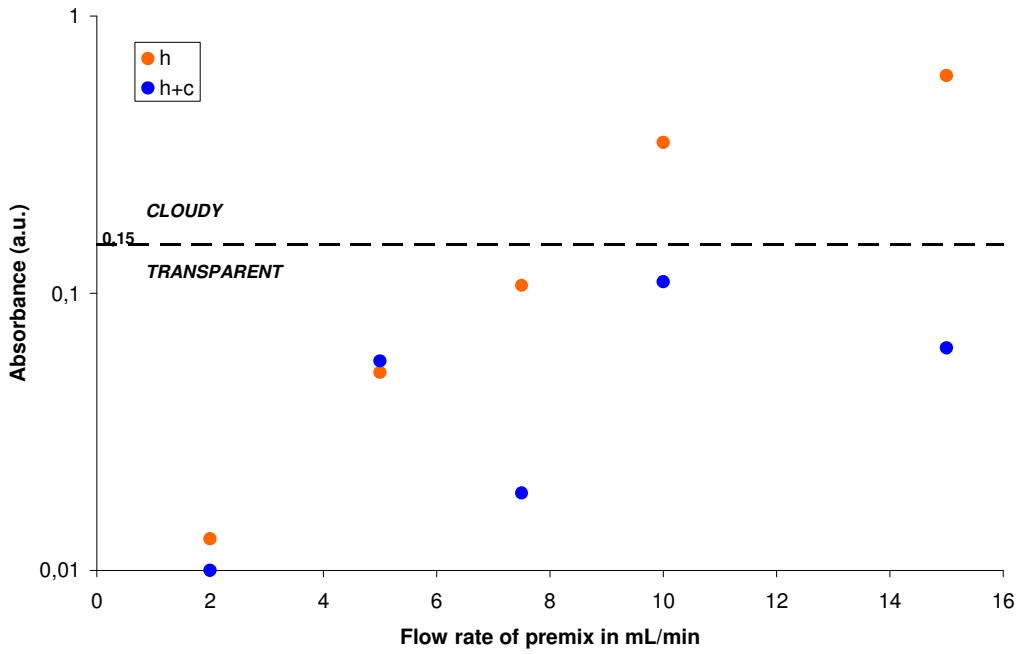

Figure 5.24: Absorbance value at λ = 540 nm of nanoemulsions containing 7.5 % (w / w) of soya bean oil in function of the flow rate used for their preparation

h=slow cooling; h+c= fast cooling, oil bath at 95 °C

However, this parameter had an effect on the optical property of the resultant emulsions. It was also seen previously that the flow rate had an impact on their viscosity. Flow rate has an important influence on the appearance of the emulsions. As a result, depending on what kind of nanoemulsion is desired, it is important to find out what is the necessary residence time of the emulsion above the HLB temperature.

Figure 5.25 presents the absorbance value of emulsions at 10 % (w / w) in soya bean oil in function of the oil bath temperature. From this graph, it was possible to deduce that an oil bath at high temperature was favourable to the preparation of clear emulsions regardless of the time of residency. Indeed, an emulsion made with an oil bath at 95 °C and which stayed 15 s above its PIT would appear more transparent than one prepared with an oil bath at 90 °C and a residency time of 35 s in that region. The picture of these samples is presented in Figure 5.26.

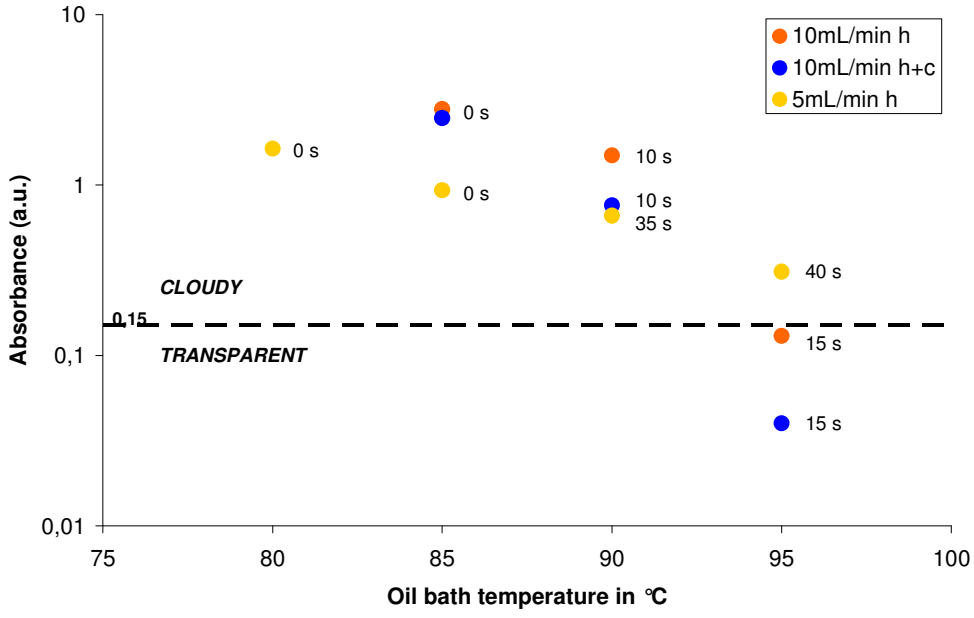

Figure 5.25: Absorbance value at λ = 540 nm of emulsions containing 10 % (w / w) of soya bean oil in function of the oil bath temperature

The legend presents the flow rate of the coarse emulsions and cooling technique used (h= slow cooling; h+c= fast cooling)

The nanoemulsion prepared at 95 °C with a flow rate at 5 mL min^{-1} was less transparent than the ones prepared at the same temperature with a shortest residency time above the PIT. This is most probably due to the gel layer that appeared when the emulsions were prepared using these parameters. After the melting of the layer, the emulsions tended to be less transparent.

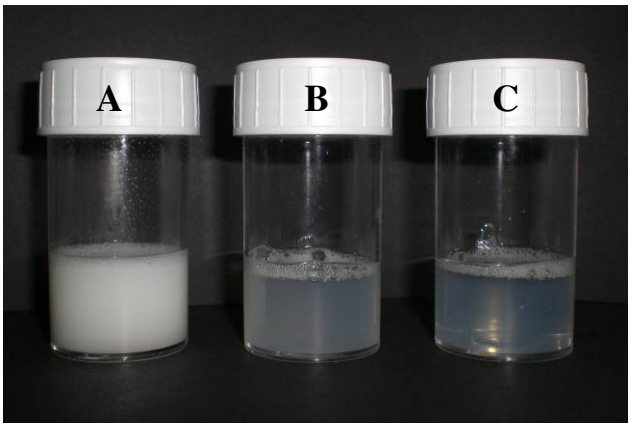

Figure 5.26: Picture of 3 samples made of 10 % (w / w) in soya bean oil

A) Coarse emulsion i.e no thermal treatment - Absorbance at λ = 540 nm → > 3,

B) emulsion prepared under T_{bath}=90 °C, slow cooling and flow rate= 5mL min^{-1} - Absorbance at λ = 540 nm → 0.66,

C) emulsion prepared under T_{bath}= 95 °C, slow cooling and flow rate= 10mL min^{-1}- Absorbance at λ = 540 nm → 0.13.

From these various observations, the important parameters in order to obtain a transparent emulsion seem to be a high oil bath temperature and a slow flow rate, though the time of residency above the PIT needs to be short enough to avoid the formation of gel.

5.4.3- Influence of the time of storage on the emulsion transparency

In Figure 5.27, the plot represents the absorbance value of fresh samples against this same variable measured 45 days later. It shows that two samples with similar measurements when fresh can end up having different absorbance values 45

days later and that two 45-day-old emulsions could share the same optical appearance even though they were not similar at the start.

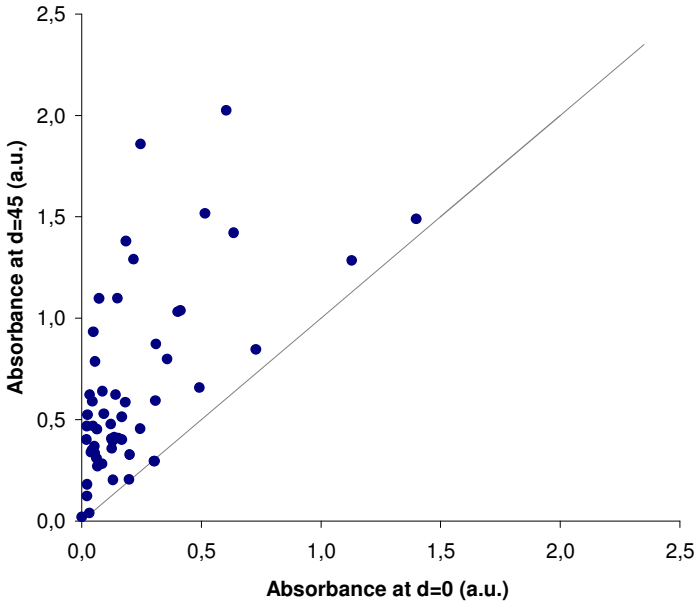

Figure 5.27: Absorbance value of samples 45 days after their preparation with the rig in function of their absorbance value on the first day (λ = 540 nm)

The curve y=x placed on the graph highlights the fact that all the aged samples were less transparent than what they were initially since all the points are above it.

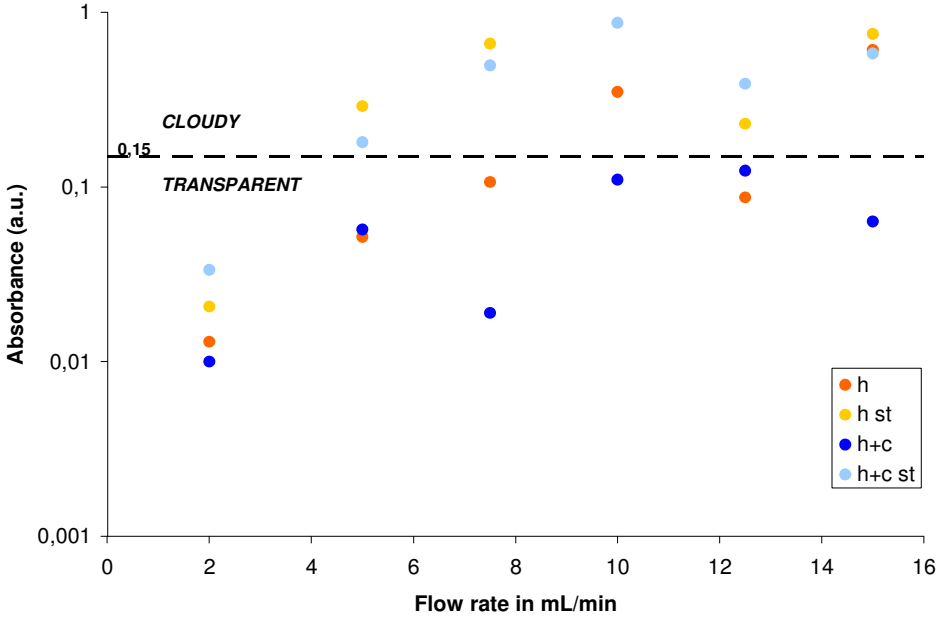

Figure 5.28: Absorbance value at λ = 540 nm of emulsions at 7.5 % (w / w) in soya bean oil in function of flow rate and their evolution with time

h= slow cooling, h+c= fast cooling and st= measurements made 45 days after preparation , T_{bath}=95 °C

Similarly as in Section 5.3.6, no experimental condition was found to particularly influence the speed of degradation in terms of transparency. Indeed, as can be seen in Figure 5.28 representing the absorbance value of emulsions at 7.5 % (w / w) in soya bean oil, the evolution of the optical properties of the samples were quite random with regards to cooling technique and flow rates. Results for other concentrations did not enable to find a parameter that would promote or prevent the samples to get more turbid with time. However, there still might be an action of the oil bath temperature on the emulsion transparency, however more experiments are needed for the analysis of this effect.

5.5- Comparison between batch and continuous processes

Batch experiments were done as described previously in Chapter 3. The same pre-emulsion as used in the continuous rig (i.e. mixtures of 5, 7.5 or 10 % (w / w) of soya bean oil and solution of Brij 97 at 22.2 % (w / w)) were employed in order to compare the results between batch and continuous processes. The samples were all heated up to 95 °C and an ice bath was used to quench the emulsions (Figure 5.29).

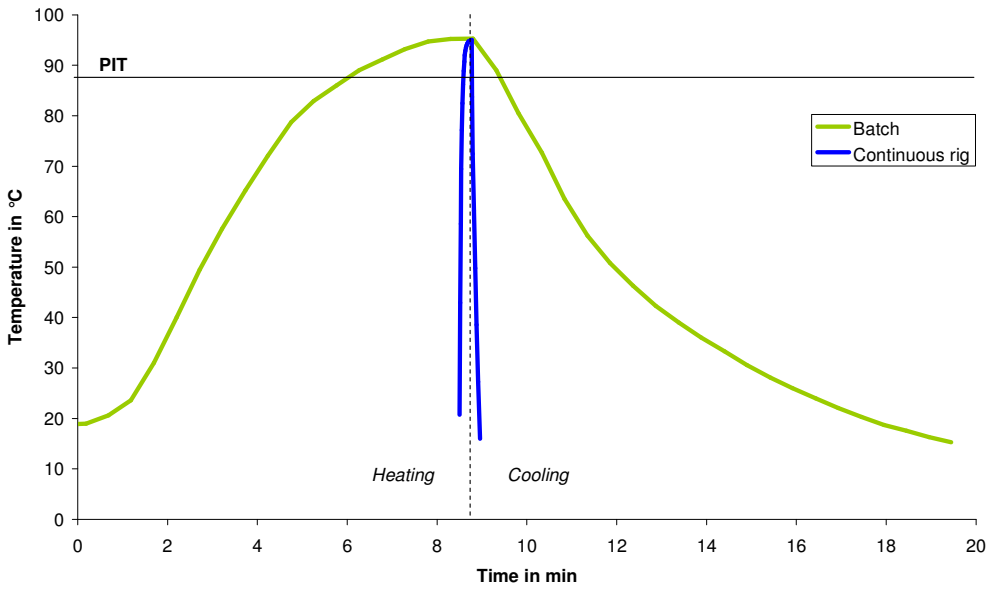

Figure 5.29: Time profiles of the batch and continuous heat treatments for an emulsion at 10 % (w / w) in soya bean oil

For both processes, fast cooling was used. Batch emulsions were heated rapidly using a bath at 95 °C.

The results of the size analyses are presented in Figure 5.30 and compared with the droplet size and size distribution of the respective nanoemulsions prepared with the rig with the oil bath set at 95 °C, the fast cooling technique and flow rate at 15mL min^{-1}. For clarity purposes, only emulsions made with this flow rate was chosen to be compared with the batch nanoemulsions on Figure 5.30. The two techniques enabled to produce very similar nanoemulsions. Indeed, on Figure 5.30, it can be seen that the average droplet size and polydispersity of the emulsions were very close to each other. The standard deviations of the batch data were larger than those of the rig. The value of all the rig nanoemulsions were comprised in the error bars of the batch emulsions. Since the standard deviations of the size analyses of the emulsions made using the continuous rig were repetitively narrower, it can be deduced that the production of emulsions with the continuous method was more reproducible than with the batch. This was probably due to the better control of the thermal treatment from one sample to the other.

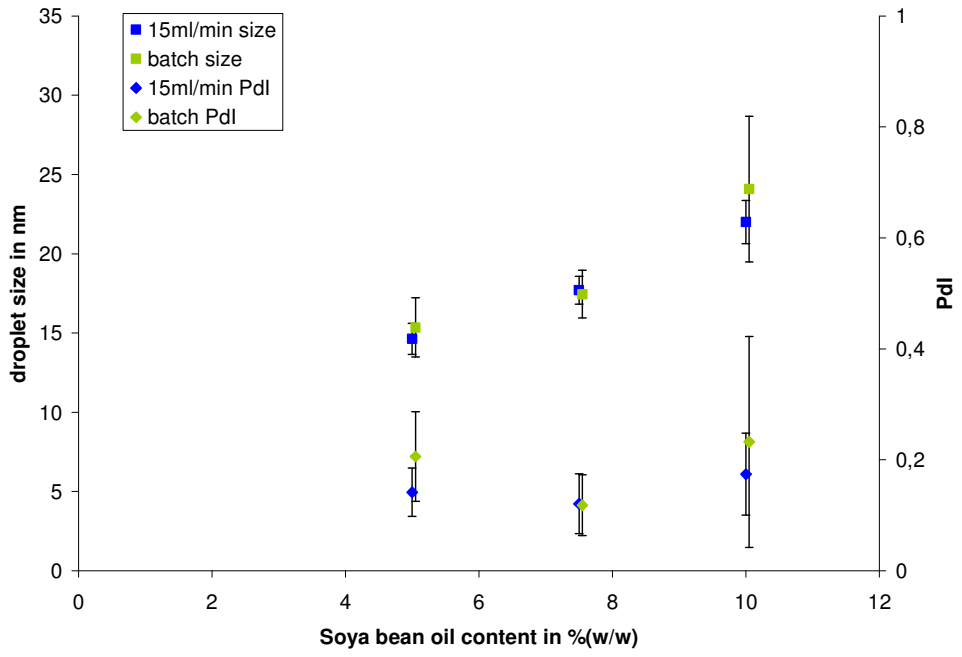

Figure 5.30: Comparison between batch and continuous processes in terms of droplet size and polydispersity index

For both processes, fast cooling was used.

In terms of transparency, it is possible to make quite clear emulsions using both techniques (see Table 5.3). Batch emulsions were mostly transparent but their trend appeared to be a bit more random than the emulsions made with the continuous rig due to the lack of reproducibility between experiments. As for the continuous process, clear emulsions can be prepared effectively if care is taken to choose the adequate flow rate. Indeed, if the flow rate is too high such as 15mL min^{-1} for a pre-emulsion at 10 % (w / w) in soya bean oil, the resultant emulsion will be cloudy. If it is too slow, there might be gel formation and risk of clogging. Actually, even though batch emulsions spent much longer at high temperatures (Figure 5.29) than the emulsion made using the continuous rig, the formation of gel was observed only once: when no condenser was used in the set up. This was thought to be the result of drying. What is more, the effect of residency time in the HLB region was not perceived at all with the batch process. Sensibility to this factor with the continuously made emulsions comes from the fact that their time of residency was much shorter than any of the batch emulsions (Figure 5.29).

Table 5.3: Absorbances at λ = 540 nm for batch and continuous processes

For both processes, fast cooling was used.

Content in oil in % (w / w)	**Abs. (a.u.) for batch process**	**Abs. (a.u.) for 10 mL min^{-1}**	**Abs. (a.u) for 15 mL min^{-1}**
5	0.21	0.02	0.04
7.5	0.08	0.02	0.06
10	0.12	0.04	0.80

5.6- Conclusion

This chapter enabled to discover the different effects of the operational parameters on the preparation of emulsions made with soya bean oil and a solution at 22.2 % (w / w) of Brij 97. The most important parameters to obtain small average size, narrow size distribution and transparency seem to be the flow rate and the oil bath temperature, two factors which are closely related. Even though, at first the flow rate of the coarse emulsion appeared to have only a small impact on the droplet size and polydispersity of resultant emulsions when the temperature of the oil bath was high, it actually played an important role when this one was put on a lower setting. Obviously, it needed to be slow enough to allow the pre-emulsion to get around the PIT region but also depending on the highest temperature reached, the amount of time necessary for the preparation of a stable emulsion required to be modulated as well. When brought to a high temperature, the emulsions needed a shortest passage in the copper coil than those at temperature close to the HLB.

Flow rate and oil bath temperature also had an important influence on the appearance of the emulsions. Flow rates which are too low would contribute to the production of gel-like emulsions but if they exceed a certain velocity, they get cloudy. High oil bath temperatures exacerbate this tendency.

Other parameters would seem to improve the emulsion properties to a lesser scale. The use of homogenized emulsions could help to get slightly better quality emulsions: more reproducible, more monodispersed and with smaller average size than emulsions prepared from simply stirred pre-emulsion. Cooling treatment was useful for the preparation of emulsions at high concentration of soya bean oil: it would promote smaller average size and polydispersity index. The impact of the cooling technique might reveal more important on larger scales, for which produced quantities will not cool down as quickly as the 15 mL samples of this study without a cooling system.

The nanoemulsions showed a very good stability over time both in terms of size and transparency, though they all got a larger average size and polydispersity

index and a more cloudy appearance over time. No process parameter was found to prevent or promote this degradation.

When using the same coarse emulsion, it was possible to get very similar nanoemulsions with both batch and rig processes. However, the rig proved to be a more reproducible method that can be modulated to obtain certain properties. Maybe the differences between these two methods would be more acute on a larger scale since the thermal treatment for the batch would probably be even less easy to control than on the laboratory scale.

Conclusions

Nanoemulsions have the potential to be transparent and very stable. To display these properties, the droplets must not only be in the nanosize range but also have a size distribution as narrow as possible. The present thesis has reported an attempt to create an experimental set-up working in continuous flow to produce monodispersed food-grade oil nanoemulsions with a low-energy emulsification method.

In order to identify the requirement for the building of the continuous rig, it was essential to understand the conditions for successful emulsification of the chosen emulsion system with the selected low-energy emulsification technique which is mainly known as a batch process. For that purpose, Soya bean oil / Brij 97 / Water nanoemulsions were prepared using the Phase Inversion Temperature (PIT) emulsification with the traditional batch method.

Brij 97 is a non-ionic ethoxylated surfactant that gets more lipophilic as the temperature increases. At low temperature, O / W macroemulsions are formed. On increasing the temperature, the O / W emulsion stability decreases and the macroemulsion finally resolves at the PIT. At higher temperature, W / O emulsions become stable. By preparing the emulsion in the region of the PIT and proceeding to cooling, the system is subjected to a transitional inversion and nanoemulsions can be produced.

Soya bean oil / Brij 97 / Water mixtures of different compositions were brought to their PIT temperatures and then cooled down with either fast or slow cooling rate. The appearance of the resultant emulsions varied from unstable white to stable transparent. Emulsions with a high proportion of soya bean oil and low content of Brij 97 tended to be whiter and less stable, especially if the cooling was slow. White emulsions presented in most cases a higher droplet size than the more transparent ones. For example, an emulsion made of 10 % (w / w) of soya bean oil, 20 % (w / w) of Brij 97 and 70 % (w / w) of water prepared under a cooling rate of 5-

16 °C min^{-1} was transparent and presented an average droplet size of 24 nm whilst it had a white appearance and an average droplet size of 64 nm when it was cooled down at a rate below 2 °C min^{-1}. Reproducible results were difficult to obtain since the batch set-up did not allow for a good temperature control. The construction of a continuous rig using heat exchangers was thought up to solve this problem.

A continuous rig was designed and built after consideration of the conditions required for a successful PIT emulsification with the batch experiments. A micropump was used to circulate the coarse emulsion of soya bean oil, Brij 97 and water into the continuous set-up at different flow rates. The first step of the PIT process is the heating up of the pre-emulsion in the PIT range. It was achieved by the use of a copper coil immersed in an oil bath set at the adequate temperature. The second step of the PIT emulsification is the rapid cooling of the emulsions. It was obtained with a micro-heat exchanger. The temperatures were controlled at the inlets and outlets of the heat exchanger using thermocouples.

The different effects of the operational parameters on the preparation of emulsions made with soya bean oil and a solution at 22.2 % (w / w) of Brij 97 with the continuous rig were studied. In order to obtain small average size, narrow size distribution and transparency, special attention needed to be paid to the flow rate and the oil bath temperature, i.e. two factors directly related to the heating treatment. Transparent nanoemulsions could be prepared with a very short residence time above the PIT temperature if the oil bath was set at a high temperature. However, an optimal flow rate had to be found. Indeed, low flow rates would promote the production of gel-like emulsions and excessive flow rates would result in cloudy emulsions.

The nanoemulsions prepared with the PIT method showed a very good stability over time in terms of both size and transparency. For instance, a fresh nanoemulsion made with 10 % (w / w) of soya bean oil in the continuous set-up displayed an average droplet size of 21 nm. 45 days later, the emulsion was still in the nanosize range with an average size increased by a mere 5 nm.

Batch and continuous set-ups enabled the preparation of nanoemulsions with similar properties when working with one emulsion composition. However, the continuous rig was a more reproducible method. It is thought that on larger scales, the rig could prove even more efficient than the batch technique for the making of reproducible nanoemulsions.

Future work on the manufacture of nanoemulsions using the continuous PIT emulsification machine could follow two possible axes. First, further improvements could be made on the rig. In the present work, a pre-emulsion was used as the feed. This coarse emulsion was prepared in batch. It would be interesting to be able to make these pre-emulsions online and vary their compositions. With this idea in mind, two pumps with variable flow rates have already been integrated in the rig: one for delivering the oil and the other for the surfactant solution. If an adequate mixer could be added to the rig, a wide range of different compositions could be produced as it enables to modify the ratio of the ingredients.

Another reason in favour of another method of mixing is the observation that homogenized pre-emulsions allowed the production of nanoemulsions which were more reproducible, more monodispersed and with smaller average size than emulsions prepared from simply stirred pre-emulsion. However, it seems contradictory to use this method of mixing when the goal of the present work is the preparation of nanoemulsion with low-energy method. An alternative way of premixing the emulsions should be looked into; online mixing might be one of these low-energy solutions.

The other axis that could be of interest is the exploration of other emulsion systems. Indeed, throughout the present thesis, the continuous rig was used exclusively with the system Soya bean oil / Brij 97 / Water. Other kind of oil and surfactants could be studied. For example, the preparation of nanoparticles using solid oils at ambient temperature such as palm oil could be investigated. Bioactives such as vitamins, minerals or other functional ingredients could also be added in the oil. Change in the composition of the emulsion system might require some rig modifications such as the length of the copper tubing in case the residency time requires being longer or shorter than the time the present set-up could allow.

References

1. Vincent, B. *Introduction to Colloid Science*. in *Spring School in Colloid Science*. 2004. University of Bristol.
2. Flanagan, J., *et al.*., *Solubilisation of soybean oil in microemulsions using various surfactant.* Food hydrocolloids, 2006. 20: p. 253-260.
3. Tadros, T.F., *et al.*., *Formation and stability of nano-emulsions.* Advances in Colloid and Interface Science, 2004. 108-109: p. 303-318.
4. Hamley, I.W., *Introduction to Soft Matter: Polymers, Colloids, Amphiphiles and Liquid Crystals*. 2000, Chichester: John Wiley & Sons, Ltd.
5. Forgiarini, A., *et al.*., *Formation of Nano-Emulsions by Low-Energy Emulsification Methods at Constant Temperature.* Langmuir, 2001. 17: p. 2076-2083.
6. Binks, B.P., *Chapter 1: Emulsions - Recent Advances in Understanding*, in *Modern Aspects of Emulsion Science*, B.P. Binks, Editor. 1998, The Royal Society of Chemistry: Cambridge.
7. Barnes, G.T. and I.R. Gentle, *Interfacial Science: An Introduction*. 2005: Oxford University Press.
8. Atkins, P. and J. de Paula, *Atkins' Physical Chemistry*, 9th Edition, P. Atkins, Editor. 2010, Oxford University Press
9. *Interaction of water and non-polar substances*. Available from the New Jersey's Science and Technology University, Federated Departments of Biological Sciences: http: / / newarkbioweb.rutgers.edu / bio301s / lecture%20slides / lec2-1.jpg.
10. Yuyama, H., *et al.*., *Preparation and analysis of uniform emulsion droplets using SPG membrane emulsification technique.* Colloids and Surfaces A: Physicochemical and Engineering Aspects, 2000. 168: p. 159-174.
11. Robins, M.M. and D.J. Hibberd, *Emulsion Flocculation and Creaming*, in *Modern Aspects of Emulsion Science*, B.P. Binks, Editor. 1998, The Royal Society of Chemistry: Cambridge.
12. Kabalnov, A.S., *Chapter 7: Coalescence in Emulsions*, in *Modern Aspects of Emulsion Science*, B.P. Binks, Editor. 1998, The Royal Society of Chemistry: Cambridge.
13. Walstra, P., *Principles of Emulsion Formation.* Chemical Engineering Science, 1993. 48(2): p. 333-349.
14. Arnaud, P., *Chimie Physique, Cours et exercices corrigés*, 5th Edition. 2001, Dunod.
15. Solans, C., *et al.*., *Nano-emulsions.* Current Opinion in Colloid and Interface Science, 2005. 10: p. 102-110.

16. Sing, A.J.F., *et al..*, *Interactions and coalescence of nanodroplets in translucent O / W emulsions.* Colloids and Surfaces A: Physicochemical and Engineering Aspects, 1999. 152(1-2): p. 31-39.
17. Sadurní, N., *et al..*, *Studies on the formation of O / W nano-emulsions, by low-energy emulsification methods, suitable for pharmaceutical applications.* European Journal of Pharmaceutical Sciences, 2005. 26(5): p. 438-445.
18. Izquierdo, P., *et al..*, *Formation and Stability of Nano-Emulsions Prepared Using the Phase Inversion Temperature Method.* Langmuir, 2002. 18: p. 26-30.
19. Morales, D., *et al..*, *A Study of the Relation between Bicontinuous Microemulsions and Oil / Water Nano-emulsion Formation.* Langmuir, 2003. 19: p. 7196-7200.
20. Usón, N., M.J. Garcia, and C. Solans, *Formation of water-in-oil (W / O) nano-emulsions in a water / mixed non-ionic surfactant / oil systems prepared by a low-energy emulsification method.* Colloids and Surfaces A: Physicochem. Eng. Aspects, 2004. 250: p. 415-421.
21. Charcosset, C., I. Limayen, and H. Fessi, *The membrane emulsification process - a review.* Journal of Chemical Technology and Biotechnology, 2004. 79(3): p. 209-218.
22. Gijsbertsen-Abrahamse, A.J., A. van der Padt, and R.M. Boom, *Status of cross-flow membrane emulsification and outlook for industrial application.* Journal of Membrane Science, 2004. 230: p. 149-159.
23. Schröder, V., *Herstellen von Öl-in-Wasser-Emulsionen mit Mikroporösen Membranen*. 1999, Technische Hochschule Karlsruhe: Karlsruhe.
24. Walstra, P., *Chapter 2: Formation of Emulsions*, in *Basic Theory*, P. Becher, Editor. 1983, Marcel Dekker, Inc.: New-York and Basel. p. 57-127.
25. Sugiura, S., *et al..*, *Interfacial Tension Driven Monodispersed Droplet Formation from Microfabricated Channel Array.* Langmuir, 2001. 17(18): p. 5562-5566.
26. Walstra, P. and P.E.A. Smulders, *Chapter 2: Emulsion Formation*, in *Modern Aspects of Emulsion Science*, B.P. Binks, Editor. 1998, The Royal Society of Chemistry: Cambridge.
27. Behrend, O. and H. Schubert, *Influence of hydrostatic pressure and gas content on continuous ultrasound emulsification.* Ultrasonics Sonochemistry, 2001. 8: p. 271-276.
28. Vladisavljevic, G.T. and R.A. Williams, *Manufacture of large uniform droplets using rotating membrane emulsification.* Journal of Colloid and Interface Science, 2006. 299: p. 396-402.
29. Williams, R.A., *et al..*, *Controlled production of emulsions using a crossflow membrane Part II: Industrial scale manufacture.* Chemical Engineering Research & Design, 1998. 76, Part A: p. 902-910.
30. King, A.G. and S.T. Keswani, *Colloid Mills: Theory and Experiment.* J. American Ceramic Society, 1994. 77(3): p. 769-777.
31. Gopal, E.S.R., *Chapter 1: Principles of emulsion formation*, in *Emulsion Science*, P. Sherman, Editor. 1968, Academic Press. p. 496.

32. Cuéllar, I., *et al.*., *More efficient preparation of parenteral emulsions or how to improve a pharmaceutical recipe by formulation engineering.* Chemical Engineering Science, 2005. 60: p. 2127-2134.
33. Brouillet, F., *et al.*., *Modification of the droplet size and distribution of parenteral emulsions by tangential microfiltration.* Journal of Membrane Science, 2003. 221: p. 199-206.
34. Nakashima, T., M. Shimizu, and M. Kukizaki, *Membrane emulsification by microporous glass.* Key Engineering Materials, 1991. 61 / 62: p. 513-516.
35. Joscelyne S.M. and G. Trägårdh, *Food emulsions using membrane emulsification: conditions for producing small droplets.* Journal of Food Engineering, 1999. 39: p. 59-64.
36. Scherze, I., K. Marzilger, and G. Muschiolik, *Emulsification using micro porous glass (MPG): surface behaviour of milk protein.* Colloids and Surfaces B: Biointerfaces, 1999. 12: p. 213-221.
37. Schröder, V. and H. Schubert, *Production of emulsions using microporous, ceramic membranes.* Colloids and Surfaces A: Physicochemical and Engineering Aspects, 1999. 152: p. 103-109.
38. Mine, Y., M. Shimizu, and T. Nakashima, *Preparation and stabilization of simple and multiple emulsions using a microporous glass membrane.* Colloids and Surfaces B: Biointerfaces, 1996. 6: p. 261-268.
39. Omi, S., *et al.*., *Synthesis of Polymeric Microspheres Employing SPG Emulsification Technique.* Journal of Applied Polymer Science, 1994. 51: p. 1-11.
40. Peng, S. and R.A. Williams, *Controlled Production of Emulsions Using a Crossflow Membrane.* Particle and Particle Systems Characterization, 1998. 15: p. 21-25.
41. Vladisavljevic, G.T., M. Shimizu, and T. Nakashima, *Permeability of hydrophilic and hydrophobic Shirasu-porous-glass (SPG) membranes to pure liquids and its microstructure.* Journal of Membrane Science, 2005. 250: p. 69-77.
42. Dowding, P.J., J.W. Goodwin, and B. Vincent, *Production of porous suspension polymer beads with a narrow size distribution using cross-flow membrane and a continuous tubular reactor.* Colloids and Surfaces A: Physicochemical and Engineering Aspects, 2001. 180(3): p. 301-309.
43. Abrahamse, A.J., *et al.*., *Analysis of droplet formation and interactions during cross-flow membrane emulsification.* Journal of Membrane Science, 2002. 204: p. 125-137.
44. Vladisavljevic, G.T., *et al.*., *Production of O / W emulsions using SPG membranes, ceramic alpha-aluminium oxide membranes, microfluidizer and a silicon microchannel plate - a comparative study.* Colloids and Surfaces A: Physicochem. Eng. Aspects, 2004. 232: p. 199-207.
45. Kawakatsu, T., *et al.*., *Production of monodispersed Oil-in-Water Emulsion Using Crossflow-Type Silicon Microchannel Plate.* Journal of Chemical Engineering of Japan, 1999. 32(2): p. 241-244.
46. Schröder, V., O. Behrend, and H. Schubert, *Effect of Dynamic Interfacial Tension on the Emulsification Process Using Microporous, Ceramic Membranes.* Journal of Colloid and Interface Science, 1998. 202: p. 334-340.

47. Christov, N.C., *et al..*, *Capillary mechanisms in membrane emulsification: oil-in-water emulsions stabilized by Tween 20 and milk proteins.* Colloids and Surfaces A: Physicochemical and Engineering Aspects, 2002. 209: p. 83-104.

48. van der Graaf, S., *et al..*, *Influence of dynamic interfacial tension on droplet formation during membrane emulsification.* Journal of Colloid and Interface Science, 2004. 277: p. 456-463.

49. Vladisavljevic, G.T. and H. Schubert, *Preparation and analysis of oil-in-water emulsions with a narrow droplet size distribution using Shirasu-porous-glass (SPG) membranes.* Desalination, 2002. 144: p. 167-172.

50. Katoh, R., *et al..*, *Preparation of food emulsions using a membrane emulsification system.* Journal of Membrane Science, 1996. 113: p. 131-135.

51. Fuchigami, T., M. Toki, and K. Nakanishi, *Membrane Emulsification Using Sol-Gel Derived Macroporous Silica Glass.* Journal of Sol-Gel Science and Technology, 2000. 19: p. 337-341.

52. Asano, Y. and K. Sotoyama, *Viscosity change in oil / water food emulsions prepared using a membrane emulsification system.* Food Chemistry, 1999. 66: p. 327-331.

53. Vladisavljevic, G.T. and H. Schubert, *Influence of process parameters on droplet size distribution in SPG membrane emulsification and stability of prepared emulsion droplets.* Journal of Membrane Science, 2003. 225: p. 15-23.

54. Lambrich, U. and H. Schubert, *Emulsification using microporous systems.* Journal of Membrane Science, 2005. 257: p. 76-84.

55. Park, S.H., T. Yamaguchi, and S.I. Nakao, *Transport mechanism of deformable droplets in microfiltration of emulsions.* Chemical Engineering Science, 2001. 56(11): p. 3539-3548.

56. Suzuki, K., I. Shuto, and Y. Hagura, *Characteristics of the Membrane Emulsification Method Combined with Preliminary Emulsification for Preparing Corn Oil-in-Water Emulsions.* Food Science and Technology International, 1996. 2(1): p. 43-47.

57. Bullón, J., A. Cárdenas, and J. Sánchez, *Emulsion Filtration Through Surface Modified Ceramic Membranes.* Journal of Dispersion Science and Technology, 2002. 23(1-3): p. 269-277.

58. Vladisavljevic, G.T. and R.A. Williams, *Recent developments in manufacturing emulsions and particulate products using membranes.* Advances in Colloid and Interface Science, 2005. 113: p. 1-20.

59. Vitale, S.A. and J.L. Katz, *Liquid Droplet Dispersions Formed by Homogeneous Liquid-Liquid Nucleation: "The Ouzo Effect".* Langmuir, 2003. 19: p. 4105-4110.

60. Ganachaud F. and J.L. Katz, *Nanoparticles and Nanocapsules created Using the Ouzo Effect: Spontaneous Emulsification as an Alternative to Ultrasonic and High-Shear Devices.* ChemPhysChem, European Journal of Chemical Physics and Physical Chemistry, 2005. 6: p. 209-216.

61. Yu, W., *et al..*, *A novel approach to the preparation of injectable emulsions by a spontaneous emulsification process.* International Journal of Pharmaceutics, 1993. 89: p. 139-146.

62. Sajjadi, S., *Nanoemulsion Formation by Phase Inversion Emulsification: On the Nature of Inversion.* Langmuir, 2006. 22: p. 5597-5603.

63. Salager, J.L., *et al.*., *Current Phenomenological Know-How and Modeling of Emulsion Inversion.* Industrial and Engineering Chemistry Research, 2000. 39(8): p. 2665-2676.

64. Salager, J.L., *et al.*., *Using emulsion inversion in industrial processes.* Advances in Colloid and Interface Science, 2004. 108-109: p. 259-272.

65. Fernandez, P., *et al.*., *Nano-emulsion formation by emulsion phase inversion.* Colloids and Surfaces A: Physicochem. Eng. Aspects, 2004. 251: p. 53-58.

66. Antón, R.E., P. Castillo, and J.L. Salager, *Surfactant-oil-water systems near the affinity inversion Part IV: Emulsion inversion temperature.* Journal of Dispersion Science and Technology, 1986. 7(3): p. 319-329.

67. Sajjadi, S., F. Jahanzad, and M. Yianneskis, *Catastrophic phase inversion of abnormal emulsions in the vicinity of the locus of transitional inversion.* Colloids and Surfaces A: Physicochem. Eng. Aspects, 2004. 240: p. 149-155.

68. Anton, N., J.P. Benoit, and P. Saulnier, *Design and production of nanoparticles formulated from nano-emulsion templates - A review.* Journal of Controlled Release, 2008. 128: p. 188-199.

69. Porras, M., *et al.*., *Properties of water-in-oil (W / O) nano-emulsions prepared by a low-energy emulsification method.* Colloids and Surfaces A: Physicochem. Eng. Aspects, 2008. 324: p. 181-188.

70. Shinoda, K. and H. Saito, *The stability of O / W Type Emulsions as Functions of Temperature and the HLB of Emulsifiers: the Emulsification by PIT-method.* Journal of Colloid and Interface Science, 1969. 30(2): p. 258-263.

71. Förster, T., W.V. Rybinsky, and A. Wadle, *Influence of microemulsion phases in the preparation of fine-disperse emulsions.* Advances in Colloid and Interface Science, 1995. 58: p. 119-149.

72. Lehnert, S., H. Tarabishi, and H. Leuenberger, *Investigation of thermal phase inversion in emulsions.* Colloids and Surfaces A: Physicochem. Eng. Aspects, 1994. 91: p. 227-235.

73. Allouche, J., *et al.*., *Simultaneous Conductivity and Viscosity Measurements as a Technique to Track Emulsion Inversion by the Phase Inversion Temperature Method.* Langmuir, 2004. 20 (6): p. 2134-2140.

74. Ghoulam, M.B., *et al.*., *Quantitative Effect of Nonionic Surfactant Partitioning on the Hydrophile-Lipophile Balance Temperature.* Langmuir, 2004. 20: p. 2584-2589.

75. Taisne, L. and B. Cabane, *Emulsification and Ripening following a Temperature Quench.* Langmuir, 1998. 14: p. 4744-4752.

76. Anton, N., J.P. Benoit, and P. Saulnier, *Particular conductive behaviors of emulsion phase inverting.* Journal of Drug Delivery Science and Technology, 2008. 18(2): p. 95-99.

77. Kunieda, H., *et al.*., *Spontaneous Formation of Highly Concentrated Water-in-Oil Emulsions (Gel-Emulsions).* Langmuir, 1996. 12: p. 2136-2140.

78. Palmer, S., *The nano diet*, in BBC Focus Magazine. 2007. p. 38-42.

79. Shakeel, F., *et al.*., *Skin permeation mechanism and bioavailability enhancement of celecoxib from transdermally applied nanoemulsion.* Journal of Nanobiotechnology, 2008. 6(8): p. 1-11.

80. Weiss, J., P. Takhistov, and J. McClements, *Functional Materials in Food Nanotechnology.* Journal of Food Science, 2006. 71(9): p. R107-R116.

81. Alléman, E., R. Burny, and E. Doelker, *Drug-Loaded Nanoparticles - Preparation Methods and Durg Targeting Issues.* European Journal of Pharmaceutics and Biopharmaceutics, 1993. 39(5): p. 173-191.

82. Spernath, L. and S. Magdassi, *A new method for preparation of poly-lauryl acrylate nanoparticles from nanoemulsion obtained by the phase inversion temperature process.* Polymers for Advanced Technologies, 2007. 18: p. 705-711.

83. Spernath, L., *et al.*., *Phase transitions in O / W lauryl acrylate emulsions during phase inversion, studied by light microscopy and cryo-TEM.* Colloids and Surfaces A: Physicochem. Eng. Aspects, 2009. 332: p. 19-25.

84. Förster, T. and W.V. Rybinski, *Chapter 12: Applications of Emulsions*, in *Modern Aspects of Emulsion Science*, B.P. Binks, Editor. 1998, The Royal Society of Chemistry: Cambridge.

85. Yoshizawa, H., *et al.*., *Microchannel O / W Nanoemulsification by Phase Inversion Temperature Method*, in *Congrès Mondial de l'Emulsion* 2006: Lyon.

86. *Zetasizer Nano Series User Manual MAN 0317*, ed. M.I. Ltd. 2004.

87. *Nanoseries and HPPS Training Manual*. 2005.

88. Lide, D., *CRC Handbook of Chemistry and Physics*, *A Ready-reference Book of Chemical and Physical Data*, 90th Edition, 2009. CRC Press Inc.

89. Malcolmson, C., D.J. Barlow, and M.J. Lawrence, *Light-Scattering Studies of Testosterone Enanthate Containing Soybean Oil / C18:1E10 / water Oil-in-Water Microemulsions.* Journal of Pharmaceutical Sciences, 2002. 91(11): p. 2317-2331.

90. *Measuring conductivity. A little theory*, in *Laboratory catalogue 2004*, Crison, Editor. 2004.

91. Malcolmson, C., *et al.*., *Effect of Oil on the Level of Solubilization of Testosterone Propionate into Nonionic Oil-in-Water Microemulsions.* Journal of Pharmaceutical Sciences, 1998. 87(1): p. 109-116.

92. Warisnoicharoen, W., A.B. Lansley, and M.J. Lawrence, *Nonionic oil-in-water microemulsions: the effect of oil type on phase behaviour.* International Journal of Pharmaceutics, 2000. 198: p. 7-27.

93. Santiago, L.G., *et al.*., *The influence of xanthan and λ-carrageenan on the creaming and flocculation of an oil-in-water emulsion containing soy protein.* Brazilian Journal of Chemical Engineering, 2002. 19(4): p. 411-417.

94. Warisnoicharoen, W., A.B. Lansley, and M.J. Lawrence, *Light-Scattering Investigations in Dilute Nonionic Oil-in-Water Microemulsions.* AAPS Pharmsci, 2000. 2(2): p. 16-26.

95. *Manual for micro annular gear pump mzr-2905 / mzr-4605 / mzr-7205*. 2005: HNP Mikrosysteme GmbH.

96. *Standard Slit Interdigital Microstructured Mixer SSIMM* in *http: / / www.imm-mainz.de / seiten / en / u_080404113958_7164.php*. 2008, IMM Institut für Mikrotechnik Mainz GmbH.
97. Hessel, V., S. Hardt, and H. Löwe, *Chapter 2: Modelling and simulation of microreactors*, in *Chemical Micro Process Engineering: Fundamentals, Modelling and Reactions*, 2004 Wiley-Vch
98. *Catalogue Chemical Process Technology*, IMM Institut für Mikrotechnik Mainz GmbH, Editor. 2006.
99. *USB-TC*. 2008, Measurement Computing Corp.
100. Coulson, J.M., *et al.*., *Chapter 9*: *Heat Transfer*, in *Chemical Engineering*, 4th Edition, 2005 Pergamon.
101. Perry, R.H. and D.W. Green, *Perry's Chemical Engineers' Handbook*, 8th Edition, 2008. McGraw-Hill.
102. Personal Communication with Daniel Metzke from IMM Institut für Mikrotechnik Mainz GmbH.
103. Robins, M.M., *Emulsions - creaming phenomena.* Current Opinion in Colloid and Interface Science, 2000. 5: p. 265-272.
104. Márquez, L., *et al.*., *Hysteresis behaviour in temperature-induced emulsion inversion.* Polymer International, 2003. 52: p. 590-593.